CANADIAN THESES ON MICROFICHE

THÈSES CANADIENNES SUR MICROFICHE

National Library of Canada
Collections Development Branch

Canadian Theses on
Microfiche Service

Ottawa, Canada
K1A 0N4

Bibliothèque nationale du Canada
Direction du développement des collections

Service des thèses canadiennes
sur microfiche

NOTICE

The quality of this microfiche is heavily dependent upon the quality of the original thesis submitted for microfilming. Every effort has been made to ensure the highest quality of reproduction possible.

If pages are missing, contact the university which granted the degree.

Some pages may have indistinct print especially if the original pages were typed with a poor typewriter ribbon or if the university sent us an inferior photocopy.

Previously copyrighted materials (journal articles, published tests, etc.) are not filmed.

Reproduction in full or in part of this film is governed by the Canadian Copyright Act, R.S.C. 1970, c. C-30. Please read the authorization forms which accompany this thesis.

AVIS

La qualité de cette microfiche dépend grandement de la qualité de la thèse soumise au microfilmage. Nous avons tout fait pour assurer une qualité supérieure de reproduction.

S'il manque des pages, veuillez communiquer avec l'université qui a conféré le grade.

La qualité d'impression de certaines pages peut laisser à désirer, surtout si les pages originales ont été dactylographiées à l'aide d'un ruban usé ou si l'université nous a fait parvenir une photocopie de qualité inférieure.

Les documents qui font déjà l'objet d'un droit d'auteur (articles de revue, examens publiés, etc.) ne sont pas microfilmés.

La reproduction, même partielle, de ce microfilm est soumise à la Loi canadienne sur le droit d'auteur, SRC 1970, c. C-30. Veuillez prendre connaissance des formules d'autorisation qui accompagnent cette thèse.

THIS DISSERTATION HAS BEEN MICROFILMED EXACTLY AS RECEIVED

LA THÈSE A ÉTÉ MICROFILMÉE TELLE QUE NOUS L'AVONS REÇUE

Canada

NL 339 (r. 85/05)

National Library of Canada
Bibliothèque nationale du Canada

Ottawa, Canada
K1A 0N4

TC –

ISBN 0-315-21344-0

CANADIAN THESES ON MICROFICHE SERVICE – SERVICE DES THÈSES CANADIENNES SUR MICROFICHE

PERMISION TO MICROFILM – AUTORISATION DE MICROFILMER

• Please print or type – Écrire en lettres moulées ou dactylographier

AUTHOR – AUTEUR

Full Name of Author – Nom complet de l'auteur

GÖKHAN COŞKUNER

Date of Birth – Date de naissance
Aug. 15, 1958

Canadian Citizen – Citoyen canadien
☐ Yes / Oui ☒ No / Non

Country of Birth – Lieu de naissance
TURKEY

Permanent Address – Résidence fixe
c/o Mineral Eng. Dept.
U of A
Edmonton, Alta.

THESIS – THÈSE

Title of Thesis – Titre de la thèse

AN EXPERIMENTAL STUDY OF A NEW APPROACH TO INSTABILITY IN POROUS MEDIA

Degree for which thesis was presented
Grade pour lequel cette thèse fut présentée
M.Sc.

Year this degree conferred
Année d'obtention de ce grade
1985

University – Université
The University of Alberta

Name of Supervisor – Nom du directeur de thèse
DR. R.G. BENTSEN

AUTHORIZATION – AUTORISATION

Permission is hereby granted to the NATIONAL LIBRARY OF CANADA to **microfilm** this thesis and to **lend** or **sell copies of the film.**

The author reserves other publication rights, and neither the thesis nor extensive extracts from it may be printed or otherwise reproduced without the author's written permission.

L'autorisation est, par la présente, accordée à la BIBLIOTHÈQUE NATIONALE DU CANADA de **microfilmer** cette thèse et de **prêter** ou de **vendre des exemplaires du film.**

L'auteur se réserve les autres droits de publication; ni la thèse ni de longs extraits de celle-ci ne doivent être imprimés ou autrement reproduits sans l'autorisation écrite de l'auteur.

ATTACH FORM TO THESIS – VEUILLEZ JOINDRE CE FORMULAIRE À LA THÈSE

Signature
Gökhan Coşkuner

Date
March 27, 1985

NL-91 (r. 84/03)

Canada

THE UNIVERSITY OF ALBERTA

AN EXPERIMENTAL STUDY OF A NEW APPROACH TO INSTABILITY IN POROUS MEDIA

by

Gökhan Coskuner

A THESIS

SUBMITTED TO THE FACULTY OF GRADUATE STUDIES AND RESEARCH

IN PARTIAL FULFILMENT OF THE REQUIREMENTS FOR THE DEGREE

OF Master of Science

IN

PETROLEUM ENGINEERING

DEPARTMENT OF MINERAL ENGINEERING

EDMONTON, ALBERTA

SPRING, 1985

THE UNIVERSITY OF ALBERTA

RELEASE FORM

NAME OF AUTHOR Gökhan Coskuner

TITLE OF THESIS AN EXPERIMENTAL STUDY OF A NEW APPROACH TO INSTABILITY IN POROUS MEDIA

DEGREE FOR WHICH THESIS WAS PRESENTED Master of Science

YEAR THIS DEGREE GRANTED SPRING, 1985

Permission is hereby granted to THE UNIVERSITY OF ALBERTA LIBRARY to reproduce single copies of this thesis and to lend or sell such copies for private, scholarly or scientific research purposes only.

The author reserves other publication rights, and neither the thesis nor extensive extracts from it may be printed or otherwise reproduced without the author's written permission.

(SIGNED) G. Coskuner

PERMANENT ADDRESS:

c/o Dept. of Mineral Engineering

The University of Alberta

Edmonton, Alberta T6G 2G6

DATED March 26, 1985

THE UNIVERSITY OF ALBERTA

FACULTY OF GRADUATE STUDIES AND RESEARCH

The undersigned certify that they have read, and recommend to the Faculty of Graduate Studies and Research, for acceptance, a thesis entitled AN EXPERIMENTAL STUDY OF A NEW APPROACH TO INSTABILITY IN POROUS MEDIA submitted by Gökhan Coskuner in partial fulfilment of the requirements for the degree of Master of Science in PETROLEUM ENGINEERING.

.....
Supervisor

.....

.....

.....

Date March 26, 1985

ABSTRACT

Whether a displacement is stable or unstable has a profound effect on how efficiently one fluid displaces another within a porous medium. As a consequence, it is of interest to be able to predict the boundary which separates stable displacements from those which are unstable. Recently, a new approach to stability theory has been developed which is based, as is earlier work, on the assumption that the immiscible displacement of one fluid by another can be treated as a moving boundary problem. In this study, the newly developed theory was first modified for a Hele-Shaw cell and then a number of experiments were conducted to validate the theory.

Sixty-three experiments, using different viscosity ratios, interfacial tension and wetting characteristics, have been performed. In general, these experiments confirmed the validity of the new theory. In particular, the stability boundary and subsequent mode boundaries are predicted correctly. Moreover, the time constant versus wavelength behaviour predicted by the theory has been verified experimentally. Also, the relative widths of oppositely directed fingers are predicted correctly. In addition, the distance travelled by the tip of the oil and water fingers with respect to the initially plane interface was found to be a linear function of time. Finally, the shape of the interface obtained in the experiments was in good agreement with the postulated functional form.

ACKNOWLEDGEMENTS

The author wishes to express his gratitude and appreciation for the guidance, encouragement and understanding of Dr. R.G.Bentsen, Professor of Petroleum Engineering, under whose supervision this investigation was conducted.

Acknowledgements are also made to Professor Dranchuk, Dr. Flock and Dr. Nandakumar for serving on the thesis commitee and for numerous beneficial discussions; to Mr. R.W.Smith who designed the cells used in the experiments and to NSERC for financial support.

The author wishes to express his gratitude to his wife, Helen, whose understanding and continued encouragement contributed to the successful completion of this study.

Table of Contents

Chapter		Page
1.	INTRODUCTION	1
2.	LITERATURE REVIEW	4
3.	STATEMENT OF THE PROBLEM	16
4.	THEORY	18
	4.1 HELE-SHAW CELL	18
	4.2 FLUID DISPLACEMENT	18
	4.3 FLOW POTENTIALS	22
	4.3.1 PERTURBATION POTENTIAL	27
	4.3.2 CAPILLARY PRESSURE POTENTIAL	29
	4.4 PERTURBATION VELOCITY	32
	4.4.1 STEADY STATE VELOCITY	32
	4.4.2 UNSTEADY STATE VELOCITY	35
	4.5 COMPATIBILITY CONDITIONS	41
	4.5.1 SIMILARITY	41
	4.5.2 SYMMETRY	42
	4.5.3 CONTINUITY	42
	4.6 CHARACTERISTIC EIGENVALUES	45
	4.7 VELOCITY OF PENETRATING FINGERS	47
	4.8 STABILITY CRITERION	48
	4.9 INITIAL CONDITION	51
5.	EXPERIMENTAL APPARATUS AND PROCEDURE	54
	5.1 DESCRIPTION OF THE EXPERIMENTAL APPARATUS	54
	5.2 EXPERIMENTAL PROCEDURE	56
6.	METHODS OF EXPERIMENTAL ANALYSIS	59
	6.1 STABILITY BOUNDARY AND MODE BOUNDARIES	59

6.2 RELATIVE FINGER WIDTHS 60

6.3 TIME CONSTANT VERSUS WAVELENGTH PLOT 61

6.4 DISTANCE TRAVELLED BY THE TIP OF THE FINGER VERSUS TIME 62

6.5 FINGER SURFACES 63

7. RESULTS AND DISCUSSION 66

SUMMARY AND CONCLUSIONS 113

REFERENCES 114

BIBLIOGRAPHY 119

APPENDIX 1 121

APPENDIX 2 127

APPENDIX 3 130

APPENDIX 4 134

APPENDIX 5 136

LIST OF TABLES

TABLE		PAGE
1.	Properties of the fluids used	57
2.	Summary of the experiments	67-70
3.	Values of c_2 at different times	107-109

LIST OF FIGURES

FIGURE PAGE

1. The Hele-Shaw Cell.....21

2. Oppositely directed oil and water fingers.....38

3. Schematic drawing of experimental apparatus.....55

4. Time constant versus wavelength plot for MCT-5+heptane and water.....71

5. Time constant versus wavelength plot for MCT-5+LA60+octylamine and water.....72

6. Time constant versus wavelength plot for MCT-5+heptane+octylamine and water.....73

7. Time constant versus wavelength plot for MCT-5 and water.....74

8. The interface at t=1424 sec. for Run 27.....78

9. The interface at t=1858 sec. for Run 27.....79

10. The interface at t=2718 sec. for Run 27.....80

11. The interface at t=3330 sec. for Run 27.....81

12. The interface et t=3685 sec. for Run 27.....82

13. The interface at t=3968 sec. for Run 27.....83

14. The interface at t=889 sec. for Run 51.....84

15. The interface at t=1092 sec. for Run 51.....85

16. The interface at t=1132 sec. for Run 51.....86

17. The interface at t=221 sec. for Run 13.....87

18. The interface at t=251 sec. for Run 13.....88

19. The interface at t=301 sec. for Run 13.....89

20. The interface at t=324 sec. for Run 13.....90

21. The interface at t=367 sec. for Run 13.....91

22. The interface at t=505 sec. for Run 13.....92

23. Distance travelled by the tip of the finger for Run 13.....97

24. Distance travelled by the tip of the finger for Run 31.....100

25. Distance travelled by the tip of the finger for Run 51.....101

26. Distance travelled by the tip of the finger for Run 33.....103

27. Distance travelled by the tip of the finger for Run 50.....104

28. Distance travelled by the tip of the finger for Run 51.....105

29. The interface at t=127 sec. for Run 31.....137

30. The interface at t=214 sec. for Run 31.....138

31. The interface at t=370 sec. for Run 31.....139

32. The interface at t=498 sec. for Run 31.....140

33. The interface at t=680 sec. for Run 33.....141

34. The interface at t=812 sec. for Run 33.....142

35. The interface at t=870 sec. for Run 33.....143

36. The interface at t=958 sec. for Run 33.....144

37. The interface at t=1008 sec. for Run 33.....145

38. The interface at t=308 sec. for Run 34.....146

39. The interface at t=413 sec. for Run 34.....147

40. The interface at t=493 sec. for Run 34.....148

41. The interface at t=525 sec. for Run 34.....149

42. The interface at t=5981 sec. for Run 42.....150

43. The interface at t=7135 sec. for Run 42.....151

44. The interface at t=7978 sec. for Run 42.....152

45. The interface at t=9976 sec. for Run 42.....153

46. The interface at t=12014 sec. for Run 42.....154

47. The interface at t=13219 sec. for Run 42.....155

48. The interface at t=14427 sec. for Run 42.....156

49. The interface at t=15092 sec. for Run 42.....157

50. The interface at t=16465 sec. for Run 42.....158

51. The interface at t=288 sec. for Run 50.....159

52. The interface at t=435 sec. for Run 50.....160

53. The interface at t=571 sec. for Run 50.....161

54. The interface at t=610 sec. for Run 50.....162

55. The interface at t=721 sec. for Run 50.....163

56. The interface at t=786 sec. for Run 50.....164

57. The interface at t=857 sec. for Run 50.....165

58. The interface at t=990 sec. for Run 50.....166

NOMENCLATURE

A	Arbitrary integration constant
A_o, A_w	Arbirary constants of integration for oil and water surface, respectively
a	Velocity of oppositely directed, two dimensional travelling waves, m/s
C_1, C_2	Principal radii of curvature of interface
c_1, c_2	Arbitrary constants of proportionality
g	Gravitational acceleration, m/s^2
h	Distance between the plates, m
k	Absolute permeability, m^2
L_x	Width of the Hele-Shaw Cell, m
L_{xo}, L_{xw}	Half-widths of oil and water fingers, respectively
M	Viscosity ratio
m	Mode number

N_g	Gravity number
n	Time constant, s^{-1}
n_w	Time constant for water finger, s^{-1}
P	Pressure, kPa
P_b	Base pressure, kPa
P_c	Capillary pressure, kPa
$P_c(t)$	Microscopic capillary pressure, kPa
P_o, P_w	Pressure in oil and water phases, respectively, kPa
q	Volumetric injection rate, m^3/s
t	Real time, seconds
V	Superficial velocity, m/s
V_c	Characteristic superficial velocity at which displacement becomes unstable, m/s
$(\vec{V}_o)$	Oil superficial velocity vector, m/s

V_{ox}, V_{oz}	X and z components of oil superficial velocity vector, respectively, m/s
$\vec{V}_w$	Water superficial velocity vector, m/s
V_{wx}, V_{wz}	X and z components of water superficial velocity vector, respectively, m/s
$(V^*_{ox})_w$, $(V^*_{oz})_w$	Oil steady state perturbation velocities in x and z direction, respectively, in the region where water is flowing, m/s
$(V^*_{wx})_o$, $(V^*_{wz})_o$	Water steady state perturbation velocities in x and z direction, respectively, in the region where oil is flowing, m/s
V_z	Average velocity of fluid passing through base of a finger, m/s
V^*_z	Perturbation velocity in the z direction, m/s
V_o	Bulk volume of an oil finger, m^3
V_w	Bulk volume of a water finger, m^3
α	Separation constant, m^{-1}

α_c	Characteristic eigenvalue for which capillary and gravity forces exactly balance viscous forces, m^{-1}
α_m	Eigenvalue for which the finger surface is being created at the greatest rate, m^{-1}
α_o, α_w	Separation constants for oil and water regions, respectively, m^{-1}
η	Frontal displacement, m
$(\eta_o)_w$	Frontal displacement of an oil finger in the region where only water is flowing, m
$(\eta_w)_o$	Frontal displacement of a water finger in the region where only oil is flowing, m
$(\eta_w)_{omax}$	Maximum length of a water finger in the region where only oil is flowing, m
θ	Angle Hele-Shaw cell makes with vertical, radians
λ_w, λ_o	Wavelenght of water and oil fingers, respectively , m

μ_o, μ_w	Oil and water viscosities, respectively, mPa.s
π	3.14159...
ρ	Density, kg/m^3
ρ_o, ρ_w	Oil and water densities, respectively, kg/m^3
σ_e	Effective interfacial tension, mN/m
σ_{ow}	Interfacial tension, mN/m
Φ	Force potential, N.m/kg
Φ_c	Capillary potential, N.m/kg
Φ_{cw}	Capillary potential for water, N.m/kg
Φ_o, Φ_w	Force potentials for oil and water, respectively, N.m/kg
$(\Phi_{cw})_o$	Capillary potential for water in the region where only oil is flowing, N.m/kg
$(\Phi_{co})_w$	Capillary potential for oil in the region where only water is flowing, N.m/kg

$(\phi_o)_o$ Oil force potential in the region where only oil is flowing, N.m/kg

$(\phi_o)_w$ Oil force potential in the region where only water is flowing, N.m/kg

$(\phi_w)_o$ Water force potential in the region where only oil is flowing, N.m/kg

$(\phi_w)_w$ Water force potential in the region where only water is flowing, N.m/kg

$(\phi_o^*)_w$ Perturbation potential for oil in the region where only water is flowing, N.m/kg

$(\phi_w^*)_o$ Perturbation potential for water in the region where only oil is flowing, N.m/kg

∇ Gradient operator

1. INTRODUCTION

Crude oil shortages may arise again in the future. One way to alleviate such shortages would be to improve recovery efficiencies in known fields, as each one percent increase in recovery efficiency adds about four billion barrels to the recoverable reserves. Hence, research effort in the area of enhanced oil recovery could pay large dividends.

Most enhanced oil recovery processes involve the displacement of one fluid by another. Thus, if recovery efficiencies are to be improved, we must come to a better understanding of fluid displacement in porous media. Whether a displacement is stable or unstable has a profound effect on how efficiently one fluid displaces another within a porous medium. Thus, it is necessary to be able to predict if a displacement is stable or unstable.

The theories of unstable immiscible displacement can be classified in two general categories. The first category consists of the theories which utilize first-order perturbation analysis and the concept of a velocity potential. These theories can deal only with the incipient finger as first-order perturbation theory is valid only if the deviations are small. If the initial perturbation applied to the displacement has a finite amplitude, first-order perturbation theory cannot be used. A velocity potential exists only for fields of flow involving a fluid of constant density and viscosity and a porous medium which is homogeneous and isotropic throughout. Therefore, it

cannot, in principle, deal with a real porous medium. Thus, the theories in the first category have some problems.

The second category includes the theories which try to account for the presence of a transition zone in the stability analysis by using Buckley-Leverett type equations. The resulting equations are solved by numerical means. There are problems with this type of approach as well. These theories utilize the capillary pressure and relative permeability curves which are obtained in stable displacements. It is debatable whether such curves apply to phenomena where the force imbalance is completely different. Numerical instabilities and numerical dispersion, which are associated with numerical methods, may also make it difficult to calculate the actual behaviour of the displacement.

Recently, a new approach to stability theory has been developed. This theory makes use of the concept of a force potential rather than that of a velocity potential and is based on the assumption that the immiscible displacement of one fluid by another can be treated as a moving boundary. Therefore, the theory is not limited by the assumptions involved in using the velocity potential. The use of force potential also makes it possible to impose additional conditions on the solution. Because a shape for the finger surfaces is postulated, there is no need for numerical solutions. As a consequence, the newly developed theory does not suffer from the problems associated with the theories in

either category. This theory has yet to be validated experimentally.

2. LITERATURE REVIEW

In 1950, Taylor[1] used small perturbation analysis, which was suggested earlier by Lamb[2], to investigate the instability of two superimposed fluids of different densities when the interface is accelerated in a direction perpendicular to itself. By neglecting interfacial tension and utilizing the velocity potentials for each fluid, Taylor[1] was able to show that this surface was stable or unstable depending upon whether the acceleration was directed from the heavier to the lighter fluid or vice versa. The experimental work of Lewis[3], which was published shortly after Taylor's[1] theoretical work, verified the theory experimentally.

The formation and the rate of growth of these instabilities were later investigated by Bellman and Pennington[4], taking into account the effects of surface tension and viscosity which were neglected by Taylor[1] in the earlier analysis. They showed that the presence of surface tension removed the instability for sufficiently small wavelengths.

In 1958, a similar method was employed by Saffman and Taylor[5] to analyse the stability of flow between two parallel plates. They assumed that the two immiscible fluids remain completely separated at the planar interface in a two-dimensional porous medium. They considered small perturbations of this interface and linearized the perturbation equations to obtain the condition for

stability. Their results indicated that the frontal zone was unstable when the effective mobility ratio behind the front exceeded that ahead of the front. They also showed that the effect of surface tension was to limit the range of disturbances which were unstable to those wavelengths greater than a critical value.

Saffman and Taylor also examined the post instability situation by trying to predict the shape of a single finger advancing at steady state in a Hele-Shaw cell. The pressure at the interface was assumed to be continuous. The use of conformal transformations enabled these authors to find several exact solutions of the equations describing the system.Their theoretical predictions for stability in a Hele-Shaw cell were confirmed by experiments, but the results regarding the post instability situation were inconclusive.

In 1958, Van Meurs and van der Poel[4] thought that it was highly questionable to apply the relative permeability concepts of conventional immiscible displacement theory to displacements dominated by viscous instabilities. Therefore, they developed a descriptive theory based on an idealized model which was tailored to viscous fingering as observed in transparent models. This theory is similar to conventional Buckley-Leverett theory in several respects.

In 1959, the analysis of instability of fluid interfaces was carried further by Chuoke, van Meurs and van der Poel[5]. Using perturbation theory, they undertook a

first-order linear stability analysis of the displacement of one fluid by another. Their theory was founded on a sharp-interface displacement model in which the displacing fluid sweeps the displaced one leaving only an immobile displaced fluid saturation (moving boundary model).

These authors derived the necessary and sufficient condition that would promote instability and viscous fingering. According to this condition for instability, the velocity has to be larger than a critical value and the wavelengths of the disturbances have to be greater than a minimum critical value which results from the effect of surface tension. They also found that the initial growth rate depended on wavelength and this dependency had an absolute maximum. Therefore, they reasoned that a real displacement was subjected to perturbations of many wavelengths at every point. The fastest growing wavelength would be expected to dominate the displacement and emerge as the observed wavelength. The experiments that were carried out in Hele-Shaw cells were in good agreement with the theory.

In 1962, Outmans' solved the perturbation equations for a sharp front between two immiscible fluids without linearizing them. He was able to consider perturbations up to fourth degree by solving the perturbation equations using the method of successive approximations. His results showed that there was a critical velocity and wavelength, in the case of linear approximations, but that the law of growth

with time of the perturbation was complicated and that the wavelength of maximum growth no longer existed. He also found that the conclusion arrived at in linear theory, that if interfacial tension is negligible the rate of growth of the initial disturbance is independent of the wave number, was not correct.

In 1964, Rachford' considered one dimensional displacement in a finite region using a simplified description of the basic flow which included the effects of a saturation distribution. Using a normal mode analysis, he linearized the perturbed equations and obtained a second order partial differential equation whose coefficients were not constants. The solution of the equation was obtained by assuming the coefficients to be constants, which is at best questionable, and by using finite difference techniques. Rachford' concluded that the existence of a transition zone, in which the saturation varies progressively, profoundly modified the characteristics of the displacement, in so far as the development of instabilities were concerned. He also showed, by using a few selected initial perturbations, that when the capillary pressure and relative permeability characteristics were those which pertained for preferentially water-wet reservoirs, and when the reservoir contained an intial water saturation, no important fingering occurred. But the results of a stability analysis based on a few selected, rather than arbitrary, initial perturbations cannot be generalized. Moreover, if the relative

permeability curves which are valid for stable displacements are used, one should not be surprised when the displacement behaves in a stable manner. It is also not certain that the solution is unaffected by the numerical dispersion associated with finite difference methods in general.

In 1971, a different approach was taken by Raghaven and Marsden[9] who considered two fluids separated by a homogeneously emulsified zone, which was treated as a third fluid. The interface between each fluid was assumed to be sharp and planar. They applied linearized small perturbation theory to this case which they called "generalized Saffman-Taylor" theory. For this problem, the two interfaces behaved independently at perturbation wavelengths small in comparison with the layer thickness; but coupling increased with the wavelength until finally the mixed zone behaved as a single interface. It was also shown that the cut-off wavenumber, above which the displacement is stable, increased as the ratio of viscous forces to capillary forces increased for a given disturbance. This same conclusion was also reached by Huang,et.al.[10]. After a linearized perturbation analysis, including the effects of a transition region, they found that the critical wavelength required for the onset of instability decreased with an increase in the ratio of viscous to capillary forces.

In 1974, Hagoort[4],as did Rachford[7], argued that the stability analysis should be based on simultaneous two phase flow. He, therefore, used the Buckley-Leverett displacement

model to derive the condition for instability. He concluded that the displacement would be unstable if the mobility ratio of the fluids behind and ahead of the shock front was greater than one, provided that the wavelength of the instabilities was smaller than the width of the porous medium. As the shock mobility ratio is considerably lower than the end-point mobility ratio, it is possible for the shock mobility ratio to be less than one at large values of the end-point mobility ratio. Hence, he attributed the lack of instability in Rachford's' studies to such a condition. In Hagoort's'' analysis the role of capillary forces did not emerge as a part of the stability analysis; therefore, he included the effects of capillarity by using energy arguments. His stability condition, as a result, does not allow for the existence of a critical wavelength. He used transparent flow models to verify the theory and obtained qualitative agreement with the theory. The use of imbibition capillary pressure and relative permeability curves to predict the behaviour of a displacement which is dominated by viscous forces is again debatable.

Gupta and co-workers presented some experiments on viscous fingering in a Hele-Shaw cell'[3] and in a bead-packed two-dimensional porous medium'[3] in 1973 and 1974, respectively. They showed that Chouke's' theory correctly predicted the number of initial fingers for a Hele-Shaw cell but could not identify the number of incipient fingers in a porous medium because the front was not sharp. In all cases,

the final state was that of a single central finger, such as that studied by Saffman and Taylor[5], irrepective of the initial number of incipient fingers. They also observed that under unstable displacement conditions local heterogeneities overrode the predicted wavelength in a Hele-Shaw cell[12]. In their experiments, the finger growth rate was linear with time for all flow rates considered; for the Hele-Shaw cell, the tail and the nose of the finger had different velocities.

In 1976, Wooding and Morel-Seytoux[14] stated that in the experiments of Gupta,et.al. it was possible that the sidewalls were influencing the results. In 1977, White,et.al.[18] carried out some immiscible displacement experiments in a Hele-Shaw cell. Their results, too, were consistent with the theory of Chuoke,et.al.[7] in that they correctly predicted the number of incipient fingers. However, contrary to the result of Gupta,et.al[12,13] the individual fingers persisted and did not merge into a single finger.White,et.al[18] state that their experiments may not have continued long enough for this phenomenon to emerge, but they share the view of Wooding and Morel-Seytoux [14] that the Gupta,et.al. experiments may have been dominated by edge effects, as their cell was relatively narrow.

In 1981, Peters and Flock[17] extended the stability analysis of Chuoke,et.al.[7] by imposing an additional boundary condition at the walls of the porous medium. This condition stated that all the velocities normal to the core

wall must vanish. The introduction of this condition allowed them to introduce the dimensions of the system into the problem. They obtained a universal scaling group and its critical value which dictated the onset of instability. Cylindrical sand packs were used in the laboratory experiments to successfully predict the onset of instability. They had to use the average dimensions of the fingers obtained experimentally to predict the value of the "effective interfacial tension" between oil and water in the porous medium which, in turn, was used in the dimensionless scaling group.

In 1984, Jerauld,et.al''·'' used a method similar to Rachford's' to consider the stability of a saturation profile of permanent form with respect to small disturbances in pressure and saturation. Their linearized stability analysis led to a generalized eigenvalue problem whose solution was found by finite differencing. Results show that when the front was unstable there was a fastest growing wavelength of disturbance tranverse to the flow''. Like Hagoort''' and Peters and Flock'', they found that stability depended on the dimensions of the system. They predicted the stability boundary of an immiscible system by using typical relative permeability and capillary pressure curves. Their results are not consistent with the use of an effective interfacial tension, as introduced by Chuoke,et.al.'

In 1984, Huang,et.al.'' used a formulation of the unstable immiscible displacement problem which was in

principle similar to the formulation of Jerauld,et.al.[8,17]. However, the numerical solution employed was different. They referred to this technique as the "matched initial values" solution scheme. Huang, et.al.[17] showed that the displacement was stable to any small disturbances provided that the viscosity ratio of oil to water was less than a critical value. For values of the viscosity ratio above the critical, the numerical results showed that the displacement was unstable to small disturbances of wavelength greater than a critical value of the wavelength. An important conclusion obtained by Huang,et.al.[17] was that the results were significantly affected by changes in the exponents of the power-law models they used to model the oil and water relative permeability curves.

In 1984, Yortsos and Huang[29] showed that the existence of a transition zone resulted in considerable attenuation of the rates of growth of the instabilities. This result is somewhat similar to the one reached by Rachford[9].

In 1985, Bentsen[21] developed a new approach to stability theory for immiscible fluids. The new approach is based on the assumption of a sharp interface between the two fluids. He used the concept of a force potential rather than that of a velocity potential which enabled him to impose additional conditions on the solution and to introduce the relative widths of the oil and the water fingers into the analysis. As a result, the instability number obtained was proportional to that obtained by Peters and Flock[7], the

proportionality constant being a function of the mobility ratio. He also showed that the width of the penetrating finger is not dictated by the characteristic eigenvalue which was obtained when viscous forces exactly balance the capillary and the gravity forces; rather it was dictated by an eigenvalue which was proportional to the critical eigenvalue. The constant of proportionality was again a function of mobility ratio. In the same paper, a method for estimating the effective interfacial tension was proposed.

Early work on the stability analysis of immiscible displacement is generally based on first-order perturbation analysis and the concept of a velocity potential[1-5,7,10,12,13,15,17]. These theories usually use a sharp interface approximation. Moreover, while they can deal with the incipient finger, they cannot deal with the subsequent growth of it. There are problems with the use of first-order perturbation theory and with the concept of a velocity potential.

A velocity potential exists only for fields of flow involving a fluid of constant density and viscosity and a porous medium which is homogeneous and isotropic throughout[22]. Therefore it cannot, in principle, deal with a real porous medium. Moreover, it is the force potential and not the velocity potential which governs the flow of fluids through porous media[23]. When the velocity potential approach is taken, if the divergence of perturbation velocity is zero, then the postulated velocity potential will satisfy

Laplace's equation[8]. But the divergence of the perturbation velocity is not zero in two phase flow in the volume averaged approach which is used in porous media. First-order perturbation theory is not rigorous and the conclusions obtained from it are not always correct, as linearization of the equations is valid only if the deviations are small. It should be noted that unless the amplitude of the developing disturbance is small compared to its wavelength, results obtained using linearized perturbation theory are invalid. Moreover, these linearized equations cannot be used if the initial perturbation applied to the displacement has finite amplitude[24].

Theories which try to incorporate the existence of a transition zone into the stability analysis by using Buckley-Leverett type equations[9,11,14,18,23] have some problems as well. In all of the approaches, except that of Hagoort[14], the resulting perturbation equations are solved by numerical means. Although this approach is seemingly more realistic, all of these theories utilize the relative permeability and capillary pressure curves which are valid for stable displacements. These curves are obtained through equations which do not include the effects of viscous fingering[23,4]. The validity of using these curves to predict unstable behaviour, and hence the results obtained in this way, should be questioned. In a stable displacement, capillary forces dominate the viscous forces and the behaviour of the system reflects this condition; but in an

unstable displacement the force imbalance is opposite which should result in a different set of capillary pressure and relative permeability curves. An additional problem arises whenever numerical methods are used in solving the equations of unstable flow. These numerical methods, in general, have numerical dispersion and numerical instabilities associated with them. As a result, it may be difficult to differentiate between the actual behaviour of the system and the effects of the numerical instabilities and the numerical dispersion.

3. STATEMENT OF THE PROBLEM

It would be helpful, in understanding the unstable displacement of immiscible fluids, to develop a theory which does not suffer from the criticism presented in the last four paragraphs of the previous chapter. In particular, this theory should be able to deal with the entire life span of the finger and should not be restricted by the assumptions involved in the use of the velocity potential. Furthermore, the theory should be simple enough to have an analytical solution and to keep the mathematics tractable. Such a theory has been developed by Bentsen[21] but it has not yet been tested experimentally. Thus, there is a need to verify this theory experimentally.

In order to test the fluid mechanics aspects of the theory, the preliminary experiments should be carried out in a simple system such as a Hele-Shaw cell. The flow in a Hele-Shaw cell satisfies the assumption of sharp interface exactly[18] and it provides a simple method for studying viscous fingering as it contains a great deal of physics without the complication of irregular or random geometry[13,24]. The problem is further simplified by replacing the effective interfacial tension by the interfacial tension measured in the laboratory.

The aim of this study is to verify experimentally the validity (or invalidity) of the new theory developed by Bentsen[21]. As the simplest laboratory system which allows the experiments to be carried out for this purpose is a

Hele-Shaw cell, these experiments will be carried out in such a system. In order to evaluate the results of immiscible fluid displacements in a Hele-Shaw cell, the theory will first be rederived for the flow conditions that prevail in such a system.

4. THEORY

4.1 HELE-SHAW CELL

A Hele-Shaw cell consists of two parallel plates separated by a small uniform gap. The viscous flow analog (Hele-Shaw cell) is based on the similarity between the differential equations governing the saturated flow in a porous medium and those describing the flow of a viscous fluid in the narrow space between two parallel planes. If the planes (plates) are separated by a distance h, then the permeability, k, by the analogy mentioned above is given by the expression[27] $k=h^2/12$. It should be noted that the equations for a porous medium are the same as those for a Hele-Shaw cell, provided that the permeability is replaced by this expression.

4.2 FLUID DISPLACEMENT

Consider two fluids which are initially separated by a plane interface in a porous medium. The displacement of one of these fluids by the other can take place under two completely different flow regimes. The first one is stable displacement during which a transition region between these two fluids will develop as they travel through a porous medium. Depending on the balance between the viscous, capillary and gravity forces and the pore size distribution, the size and the shape of this transition region changes. Conventional displacement theory[28] can predict the shape of

the saturation profile in this case. If the displacement is stable and all the flow paths are identical in size and shape, these two fluids will continue to be separated by a sharp front or saturation discontinuity during the displacement. This kind of displacement can be modelled as a moving boundary problem.

The second type of displacement is unstable displacement. In this kind of displacement the interface separating the two fluids becomes unstable causing viscous fingers to appear. In this case, the heterogeneities in the porous medium and the balance between viscous, capillary and gravity forces will determine the extent of viscous fingering.

In the development of the theory, it will be assumed that the fluids are initially separated by a plane interface. That is, the displacement will be treated as a moving boundary problem. The use of a Hele-Shaw cell not only simplifies the problem as it is an idealized porous medium, but also enables attention to be focussed on the most important aspect of the problem: the balance of forces which exists at the interface separating the two fluids. As a consequence , the effect of pore size distribution on how the perturbed interface will grow is absent in the analysis and in the experiments.

Therefore, consider the displacement of oil by water at a constant velocity, V, normal to the interface which is treated as a moving boundary. The displacement takes place

in a Hele-Shaw cell, which is assumed to be infinitely long, as shown in Fig.1 . The origin of the coordinate axes is assumed to be embedded in the plane of the unperturbed interface which moves with the velocity V in an Eulerian frame of reference but is stationary in a Lagrangian frame of reference; the z axis is inclined at an angle θ to the upward vertical.

To determine whether a perturbation of the interface separating the two fluids will grow, one must be able to specify a potential at each point on either side of the interface for each fluid. The approach taken here is to define a force potential for the water on the oil side of the interface and then on the water side of the interface. Then, the perturbation potential is defined to be the difference, evaluated at the same point on the interface, between these two potentials. Finally, the perturbation velocity for the water finger is found by applying the appropriate form of Darcy's law to the perturbation potential. A similar approach is followed for the oil finger.

Certain conditions must be met if the growth of two or more pairs of oppositely directed, contiguous fingers is to be compatible. If these compatibility conditions are combined with the equations for the perturbation velocities, a system of equations arise which may be solved for the eigenvalues which dictate the width of the finger. As the displacement takes place within the confines of a Hele-Shaw

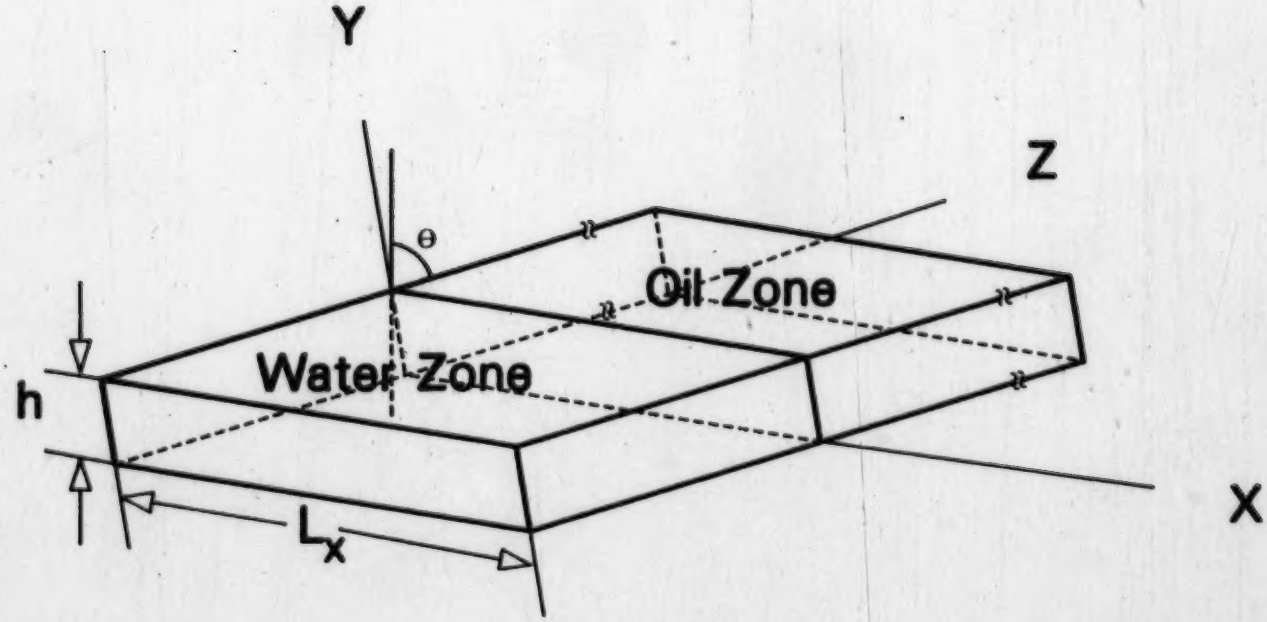

FIG.1 A HELE-SHAW CELL

cell, geometry dictates that only certain of the infinitude of possible wavelengths can fit within the Hele-Shaw cell. Thus, the superficial velocity at which the displacement becomes unstable can be found by choosing the eigenvalue which dictates the largest wavelength which can fit in the Hele-Shaw cell. The details of this approach are presented in the following sections.

4.3 FLOW POTENTIALS

The force potential, Φ, was first suggested by Hubbert[22] It is the mechanical energy per unit mass of a given fluid at any arbitrary point in space. The potential of a fluid at a specified point is, accordingly, the reversible work required to transform a unit mass of fluid from an arbitrary standard state to the state at the point under consideration. The force potential has a value not only at all points occupied by that fluid, but also at all exterior points capable of being occupied by that fluid. Let us now consider two fluids in contact with each other in the porous medium. If the fluids are immiscible, they will always be separated by a fluid interface on opposite sides of which the pressures will have a difference P (capillary pressure). To deal with this circumstance it is necessary to extend the definition of force potential for a fluid to include the work done against the interfacial capillary pressure[22]. If this is done, then the potential of any fluid in any region is defined by

$$\Phi = gzCos\theta + \int_{P_b}^{P + P_c} \frac{dP}{\rho} \qquad (1)$$

In this equation, the density ρ must be a function of pressure only. Equation 1 can be further simplified by assuming that the fluids under consideration are incompressible. If this is done, Equation 1 reduces to the simpler form

$$\Phi = gzCos\theta + \frac{P - P_b}{\rho} + \Phi_c \qquad (2)$$

where

$$\Phi_c = \frac{P_c}{\rho} \qquad (3)$$

In dealing with several fluids, there will be as many different potentials as there are fluids; at each point in space, therefore, regardless of which fluid occupies that

space, there will be a particular value for each of the several potentials. Now,if z represents the elevation of a point on the interface, then it is necessary to think of both fluids being injected on the same side of the existing interface against the pressure of the fluid that occupies that same side of the interface. Therefore, the injection will be made against the pressure of water on the water side of the interface. In this case, if the injected fluid is water, the capillary pressure potential of the water is zero; but if the injected fluid is oil, then the capillary pressure potential of the oil will be the appropriate non-zero value which can be calculated using Equation 3. Similarly, the injection can be made against the pressure of the oil on the oil side of the interface. In this case, if oil is the injected fluid, the capillary pressure potential of the oil will be zero; but if water is the injected fluid, the capillary pressure potential of the water will be the appropriate non-zero value which again can be calculated using Equation 3. It makes no difference in the results which of these approaches are employed, but one or the other must be used.

On the oil side of the interface, the potentials of the water and the oil are given, respectively, by

$$(\phi_w)_o = gz\cos\theta + \frac{P_o - P_b}{\rho_w} + (\phi_{cw})_o \qquad (4)$$

and

$$(\phi_o)_o = gz\cos\theta + \frac{P_o - P_b}{\rho_o} \qquad (5)$$

Solving for $P_o - P_b$ from Equation 5 and substituting this result into Equation 4 gives, for the potential of water on the oil side of the interface,

$$(\phi_w)_o = \frac{\rho_w - \rho_o}{\rho_w} gz\cos\theta + \frac{\rho_o}{\rho_w} (\phi_o)_o + (\phi_{cw})_o \qquad (6)$$

where $(\phi_o)_o$, the potential of the oil on the oil side of the interface is defined by Darcy's law, as follows,

$$\vec{V}_o = - \frac{h^2 \rho_o}{12\mu_o} \nabla(\phi_o)_o \qquad (7)$$

and

$$V_{ox} = 0 \quad ; \quad V_{oz} = V \qquad (8)$$

Following the same procedure for the water side of the interface, the potentials of the water and the oil, respectively, are

$$(\phi_w)_w = gz\cos\theta + \frac{P_w - P_b}{\rho_w} \tag{9}$$

and

$$(\phi_o)_w = gz\cos\theta + \frac{P_w - P_b}{\rho_o} - (\phi_{co})_w \tag{10}$$

Eliminating $P_w - P_b$ from Equation 10 by replacing it from Equation 9 gives, for the potential of the oil on the water side of the interface,

$$(\phi_o)_w = -\frac{(\rho_w - \rho_o)}{\rho_o} gz\cos\theta + \frac{\rho_w}{\rho_o}(\phi_w)_w - (\phi_{co})_w \tag{11}$$

where $(\phi_w)_w$, the potential of water on the water side of the interface, is defined by Darcy's law, as follows,

$$\vec{V}_w = - \frac{h^2 \rho_w}{12 \mu_w} \nabla (\Phi_w)_w \qquad (12)$$

and

$$V_{wx} = 0 \quad ; \quad V_{wz} = V \qquad (13)$$

4.3.1 PERTURBATION POTENTIAL

Consider the potential of the water on the oil side of the interface, $(\Phi_w)_o$, and on the water side of the interface, $(\Phi_w)_w$. If the interface is planar these two potentials are equal. If, however, the interface is perturbed these potentials will not be equal. Consequently, a finger of water will penetrate the oil, provided that, on the interface, $(\Phi_w)_w > (\Phi_w)_o$. Therefore, let a perturbation potential for the water in the region where oil is flowing, $(\Phi_w^*)_o$, be defined as

$$(\phi^*_w)_o = (\phi_w)_o - (\phi_w)_w \tag{14}$$

Upon introducing Equation 6 into Equation 14, one obtains

$$(\phi^*_w)_o = \frac{\rho_w - \rho_o}{\rho_w} gz\cos\theta + \frac{\rho_o}{\rho_w}(\phi_o)_o - (\phi_w)_w + (\phi_{cw})_o \tag{15}$$

While a water finger penetrates into the oil, an oil finger also penetrates into the water because of material balance demands. An oil finger will grow in the minus z direction, provided that $(\phi_o)_o > (\phi_o)_w$. Therefore, let the perturbation potential of the oil in the region where water is flowing, $(\phi^*_o)_w$, be defined as

$$(\phi^*_o)_w = (\phi_o)_w - (\phi_o)_o \tag{16}$$

Introducing Equation 12 into Equation 16 leads to

$$(\Phi_o^*)_w = -\frac{\rho_w - \rho_o}{\rho_o} gz\cos\theta + \frac{\rho_w}{\rho_o}(\Phi_w)_w - (\Phi_o)_\rho - (\Phi_{co})_w \qquad (17)$$

4.3.2 CAPILLARY PRESSURE POTENTIAL

The pressure difference across the boundary, η, separating the displaced fluid from the displacing fluid, is related to the curvature of this boundary. Therefore, it is necessary to know how this boundary evolves over time to determine the capillary pressure potential. In order to determine the shape of the interface, the potentials on either side of the interface satisfying the appropriate boundary and initial conditions have to be ascertained. In particular, these potentials have to satisfy an appropriate continuity equation, initial condition, the boundary conditions on the external boundaries, and dynamic and kinematic conditions on the interface. An exact analytical solution for the moving boundary problem employing presently available mathematical tools is complicated because the boundary conditions at the interface are given on an a priori, unknown surface $z=\eta$. Therefore, in order to avoid these difficulties, a shape for the perturbed interface will be assumed. It is supposed that a finger may be modelled as

a symmetric, one-dimensional standing wave whose amplitude continuously increases with time. It is postulated that the differential equation describing the evolution of such a wave will take the form

$$-\frac{1}{a^2 f(t)}\frac{\partial^2 \eta}{\partial t^2} = \frac{\partial^2 \eta}{\partial x^2} \qquad (18)$$

where $\eta(x,t)$ is the distance travelled by the interface in the z direction with respect to the initially straight interface; a is the velocity of the oppositely directed, one dimensional travelling waves; and $f(t)$ is a function of time which will be defined later. The solution of Equation 18 by separation of variables, using the appropriate boundary conditions, will take the form (see Appendix 1)

$$\eta(x,t) = \mathrm{Cos}(\alpha x)T(t) \qquad (19)$$

where

$$\alpha = \frac{(2m-1)\pi}{2L_x} \quad ; \quad m = 1,2,3... \tag{20}$$

α being the separation constant. It is also equal to the eigenvalues for this case of two dimensional flow. The width of the cell is L_x.

Once the functional form defining the behaviour of the interface is found, the pressure difference across this interface can be shown to be (see Appendix 2)

$$P_c = P_w - P_o = \sigma_{ow} \left(\frac{2}{h} + \alpha^2 \eta\right) \tag{21}$$

For the region where oil is flowing, the capillary pressure potential of the water can be found by substituting Equation 21 into Equation 3 , yielding

$$(\phi_{cw})_o = \frac{\sigma_{ow}}{\rho_w} \left(\frac{2}{h} + \alpha_w^2 (\eta_w)_o\right) \qquad (22)$$

The capillary pressure potential of the oil in the region where water is flowing is found in a similar manner ,

$$(\phi_{co})_w = \frac{\sigma_{ow}}{\rho_o} \left(\frac{2}{h} + \alpha_o^2 (\eta_o)_w\right) \qquad (23)$$

4.4 PERTURBATION VELOCITY

4.4.1 STEADY STATE VELOCITY

In order to obtain the steady state perturbation velocities, Darcy's law will be used. The perturbation velocity for water in the region where oil is flowing is given by

$$(\vec{V}^{*}_{w})_{o} = - \frac{h^2 \rho_o}{12\mu_o} \nabla(\phi^{*}_{w})_{o} \qquad (24)$$

where the perturbation potential $(\phi^{*}_{w})_{o}$ is obtained by substituting Equation 22 into Equation 15. If this final expression is introduced into Equation 24, the perturbation velocity of water, in the region where oil is flowing, can be shown, in the x direction, to be

$$(V^{*}_{wx})_{o} = - \frac{h^2}{12\mu_w} a^2_w \sigma_{ow} \frac{\partial(\eta_w)_o}{\partial x} \qquad (25)$$

and by defining (see Appendix 3)

$$N_g = \frac{(\rho_w - \rho_o)\ h^2 g \cos\theta}{12\mu_w V} \qquad (26)$$

$$M = \frac{\mu_o}{\mu_w} \tag{27}$$

can be shown, in the z direction, to be

$$(V^*_{wz})_o = V(M-1-N_g - \frac{h^2}{12\mu_w} \frac{\sigma_{ow}}{V} \alpha_w^2) \tag{28}$$

The perturbation velocity of the oil finger in the region where water is flowing is obtained in a similar manner. The perturbation potential $(\phi^*_o)_w$ is obtained by introducing Equation 23 into Equation 17 and by substituting this final expression into Darcy's law to obtain

$$(V^*_{ox})_w = - \frac{1}{M} \frac{h^2}{12\mu_w} \sigma_{ow} \alpha_o^2 \frac{\partial(\eta_o)_w}{\partial x} \tag{29}$$

and

$$(V^{*}_{oz})_w = - \frac{V}{M} \left(M-1-N_g - \frac{h^2}{12\mu_w} \frac{\sigma_{ow}}{V} \alpha_o^2\right) \qquad (30)$$

The Darcy velocity of a finger can be obtained by adding the perturbation velocity in the z direction to the superficial velocity. If Equations 25 and 28 are compared with Equations 29 and 30, it is seen that the two sets of equations differ by a factor M, but apart from this difference they yield the same conditions for the growth of an oil finger into the water region and a water finger into the oil region. This also means that these two fingers will have different sizes, although their shapes will be similar.

4.4.2 UNSTEADY STATE VELOCITY

The unsteady state velocity is the velocity of the finger between the time at which it starts to form and the time after which it advances at a constant steady state velocity which was dealt with in the previous section. Therefore, the function f(t) must be known in order to evaluate how a finger begins to grow. The true functional form of both the functions f(t) and T(t) is not known, as the physics of how a finger starts to grow is not well understood. However, an inspection of Equation 28 (or 30)

and the experimental work of Lewis[3] suggests that the rate of penetration of a finger must approach a steady state value. Moreover, it is desirable that both the amplitude of the finger and its rate of growth be zero at t=0. These requirements can be met by choosing the functional form for T(t) as

$$T(t) = \frac{A}{\alpha} \ln\mathrm{Cosh}(\alpha a t) \tag{31}$$

In Appendix 1, it is shown that, if Equation 31 is given then the function f(t) is defined by

$$f(t) = \frac{\mathrm{Sech}^2(\alpha a t)}{\ln\mathrm{Cosh}(\alpha a t)} \tag{32}$$

Hence, the equation of the surface of the standing wave can be found by introducing Equation 31 into Equation 19 , to obtain

$$\eta(x,t) = \frac{A}{a} \text{Cos}(ax)\,\text{lnCosh}(aat) \tag{33}$$

In Equation 33, $\eta(x,t)$ gives the displacement of any point on the initially plane interface as a function of time. The velocity of each point on the interface can be found by differentiating Equation 33 with respect to time, t,

$$\frac{\partial \eta}{\partial t} = \text{AaCos}(ax)\,\text{Tanh}(aat) \tag{34}$$

Now, this velocity is integrated over the total base area for each type of finger to find the total flow rate, q, passing through the finger base (see Fig.2). The general expression for this total flow rate is given by

$$q = \frac{Aah}{a}\,\text{Tanh}(aat) \tag{35}$$

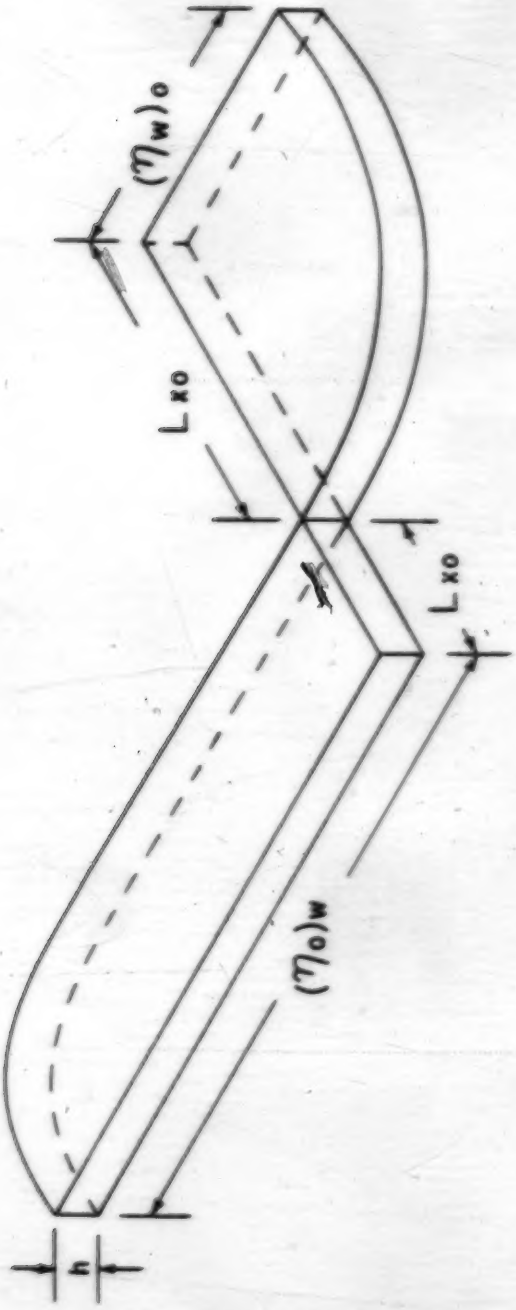

FIG.2 OPPOSITELY DIRECTED PAIR OF OIL AND WATER FINGERS

The average velocity of a finger in the z direction is found by dividing the total flow rate by the area of the base of the finger and by introducing Equation 20 into the resulting equation,

$$V_z = \frac{2Aa}{\pi} \text{Tanh}(\alpha a t) \tag{36}$$

The long time form of this average velocity should be equal to the steady state perturbation velocity, which is given by

$$V_z = \frac{2Aa}{\pi} \tag{37}$$

as the hyperbolic tangent approaches one for large values of its argument. If it is assumed that Equation 37 is equal to the steady state perturbation velocity, V_z, as defined by Equation 28 (or 30), it follows that

$$a = \frac{\pi V_z^*}{2A} \tag{38}$$

Finally, the expression for the finger surface is obtained by introducing Equation 38 into Equation 33

$$\eta(x,t) = \frac{A}{a} \cos(ax) \ln\cosh\left(\frac{\pi}{2} \frac{a}{A} V_z^* t\right) \tag{39}$$

4.5 COMPATIBILITY CONDITIONS

It is necessary to impose certain conditions on both the water and the oil fingers, if it is desired that the growth of two or more pairs of oppositely directed fingers be compatible. Thus, conditions of symmetry and similarity of fingers and continuity of the fluid contained in each type of finger are imposed on the solution.

4.5.1 SIMILARITY

The first condition to be imposed on the fingers is that an oil finger should be similar in shape to a water finger. Similarity can be guaranteed by demanding that the unsteady state velocity vectors for the oil fingers be colinear with the velocity vectors for the water fingers at equivalent locations on the surface of each finger. Thus, an oil finger will be similar in shape to a water finger, but the sizes will be different owing to the fact that these colinear velocity vectors have different magnitudes. The colinearity of the velocity vectors of oil and water fingers can be guaranteed by demanding that the initial accelerations of both fingers are equal at equivalent locations. The application of this condition yields the following relationship,

$$a_o^3 = M a_w^3 \qquad (40)$$

where by definition, $\lambda=2\pi/\alpha$; therefore,

$$\lambda_w = M^{1/3}\lambda_o \qquad (41)$$

Hence, the wavelength of a water finger is $M^{1/3}$ times that of an oil finger.

4.5.2 SYMMETRY

The instability conditions are equivalent for both types of fingers. As a consequence, the roots of the oppositely directed pairs of fingers must be located symmetrically within the straight interface which initially separated the two fluids. This condition can be fulfilled by requiring that the integral values of m for both the oil and the water fingers be the same. This condition implies that there will be as many oil fingers as there are water fingers, and that the total cross-sectional area of the bases of each set of fingers will be independent of the number of fingers (see Appendix 4).

4.5.3 CONTINUITY

The final compatibility condition is the material balance requirement. The volume of fluid contained in each type of finger is found by integrating the appropriate form

of Equation 39 over the base area of each type of finger (see Fig.2) to obtain

$$V_w = \frac{A_w h}{\alpha_w^2} \ln\text{Cosh} \left(\frac{\pi}{2} \alpha_w \frac{(V^*_{wz})_o}{A_w} t \right) \tag{42}$$

and

$$V_o = \frac{A_o h}{\alpha_o^2} \ln\text{Cosh} \left(\frac{\pi}{2} \alpha_o \frac{(V^*_{oz})_w}{A_o} t \right) \tag{43}$$

The volume of water contained in a water finger must be equal to the volume of oil contained in an oil finger at all times, if material balance requirements are to be met. Thus, Equation 42 is equated to Equation 43 and the following two equations are obtained,

$$\frac{A_w}{\alpha_w^2} = \frac{A_o}{\alpha_o^2} \tag{44}$$

and

$$\frac{\alpha_w}{A_w} (V^*_{wz})_o = \frac{\alpha_o}{A_o} (V^*_{oz})_w \tag{45}$$

These two equations can be combined to show that

$$\frac{(V^*_{wz})_o}{\alpha_w} = \frac{(V^*_{oz})_w}{\alpha_o} \tag{46}$$

The continuity requirement for the perturbation velocities in the x direction is obtained by substituting the appropriate form of Equation 33 into Equations 25 and 29. Therefore, at equivalent locations on each finger,

$$\frac{(V^*_{wx})_o}{(V^*_{ox})_w} = \frac{\alpha^2_w A_w}{(1/M)\alpha^2_o A_o} \tag{47}$$

Introducing Equations 40 and 44 into Equation 47 leads to, at equivalent locations on each finger,

$$\frac{(V^*_{wx})_o}{\alpha_w} = \frac{(V^*_{ox})_w}{\alpha_o} \tag{48}$$

Equations 46 and 48 guarantee that continuity is met.

4.6 CHARACTERISTIC EIGENVALUES

The eigenvalue at which the perturbation velocity is zero is termed the characteristic eigenvalue. Therefore, by setting the right hand side of Equation 28 (or 30) to zero, the square of the characteristic eigenvalue is found to be

$$\alpha_c^2 = \frac{12\mu_w V(M-1-N_g)}{h^2\sigma_{ow}} \tag{49}$$

The eigenvalue defined in this way is characteristic because it is the eigenvalue at which the viscous forces exactly balance the capillary and gravity forces. If the characteristics of the medium and the fluids are the same, a different characteristic eigenvalue is obtained for each different value of the superficial velocity. In particular, as the superficial velocity is increased there exists the

possibility of fingers being formed with smaller and smaller wavelengths, as the wavelength is inversely proportional to the eigenvalue. The question thus arises as to which of these wavelengths will dominate. For every finger wavelength there is a time constant, n, which determines how fast each wavelength will grow. From Equation 39, this time constant is

$$n = \frac{\pi}{2} \frac{\alpha}{A} V_z^* \tag{50}$$

The dominant finger is the one for which new surface is created at the maximum rate; i.e., it is the one for which the time constant as defined by Equation 50 is a maximum. To find the maximum time constant which corresponds to the dominant eigenvalue, α_m, the time constant, n, is differentiated with respect to the eigenvalue and set to zero' after introducing Equation 28 (or 30) into Equation 50. This results in

$$\alpha_m^2 = \frac{4\mu_w V(M-1-N_g)}{h^2 \sigma_{ow}} \tag{51}$$

Introduction of Equation 49 into Equation 51 leads to

$$\alpha_m^2 = \frac{1}{3}\alpha_c^2 \tag{52}$$

Therefore, the eigenvalue of the dominant finger occurs at one-third of the critical eigenvalue in terms of the squared eigenvalues. It should also be noted that the critical eigenvalue corresponds to zero growth rate for a finger; hence, it can also be obtained by equating Equation 50 to zero and solving for the eigenvalue.

4.7 VELOCITY OF PENETRATING FINGERS

Equations 28, 30, 40 and 46 represent a system of four equations with four unknowns which are $(V^*_{oz})_w$, $(V^*_{wz})_o$, α_o and α_w. By solving this system of equations, it may be shown that

$$(V^*_{wz})_o = \frac{M^{2/3}-1}{M^{4/3}+1}\,\frac{h^2}{12\mu_w}\,\sigma_{ow}\alpha_w^2 \tag{53}$$

where

$$\alpha_w^2 = \frac{V(M-1-N_g)\mu_w}{(h^2/12)\sigma_{ow}} \frac{M^{4/3}+1}{M^{2/3}(M^{2/3}+1)} \tag{54}$$

Equation 54 suggests that there is a unique wavelength corresponding to each superficial velocity of the displacement. The perturbation velocity in the z direction can be further simplified by introducing Equation 54 into Equation 53 which yields

$$(V^*_{wz})_o = \frac{V(M-1-N_g)}{M^{2/3}+1} \frac{M^{2/3}-1}{M^{2/3}} \tag{55}$$

Therefore, the perturbation velocity of a water finger is proportional to the superficial velocity and the constant of proportionality is a function of mobility ratio.

4.8 STABILITY CRITERION

If it is assumed that the Hele-Shaw cell is infinitely long and wide, then the viscous fingering of water into oil will be dictated only by the viscous, capillary and gravity forces. This is reflected in Equation 54, as each finger

wavelength is not a function of the dimensions of the system. But it is not possible to obtain all the wavelengths, in reality, for two reasons. First, as the displacement takes place within the confines of the Hele-Shaw cell, only those wavelengths smaller than a critical size can be observed. Second, Equation 18 is a linear partial differential equation. This suggests that a linear superposition of the harmonics should be possible. However, because of the way in which the parameters α and A (see Sec. 4.9) are defined, such a linear superposition of the individual harmonics is not possible. This problem may arise because the underlying process is non-linear. As a result, only those wavelengths corresponding to individual harmonics can propagate.

In order to determine the effect of the boundaries of the Hele-Shaw cell, α has to be defined in terms of the dimensions of the system. Before proceeding with the analysis, it is necessary to modify Equation 20 by deleting the (2m-1) term from it, i.e.

$$\alpha = \frac{\pi}{2L_x} \tag{56}$$

The effect of parameter m which was deleted from Equation 20 is reintroduced into the analysis through the symmetry condition which is imposed on the initially straight interface in which the roots of the oil and water fingers are embedded. This symmetry condition demands that

$$L_{xo} + L_{xw} = \frac{L_x}{m} \tag{57}$$

Introducing Equation 56 into Equation 57 yields

$$\frac{L_{xw}}{L_x} = \frac{1}{m} \left(\frac{\alpha_o}{\alpha_o+\alpha_w}\right) \tag{58}$$

Finally, combining Equation 58 with Equation 40 and introducing the result into Equation 57 leads to

$$\alpha_w^2 = \frac{\pi^2 m^2}{4} \frac{(M^{1/3}+1)^2}{M^{2/3}} \frac{1}{L_x^2} \tag{59}$$

Equation 59 expresses the wavelength as a function of the dimensions of the system. In order to find the marginal stability boundary, Equation 59 has to be used in conjunction with Equation 54. The instability can be observed only if the wavelength of the finger is small

enough to fit inside the Hele-Shaw cell. Therefore, the largest wavelength which can fit within the confines of the Hele-Shaw cell determines the onset of instability. This largest wavelength corresponds to the smallest eigenvalue and is obtained from Equation 59 by setting m=1 . Once the largest wavelength that can be formed within the Hele-Shaw cell is found, the superficial velocity associated with it can be found from Equation 54. Hence, the displacement will be stable provided that

$$I_{sr} = \frac{\mu_w V(M-1-N_g)}{h^2 \sigma_{ow}} \frac{(M^{4/3}+1)48L_x^2}{(M^{1/3}+1)^2(M^{2/3}+1)} \leq \pi^2 \qquad (60)$$

It should be noted that the instability number defined by Equation 60 is proportional to the one proposed by Peters and Flock'', the constant of proportionality being a function of mobility ratio. The function of mobility ratio enters the problem because proper account was taken of the fact that the widths of the water and oil fingers are different.

4.9 INITIAL CONDITION

The differential equation (Equation 18) which was postulated to describe finger growth is second order with respect to time. This results in two parameters in the time

part of the solution which was given as Equation 32. These two parameters are A and a. Parameter a was defined in Equation 39 but the second parameter is yet to be defined. Before defining A, it is useful to define a compatibility condition relating the value of A for an oil finger to that for a water finger. Upon inserting Equation 40 into Equation 44, one obtains

$$A_o = M^{2/3} A_w \tag{61}$$

Parameter A can be defined by imposing an initial condition on the solution as A depends upon the initial rate of acceleration of a water finger.

In order to impose the initial condition, it is necessary to look first at the unsteady state finger velocity. The average velocity of water passing through the base of a finger during the unsteady state period is given by Equation 36. If Equation 38 is substituted into Equation 36, it is seen that this average velocity is proportional to a function of time. Moreover, the constant of proportionality, V_z, is not an explicit function of m, as can be seen from Equation 55. Therefore, the constant of proportionality relating the average velocity of water passing through the base of a water finger to a function of

time is independent of the number of fingers propagating. This suggests that the final compatibility condition can be obtained by requiring that the constant of proportionality relating acceleration to a function of time should be independent of the number of fingers propagating. If the initial rate of acceleration is calculated by differentiating Equation 36 with respect to t and introducing Equation 38, it is seen that the constant of proportionality relating acceleration to a function of time has an m/A_w term in it. Therefore, choosing

$$A_w = c_2 m \tag{62}$$

makes the constant of proportionality independent of the number of fingers propagating. The constant of proportionality c_2 in Equation 62 cannot be estimated theoretically as it is not possible to give a theoretical estimation for A_w. This not a serious problem, however, as the characteristic behaviour of the displacement (such as time constant versus wavelength) may be obtained by choosing $c_2=1$. The actual value of c_2 can be obtained from the experimental data, as will be shown later.

5. EXPERIMENTAL APPARATUS AND PROCEDURE

5.1 DESCRIPTION OF THE EXPERIMENTAL APPARATUS

The experimental set-up consisted of two Hele-Shaw cells of different lengths joined by a dam which separated the two cells (see Fig. 3). An "O" ring, by phsically separating the water from the oil, prevented the fluids in the cells from coming into contact with each other. Each Hele-Shaw cell consisted of flat sheets of glass of approximately 10 mm thickness. The glass sheets were clamped together by an aluminum housing and separated by strips of teflon to provide the desired gap thickness of 1.016 mm. The lengths of the cells were 100 cm and 20 cm respectively, and they were both 20.32 cm wide. The inlet and outlet ends were connected to small reservoirs of water and oil respectively. These reservoirs had screens in them to disperse the incoming and outgoing fluids along the width of the cells, thus providing a uniform entrance for displacing fluid into the cell and a uniform discharge of displaced fluid from the cell. A Ruska Pump was used to obtain a constant injection rate of the desired magnitude over the range of 8.5 cc/hr to 560 cc/hr.

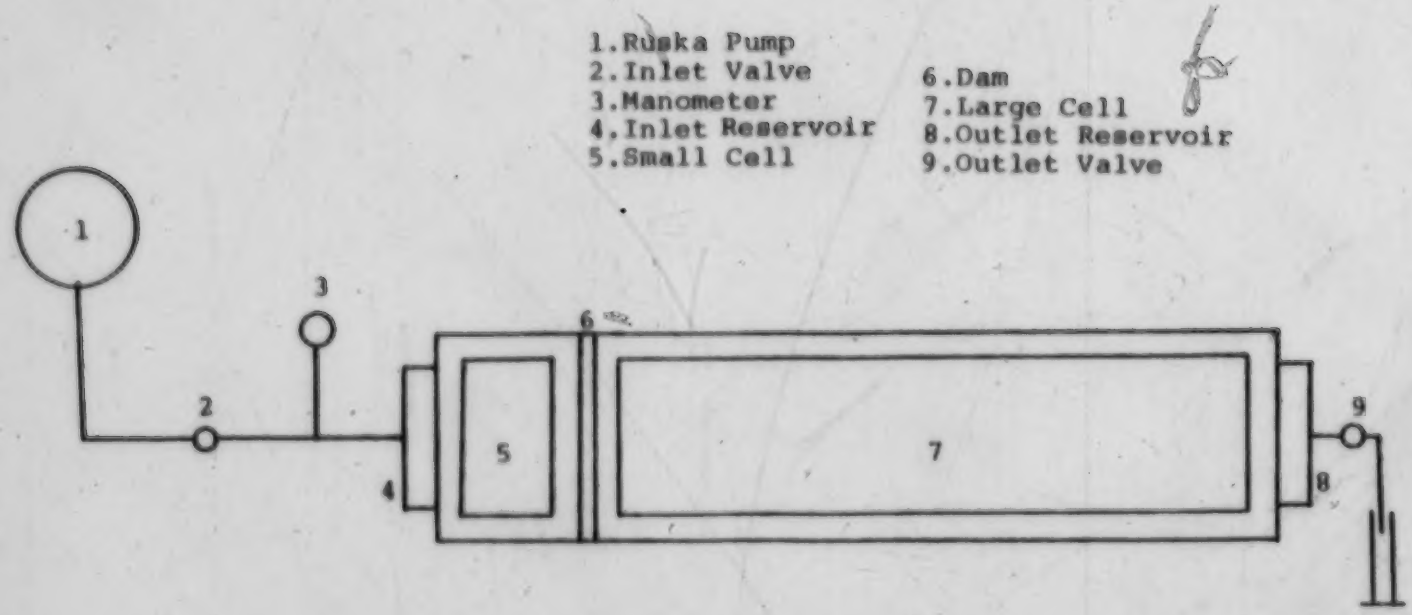

FIG.3 SCHEMATIC DRAWING OF EXPERIMENTAL APPARATUS

5.2 EXPERIMENTAL PROCEDURE

The first five experiments were carried out with a Hele-Shaw cell having a gap width of 0.5 mm and using refined oil and water as fluids; but very strong and irregular capillary effects, similar to the effects observed by Perkins and Johnston[21], were observed. Therefore, it was decided to carry out the experiments in the cell which had a gap width of 1.016 mm. It was observed that this increase in gap width eliminated the problems encountered in the cell with 0.5 mm gap width. This gap width is within the range used by various researchers[8,7,12,18,20] which varies between the values of 0.4 mm and 1.6 mm.

The glass surfaces were preferentially wet by water. The first 23 experiments were carried out under water-wet conditions. Then the wettability was changed from water-wet to oil-wet to improve the reproducibility of the experiments' after the 23rd experiment. The change in wettability was achieved by adding n-octylamine to the refined oil. An organic dye was also added to the oil in order to distinguish it visually from the water. The oils used were obtained from Imperial Oil Refinery in Edmonton and they were paraffinic base oils of different SAE grades. Oil was mixed with heptane to produce the desired range of viscosities for some of the experiments. The density, viscosity and the interfacial tension between the oils and the water is given in Table 1.

TABLE.1

PROPERTIES OF THE FLUIDS USED

FLUID	DENSITY (gm/cc)	VISCOSITY (cp)	σ_{ow} (dynes/cm)
Water	0.9978	1.00	-
MCT5	0.8594	30.40	25.2
MCT5+Heptane	0.8245	5.54	24.7
MCT5+Heptane+n-octylamine	0.8195	6.46	11.1
MCT5+LA60+n-octylamine	0.8510	11.46	14.8

The Hele-Shaw cell was tested for bulging under pressure by using a caliper which could measure changes within 0.025 mm. The cell did not change its separation thickness under the pressure developed by the maximum rate that was used in the experiments.

Before each run, both cells were cleaned using acetone. After assembling the cells with the dam in between, the small cell was filled with water and the large cell was

filled with oil. In the case of the oil-wet runs, the fluids were left in the cells overnight so that the glass surfaces would become oil-wet. The next step was to place the cell on a horizontal table and remove carefully the "O" ring separating the two fluids so that the interface separating the two fluids was not deformed. At this point, the initially straight interface, which is one of the assumptions in the theory, was obtained. The experiments started after opening inlet and outlet valves and turning on the Ruska Pump which was preset to the desired injection rate. The "O" ring groove in the dam provided the initial perturbations to the interface between the oil and the water. As the interface moved away from the dam into the large cell, a camera was used to record its movements on a videotape to be analyzed later. The rate of the Ruska Pump was also double checked by collecting liquid at the outlet for a certain time interval and calculating the flow rate independently. The Reynolds number for each experiment was well below one, indicating that the creeping flow assumption was met. The creeping flow assumption holds as long as the Reynolds number is much smaller than one. The thickness of the gap separating the two plates was used as the characteristic length in the defining equation for the Reynolds number ($= Vh\rho/\mu$) .

After each experiment, the experimental profiles were traced from the video monitor onto tracing paper; later, these profiles were transferred to a graph paper.

6. METHODS OF EXPERIMENTAL ANALYSIS

6.1 STABILITY BOUNDARY AND MODE BOUNDARIES

Although from the point of view of fluid mechanics there is a unique wavelength corresponding to each superficial velocity (see Equation 54), geometry dictates that only certain wavelengths will actually fit in the confines of a porous medium (see Equation 59). Hence, a superficial velocity above which a certain mode should be observed can be obtained by equating Equation 59 to Equation 54, setting m to the desired mode and solving for the superficial velocity, i.e.,

$$V = \frac{\pi^2 m^2}{4L_x^2} \frac{(h^2/12)\sigma_{ow}}{(M-1-N_g)\mu_w} \frac{(M^{1/3}+1)^2(M^{2/3}+1)}{M^{4/3}+1} \qquad (63)$$

The largest wavelength (m=1) that can fit in the porous medium will determine the stability boundary which was shown in Equation 60. Therefore, by setting m=1 in Equation 63, the superficial velocity, V_1, below which the displacement is stable, can be obtained. This also means that above V_1 the displacement will exhibit the first mode configuration; i.e., by setting m=1 the lower boundary of the first mode is obtained. The lower boundary of the second mode (upper boundary of the first mode) is obtained by setting m=2 in

Equation 63 and solving for the velocity V_2. The higher mode boundaries, V_3,V_4,etc. are calculated in the same manner by setting m=3,4,etc. in Equation 63.

6.2 RELATIVE FINGER WIDTHS

For any particular mode, the corresponding eigenvalue for a water finger can be calculated from Equation 59. The relationship between eigenvalue and wavelength is given by Equation 64 :

$$\lambda_i = \frac{2\pi}{\alpha_i} \; ; \; i = o,w \tag{64}$$

Once the wavelength for the water finger is calculated, the wavelength for the oil finger is obtained from Equation 41; Equation 64, in turn, gives the eigenvalue of the oil finger. Next, the relative widths of the oil and water fingers, L_{xo} and L_{xw}, are calculated by making use of the modified form of Equation 20, which is given by the following equation.

$$\alpha_i = \frac{\pi}{2L_{xi}} \; ; \; i = o,w \tag{65}$$

6.3 TIME CONSTANT VERSUS WAVELENGTH PLOT

For a specific mode, a superficial velocity V which corresponds to the lower boundary of the mode is given by Equation 63. Let us now consider an infinite system in which one fluid is displacing another with this superficial velocity V. The time constant is given by Equation 50; for a water finger this equation becomes

$$n_w = \frac{\pi}{2} \frac{a_w}{A_w} (V^*_{wz})_o \tag{66}$$

where the perturbation velocity for a water finger is given by Equation 28, and A_w is given by Equation 62. If c_2 is set equal to one, Equation 62 becomes

$$A_w = m \tag{67}$$

Insertion of Equations 27 and 67 into Equation 66 leads to

$$n_w = \frac{\pi}{2m} a_w V \left(M-1-N_g - \frac{h^2}{12\mu_w} \frac{\sigma_{ow}}{V} a_w^2\right) \tag{68}$$

Hence, Equation 68 enables the time constant, n_w , to be estimated for each wavelength, λ_w , for a fixed superficial velocity V. This relationship is continuous owing to the fact that the system under consideration is infinite in size. When the finite geometry of the system is considered, it is seen that only certain modes are possible, those whose wavelengths can be calculated from Equation 59.

When a certain mode is obtained in a porous medium, there is enough energy available to produce all the modes which are smaller than the observed mode. Therefore, although the n_w versus λ_w curve is continuous from the fluid mechanics point of view (infinite system) , the effect of the finite size of the system is to allow only those wavelengths smaller than some critical size. This also means that in actual experiments only certain wavelengths, those corresponding to the geometrically defined modes on the continuous curve, can be observed. Thus, the wavelengths corresponding to the smaller modes are calculated from Equation 59 and these wavelengths are used in Equation 68 to calculate the corresponding time factors on the continuous curve for the smaller modes.

6.4 DISTANCE TRAVELLED BY THE TIP OF THE FINGER VERSUS TIME

For each position of the interface that was traced from the video monitor, the imaginary stable interface was located on the graph; and the distances travelled by the tip of the oil and water fingers were measured with respect to

this imaginary stable interface. A plot of distance travelled by the tip of the finger versus time was then constructed for the run. In most of the plots, two definite trends were observed for each finger, therefore, a two-piece linear regression model was used to get two straight lines which fitted these trends. The first piece of the linear regression model was forced to go through the origin in accordance with the initially undisturbed interface. The ratio of viscous forces to capillary forces , that is the capillary number, N_c , indicated on these plots is derived in Appendix 3.

6.5 FINGER SURFACES

When Equation 39 is written for a specific type of finger, it becomes, for a water finger,

$$(\eta_w)_o = \frac{A_w}{\alpha_w} \cos(\alpha_w x) \ln\cosh\left(\frac{\pi}{2} \frac{\alpha_w}{A_w} (V^*_{wz})_o t\right) \qquad (69)$$

and, for an oil finger,

$$(\eta_o)_w = \frac{A_o}{\alpha_o} \cos(\alpha_o x) \ln\cosh\left(\frac{\pi}{2} \frac{\alpha_o}{A_o} (V^*_{oz})_w t\right) \qquad (70)$$

In these equations α_w and α_o are calculated from Equations 59 and 40, respectively. Moreover, the perturbation velocities for water and oil are calculated from Equations 55 and 48 respectively. At this point, the only parameter remaining to be defined is the constant c_2. This constant may be estimated by making use of the experimental value of the distance travelled by the tip of the water finger, i.e. the maximum distance travelled by the water finger, $(\eta_w)_{omax}$, in the following manner : When $(\eta_w)_o = (\eta_w)_{omax}$ then $\cos\alpha_w x=1$. Therefore, from Equation 69,

$$(\eta_w)_{omax} = \frac{mc_2}{\alpha_w} \ln\cosh\left(\frac{\pi}{2} \frac{\alpha_w}{mc_2} (V^*_{wz})_o t\right) \qquad (71)$$

Now, in this equation, the only unknown is c_2, which can be calculated by trial and error. Once this is done, Equations 69 and 70 can be utilized to define the surfaces of the water and oil fingers between the intervals $(0,L_{xo})$ and $(0,L_{xw})$ respectively.

A computer programme has been written to calculate the surfaces of the water and oil fingers at each time for a single run. Except for the first mode (see Fig. 2), the sum of the half-widths of the oil and water fingers, $L_{xo}+L_{xw}$, does not add up to the width of the Hele-Shaw cell, L_x. This means that when one-half of an oil finger is placed next to

one-half of a water finger, these fingers will not occupy the whole width of the Hele-Shaw cell unless they are in the first mode. Therefore, after calculating the finger surfaces between $(0,L_{xo})$ and $(0,L_{xw})$, the programme arranges the surface data so that the oil and water fingers are placed one after the other to fill the entire width of the Hele-Shaw cell for the given mode when the mode number is larger than one.

In order to compare the finger surfaces which are experimentally obtained with the ones that are theoretically calculated, the experimental profiles were digitized using a calcomp digitizer. Next, the calculated profiles were superimposed on the digitized ones for comparison purposes. When the interface obtained from the experiments was plotted, it was found that the interface had to travel far enough from the dam so that the inlet end effects (uneven perturbation) would disappear in order that the expected mode could be observed. This is why all these plots start at times larger than zero.

7. RESULTS AND DISCUSSION

The results of the sixty-three Hele-Shaw cell experiments carried out are summarized in Table 2. The first five runs are not listed in the table because of experimental problems brought about by the very strong capillary effects due to small plate separation (0.5 mm). All the runs listed were carried out within a Hele-Shaw cell which had a plate separation of 1.016 mm. All the experiments were carried out horizontally, except Runs 59, 61, 62 and 63, which were carried out at $\Theta = 86.2°$. In Table 2, a dash shows that something went wrong with the experiment; a question mark shows that the interface could not be classified as being in a certain mode or that the mode observed was the closest to the one shown. Arrows indicate the manner in which the experimental mode changed within the time span of the experiment. The calculation of the upper and lower mode boundaries for any given mode was explained in Section 6.1. The superficial velocity presented in Column 3 was in between the upper and the lower values dictated by the maximum theoretical mode shown in Column 4. A time constant versus wavelength plot for each pair of fluids at each mode was calculated as described in Section 6.3. These plots are shown in Figures 4, 5, 6 and 7. In these plots, each individual curve is marked with different symbols. The number of points on each curve indicates the maximum mode which corresponds to that curve, e.g. as the uppermost curve in Fig.4 has four points, it corresponds to

TABLE.2

SUMMARY OF THE EXPERIMENTS

No.	M	VELOCITY (cm/min)	THEORETICAL MODE		EXPERIMENTAL MODE
			Max.	Most Probable	
6	5.54	3.229	2	1	2(?)→1
7	5.54	3.229	2	1	2→1
8	5.54	0.484		Stable	Stable
9	5.54	0.645	1	1	1
10	5.54	1.130	1	1	1
11	5.54	0.969	1	1	1
12	5.54	5.166	3	2	–
13	5.54	5.166	3	2	3→2
14	5.54	3.938	2	1	2→1
15	5.54	3.938	2	1	2→1
16	5.54	3.845	2	1	?→1→2
17	5.54	6.458	3	2	4→1
18	5.54	6.458	3	2	4→?
19	5.54	3.938	2	1	3→2→1
20	5.54	6.458	3	2	4→1
21	5.54	6.458	3	2	4→1
22	5.54	5.166	3	2	3→2
57	5.54	0.323		Stable	Stable

TABLE.2 (Continued)

SUMMARY OF THE EXPERIMENTS

No.	M	VELOCITY (cm/min)	THEORETICAL MODE		EXPERIMENTAL MODE
			Max.	Most Probable	
23	6.46	0.282	1	1	1
24	6.46	0.282	1	1	–
25	6.46	0.657	1	1	2→1
26	6.46	0.738	2	1	2→1
27	6.46	1.058	2	1	2→1
28	6.46	1.058	2	1	2→?
29	6.46	1.937	3	2	3→1
30	6.46	2.583	3	2	3→1
31	6.46	3.229	4	3,2	4→2→1
32	6.46	3.875	4	3,2	4→2→1
33	6.46	4.521	5	3,4,2	4→2
34	6.46	3.798	4	3,2	?→2→1
35	6.46	4.230	4	3,2	4→3→2(?)
36	6.46	4.876	5	3,4,2	4,5→1→2(?)
37	6.46	4.876	5	3,4,2	5→2
38	6.46	4.876	5	3,4,2	4,5→3→1

TABLE.2 (Continued)

SUMMARY OF THE EXPERIMENTS

No.	M	VELOCITY (cm/min)	THEORETICAL MODE		EXPERIMENTAL MODE
			Max.	Most Probable	
39	6.46	4.876	5	3,4,2	4→3→1
40	6.46	4.876	5	3,4,2	–
41	6.46	4.876	5	3,4	–
58	6.46	0.100		Stable	Stable
42	11.46	0.222	1	1	1
43	11.46	0.178	1	1	?
44	11.46	0.844	2	1	1→2→1(?)
45	11.46	1.012	3	2,1	?→2
46	11.46	1.558	3	2,1	3(?)
47	11.46	1.493	3	2,1	3(?)→2
48	11.46	1.937	4	3,2	4→1
49	11.46	1.937	4	3,2	4→3→1
50	11.46	2.583	4	3,2	4,3→2→3
51	11.46	3.229	5	3,4,2	4→2
52	11.46	3.229	5	3,4,2	4→2
53	11.46	3.229	5	3,4,2	5→2
54	11.46	3.229	5	3,4,2	?→4(?)

TABLE.2 (Continued)

SUMMARY OF THE EXPERIMENTS

No.	M	VELOCITY (cm/min)	THEORETICAL MODE		EXPERIMENTAL MODE
			Max.	Most Probable	
55	30.40	0.040		Stable	?
56	30.40	0.071	1	1	1(?)
59	30.40	9.090	12	5–9	5,7→4→3→1
60	30.40	6.458	11	5–9	5,4→2→1
61	30.40	1.130		Stable	?
62	30.40	1.130		Stable	Stable
63	30.40	1.937	6	4,3	6,4→3→1

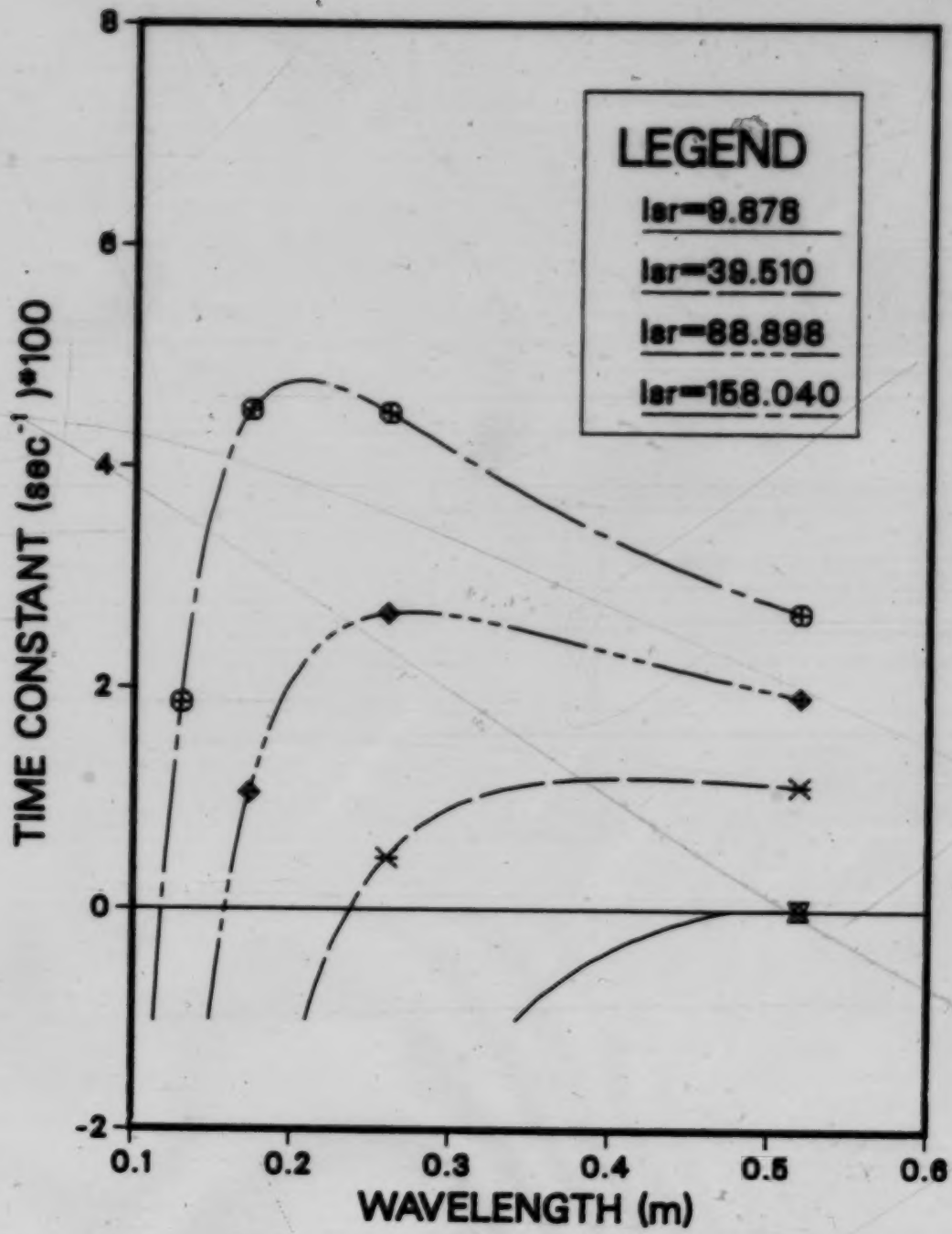

FIG.4 TIME CONSTANT VS. WAVELENGTH PLOT FOR MCT-5+HEPTANE AND WATER

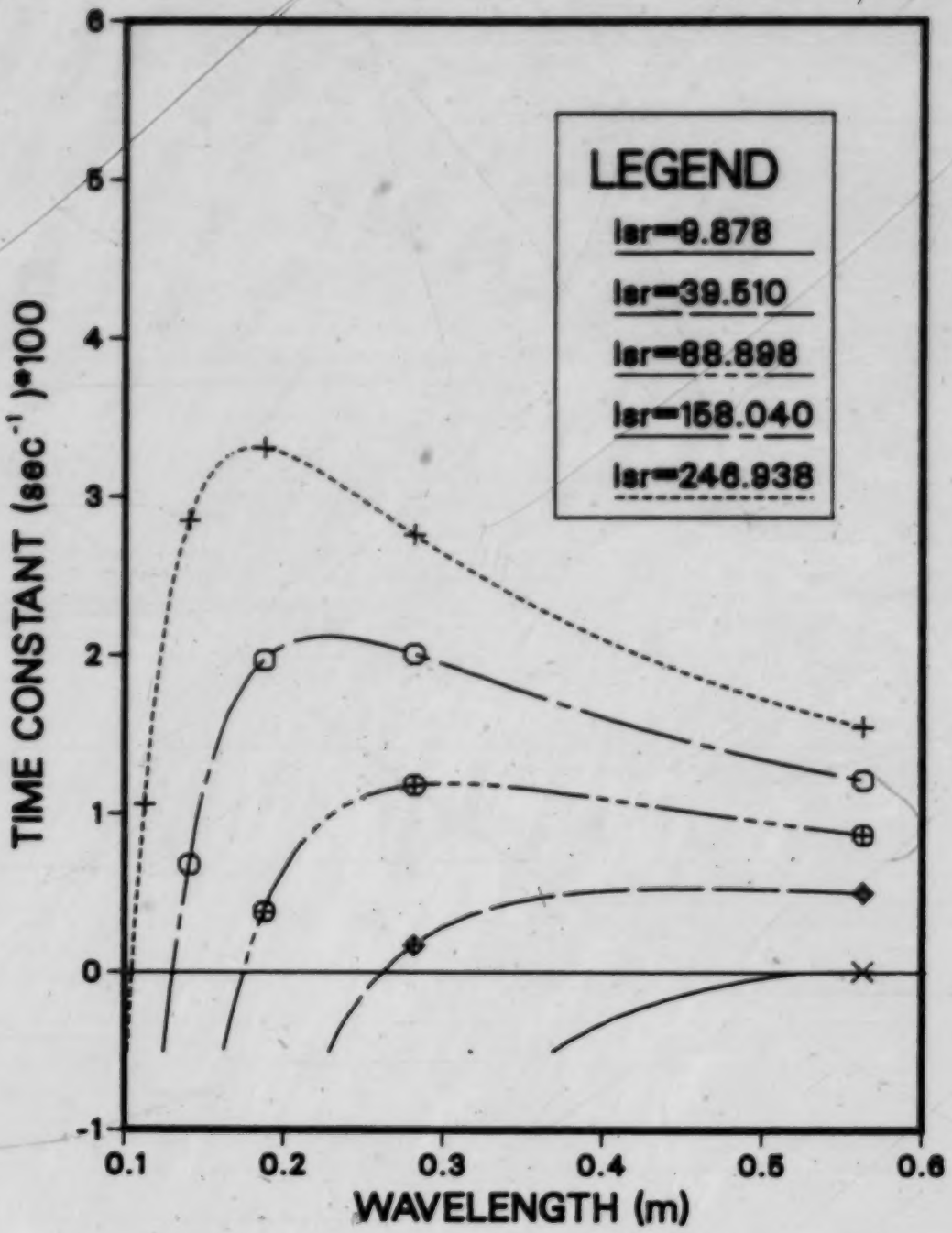

FIG.5 TIME CONSTANT VS. WAVELENGTH PLOT FOR MCT-5+LA60+OCTYLAMINE AND WATER

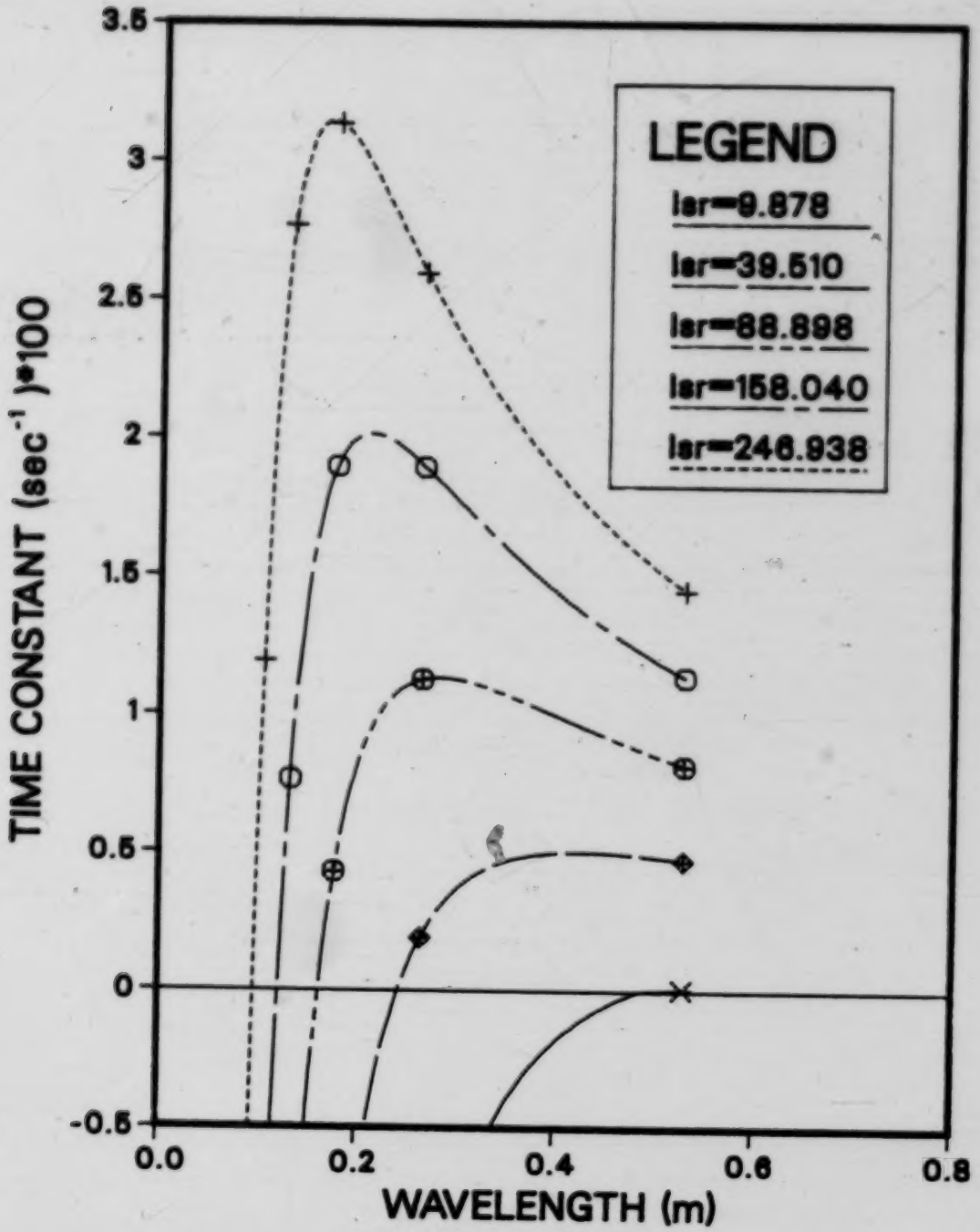

FIG.6 TIME CONSTANT VS. WAVELENGTH PLOT FOR MCT-5+HEPTANE+OCTYLAMINE AND WATER

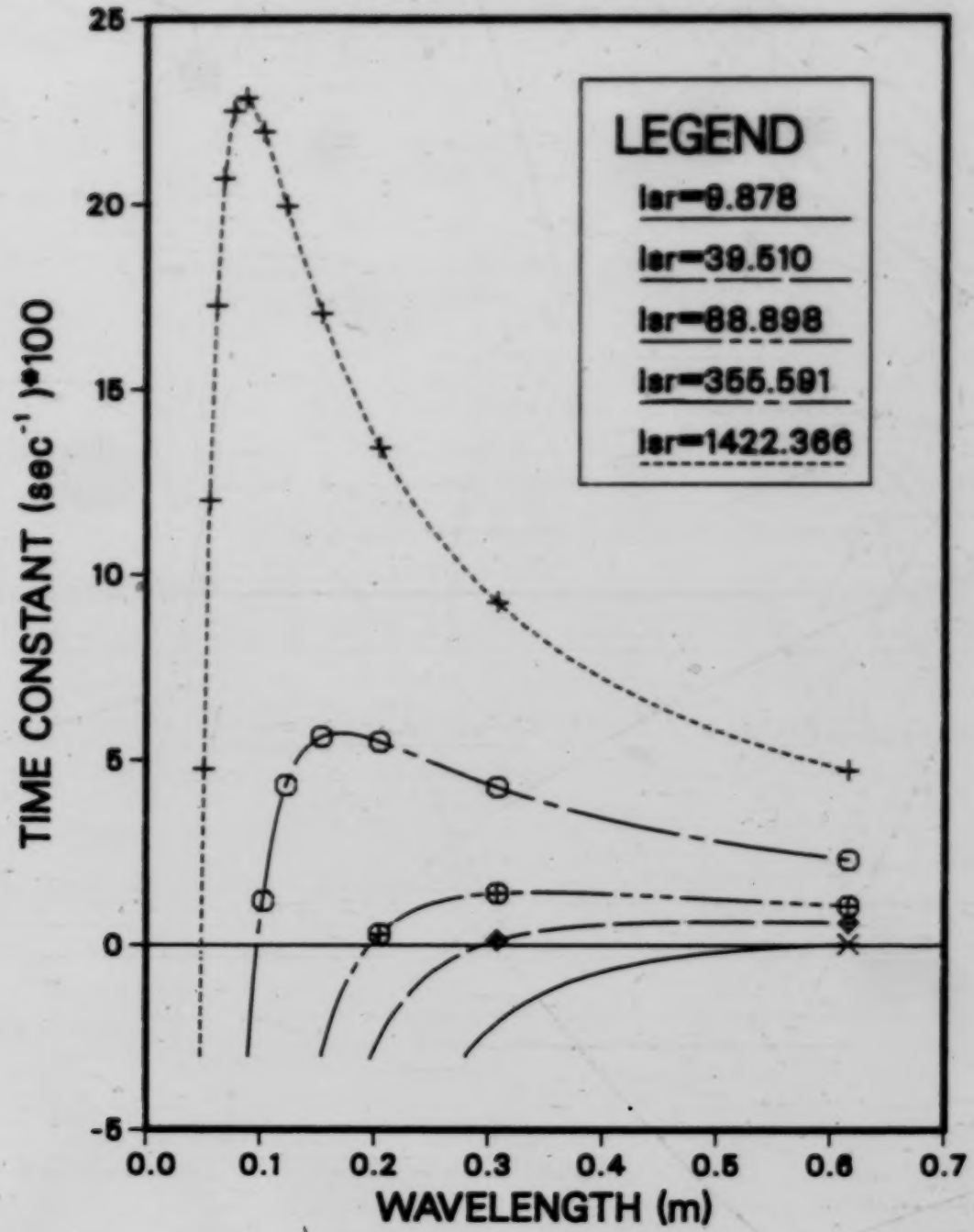

FIG.7 TIME CONSTANT VS. WAVELENGTH PLOT FOR MCT-5 AND WATER

fourth mode. The point on the extreme right corresponds to the first mode, while the point on the extreme left corresponds to the fourth mode on this curve. For a particular maximum mode, the most probable mode is the one which has the maximum time constant. The most probable modes are shown in Table 2 for each run; if the time constants of several modes are very close to each other, these modes appear as the most probable modes in Column 5. For example, Experiments 48, 49, 50 in Table 2 indicate that, for a maximum mode of 4, most probable modes are 3 and 2. This is because modes 3 and 2 are both very close to the maximum on the time constant versus wavelength curve for mode 4 (second curve from the top) in Fig. 5 .

The theory predicted the stability boundary correctly for all the fluid pairs considered except in the case of the MCT5-Water system (M=30.4) which had a very low stability boundary under horizontal flow conditions. Below this boundary, selective entry effects, which have also been reported in the literature[2] for similar flow conditions, were observed. The capillary forces were so dominant at these low rates that the effects of heterogeneities (in wettability, dust particles on the glass surfaces) overrode the stable shape of the front which was expected. But, when the system was tilted, which increased the stability boundary by an order of magnitude, the stability boundary was correctly predicted again. Similarly, the stability boundary for horizontal flow of the MCT5+LA60-Water system

(M=11.46) was too low to be checked.

It was seen in Section 6.1 that there is a range of velocities over which a certain mode can be obtained. In the plots of time constant versus wavelength (Figs. 4, 5, 6, 7), it can be observed that, for any curve, the most probable mode is a smaller mode than the maximum mode for which that particular curve was plotted. Therefore, at a certain stability number, the displacement should start at the maximum possible mode as there is enough energy to drive the interface at the corresponding wavelength; but the mode which has the largest time constant (the most unstable mode or the most probable mode) should emerge as the dominant mode over time. Thus, in order to analyze the mode boundaries subsequent to the stability boundary, it is necessary to look at the data presented in Table 2 in conjunction with the time constant versus wavelength behaviour associated with the superficial velocity of the experiment.

At low values of the instability number, Isr, the plot of time constant versus wavelength possesses a very broad maximum (see Figs. 4, 5, 6, 7) and as a consequence there is usually more than one mode which has a time constant close to the maximum. At the higher stability numbers, even though the maximum gets sharper, there are still a number of modes which have time constants close to the maximum value. This means that, in an experiment, any one of these modes could dominate, which was observed to be the case.

The procedure described in Section 6.5 was undertaken so that the plots of the experimentally obtained profiles could be superimposed on the theoretically calculated ones. Figures 8, 9, 10, 11, 12, 13 show this plot for a first mode; Figures 14, 15, 16 show the profiles for a second mode and Figures 17, 18, 19, 20, 21, 22 show the profiles for a third mode. Some additional plots can be found in Appendix 5 for Runs 31, 33, 34, 42 and 50.

The theory assumes that the porous medium under consideration is a part of an infinite system; that is, it does not consider any boundary effects. Under laboratory conditions, however, the boundaries have an effect on the shape of the interface due to the no-slip condition which is present at the sidewalls. Therefore, the interface tends to be distorted at the sidewalls because of the drag. Small distortions are present in all the plots of the interface in Figures 8 to 22 and 29 to 58. This effect can best be observed in Figures 29 to 32, 42 to 48 and 51 to 58 in Appendix 5.

It was assumed, while developing the theory, that the roots of the fingers remain fixed on the initially straight interface. However, it was found that this was not the case when the fingers were developing, i.e. early in the experiment (see Figs. 17, 18, 38, 42, 43, 44) and when the experimental mode changed (see Figs. 8, 9, 10, 22, 29, 30, 41, 51, 52, 53).

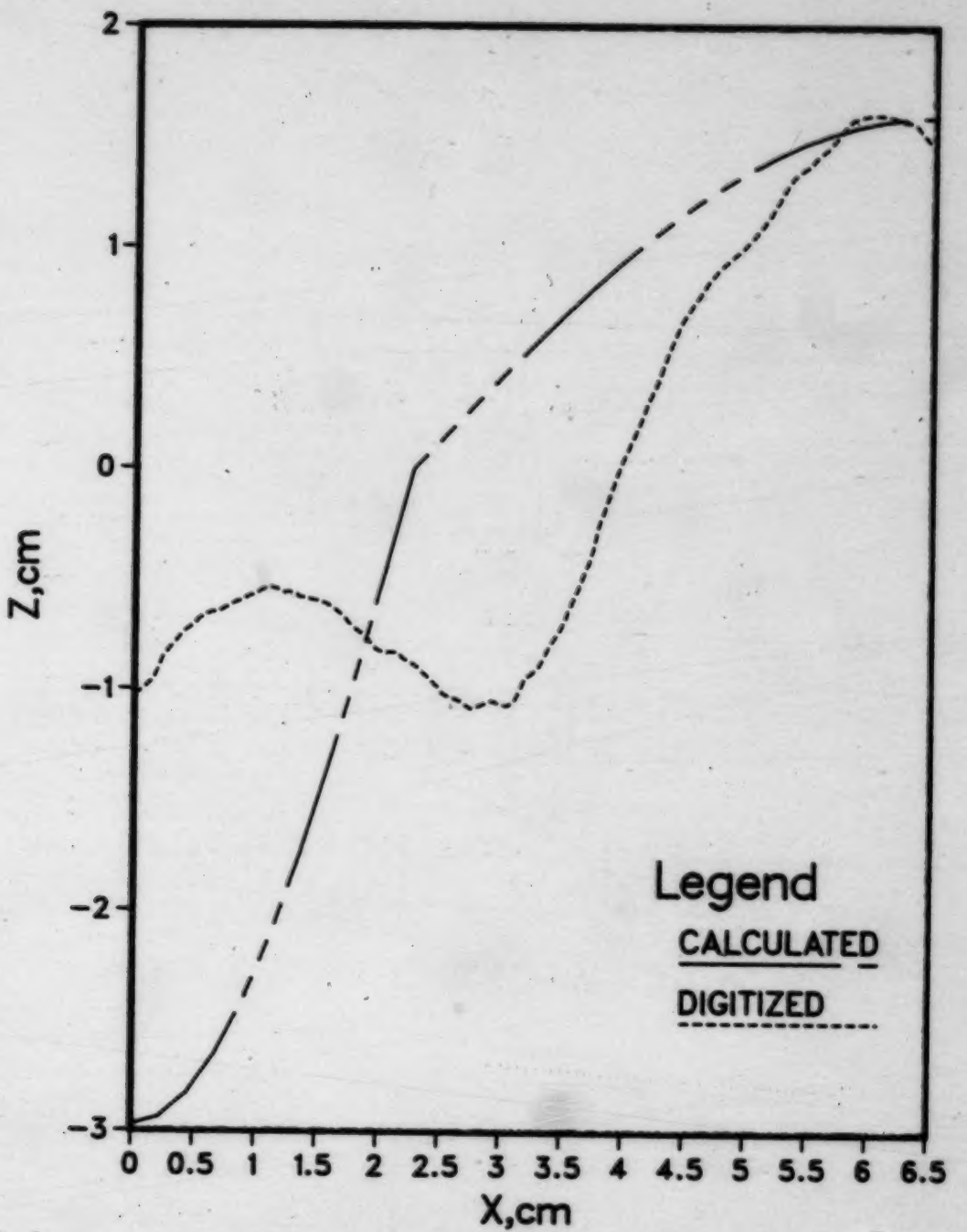

FIG.8 THE INTERFACE AT T=1424 SEC. FOR RUN 27

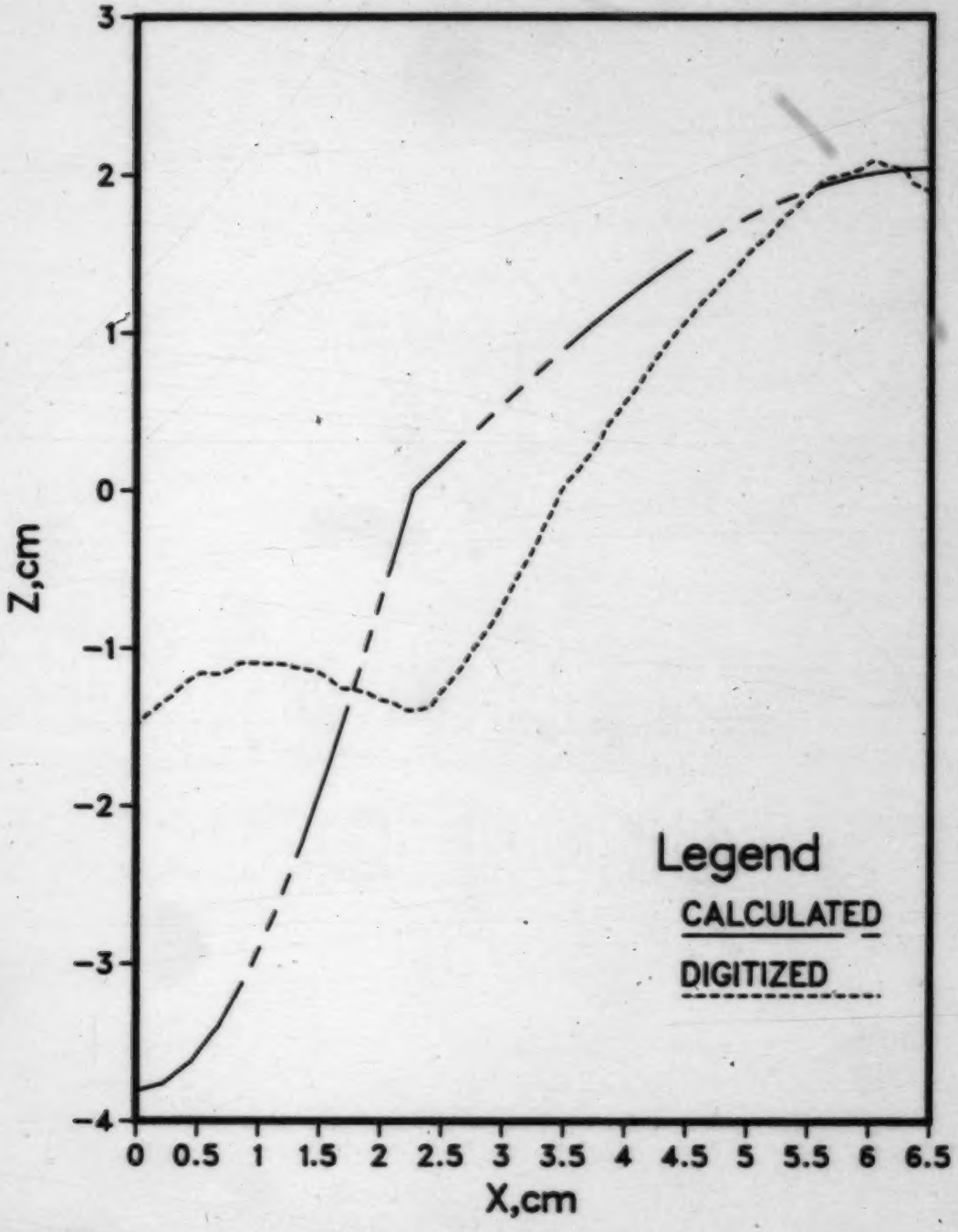

FIG.9 THE INTERFACE AT T=1858 SEC. FOR RUN 27

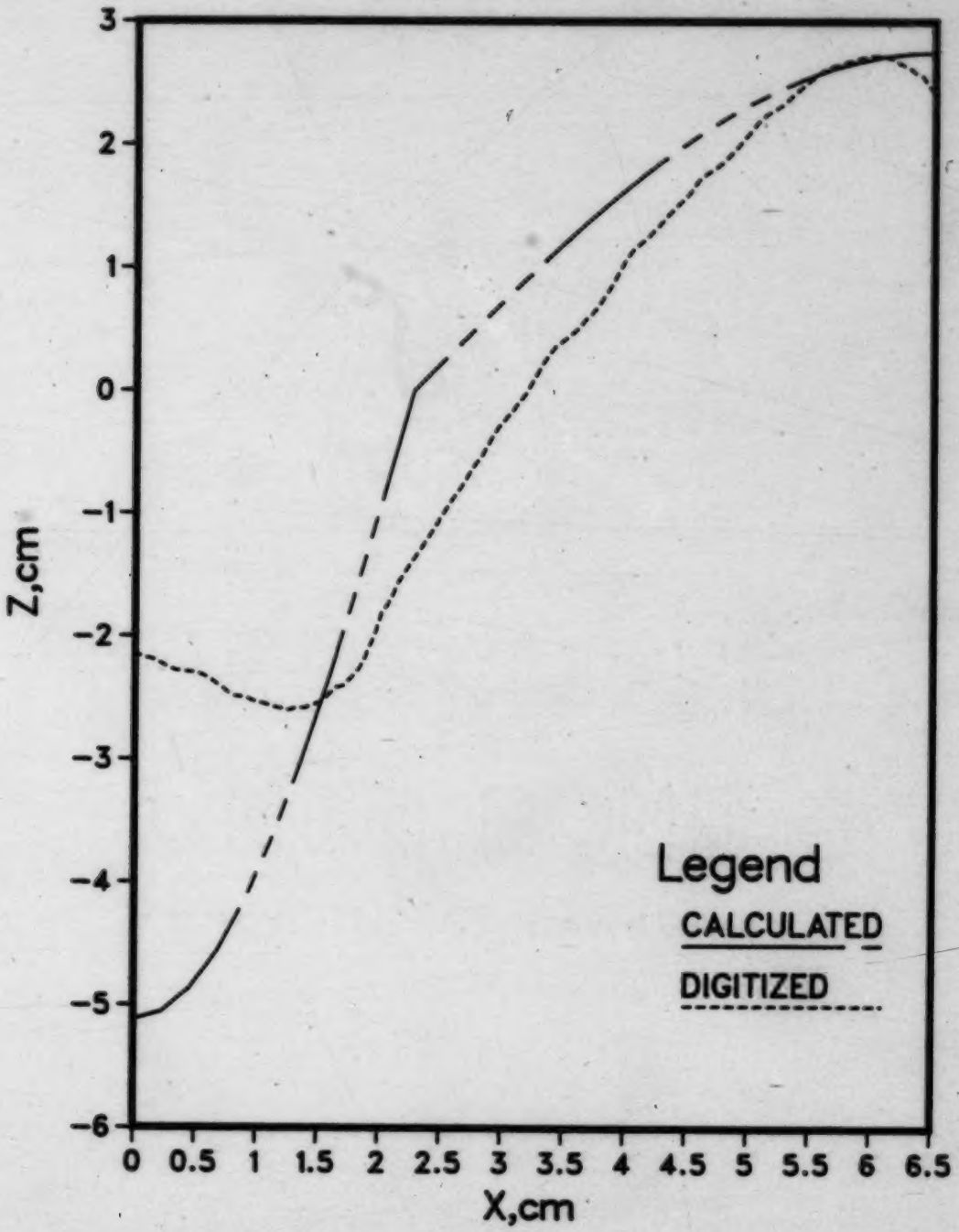

FIG.10 THE INTERFACE AT T=2718 SEC. FOR RUN 27

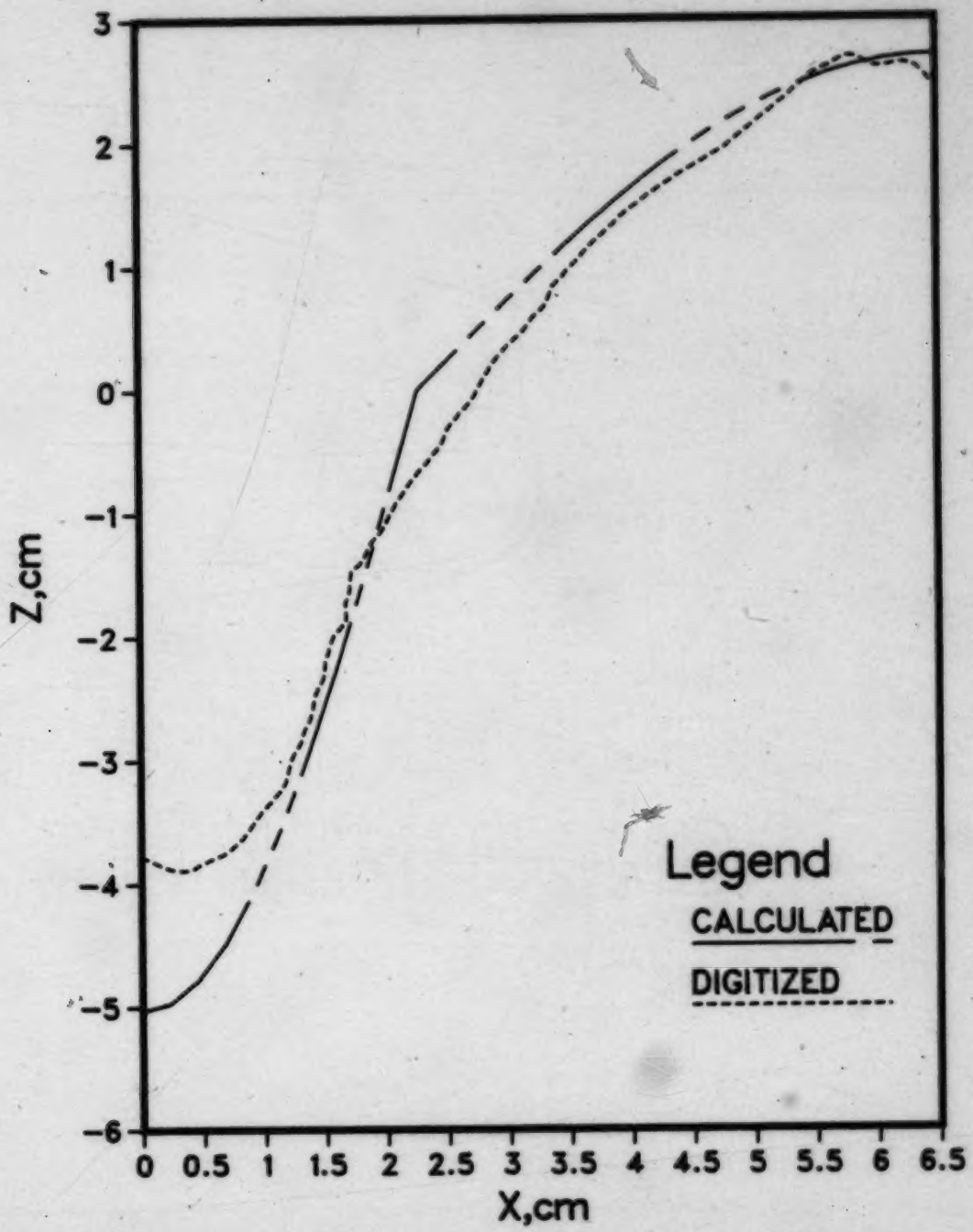

FIG.11 THE INTERFACE AT T=3330 SEC. FOR RUN 27

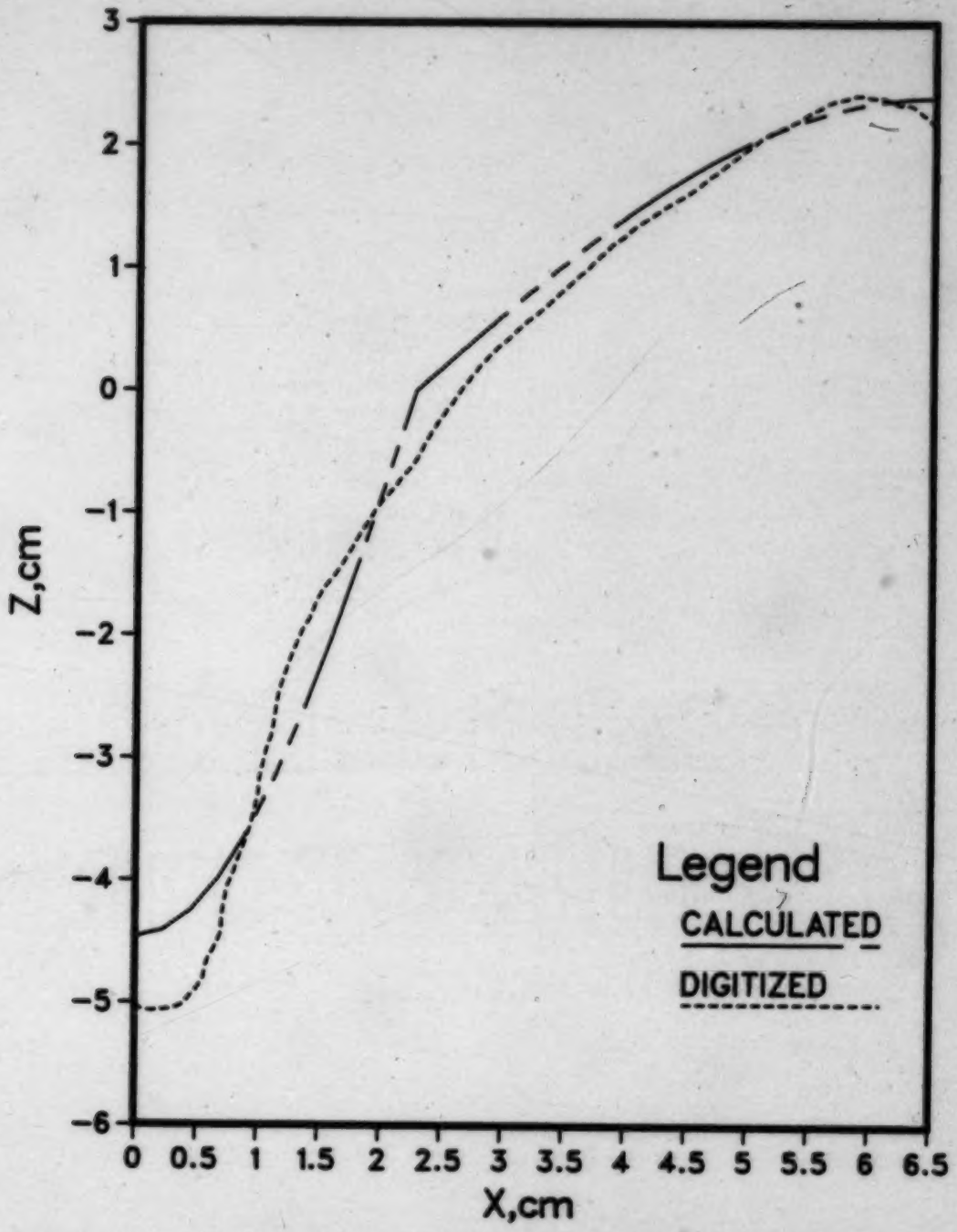

FIG.12 THE INTERFACE AT T=3685 SEC. FOR RUN 27

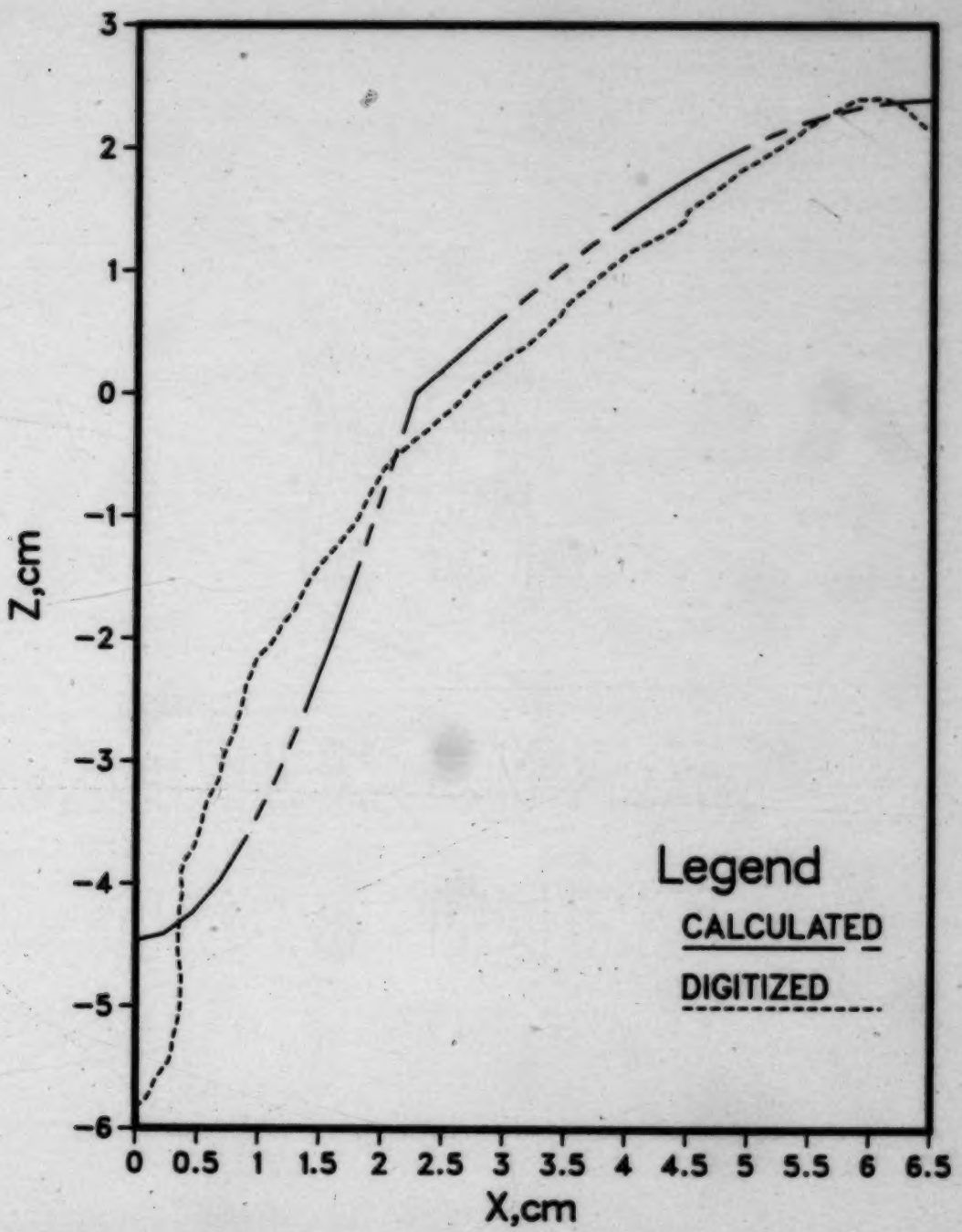

FIG.13 THE INTERFACE AT T=3968 SEC. FOR RUN 27

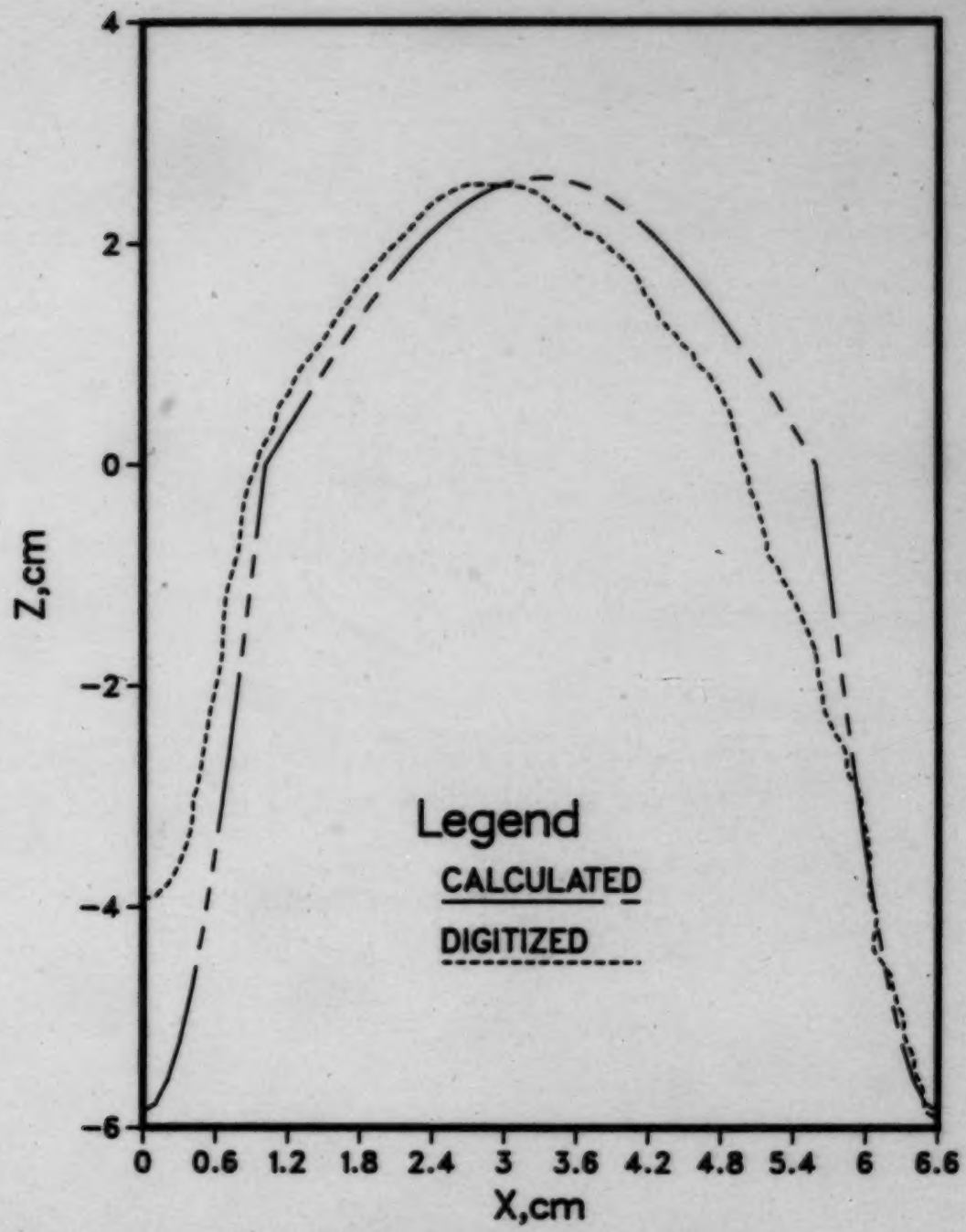

FIG.14 THE INTERFACE AT T=889 SEC. FOR RUN 61

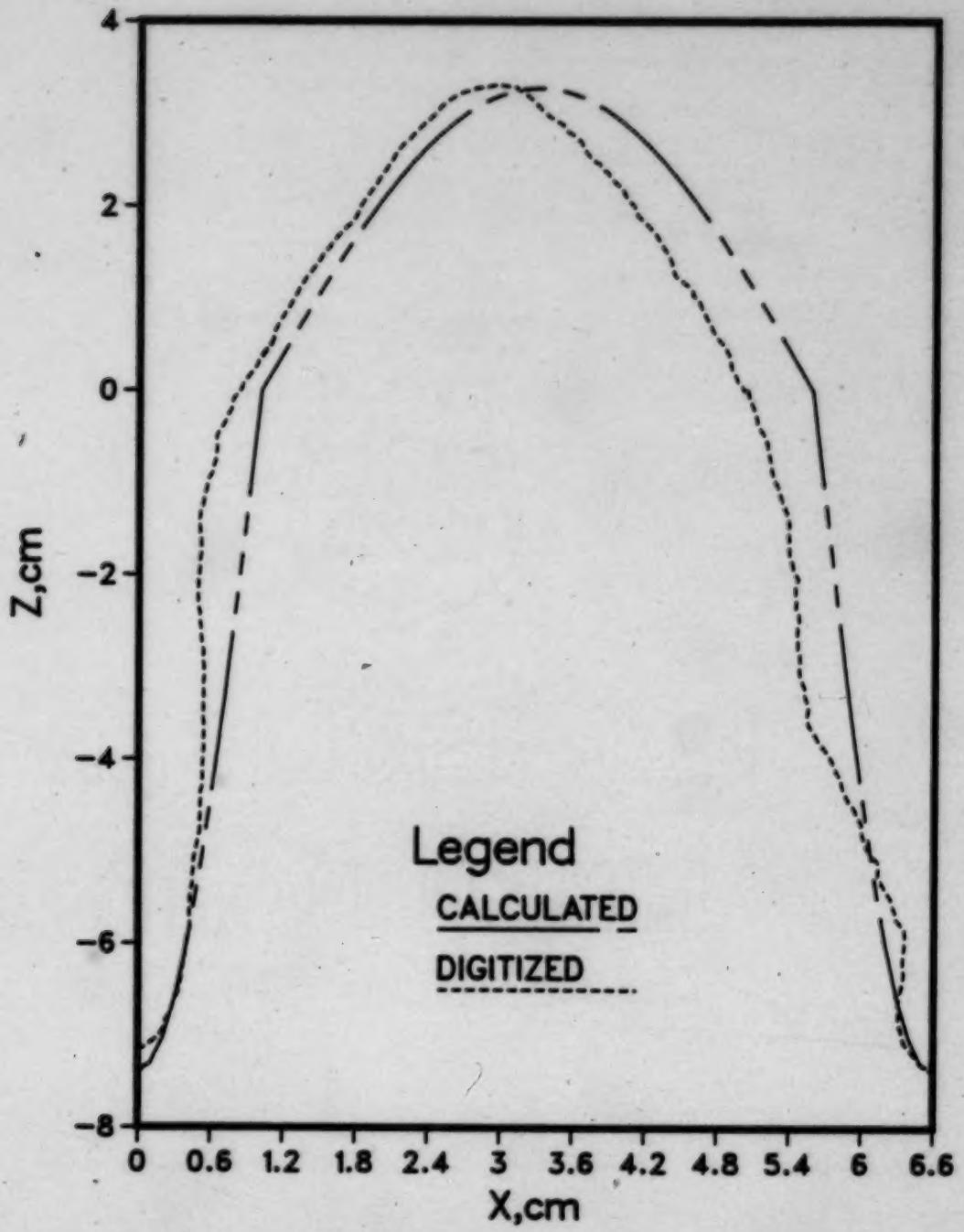

FIG.15 THE INTERFACE AT T=1092 SEC. FOR RUN 51

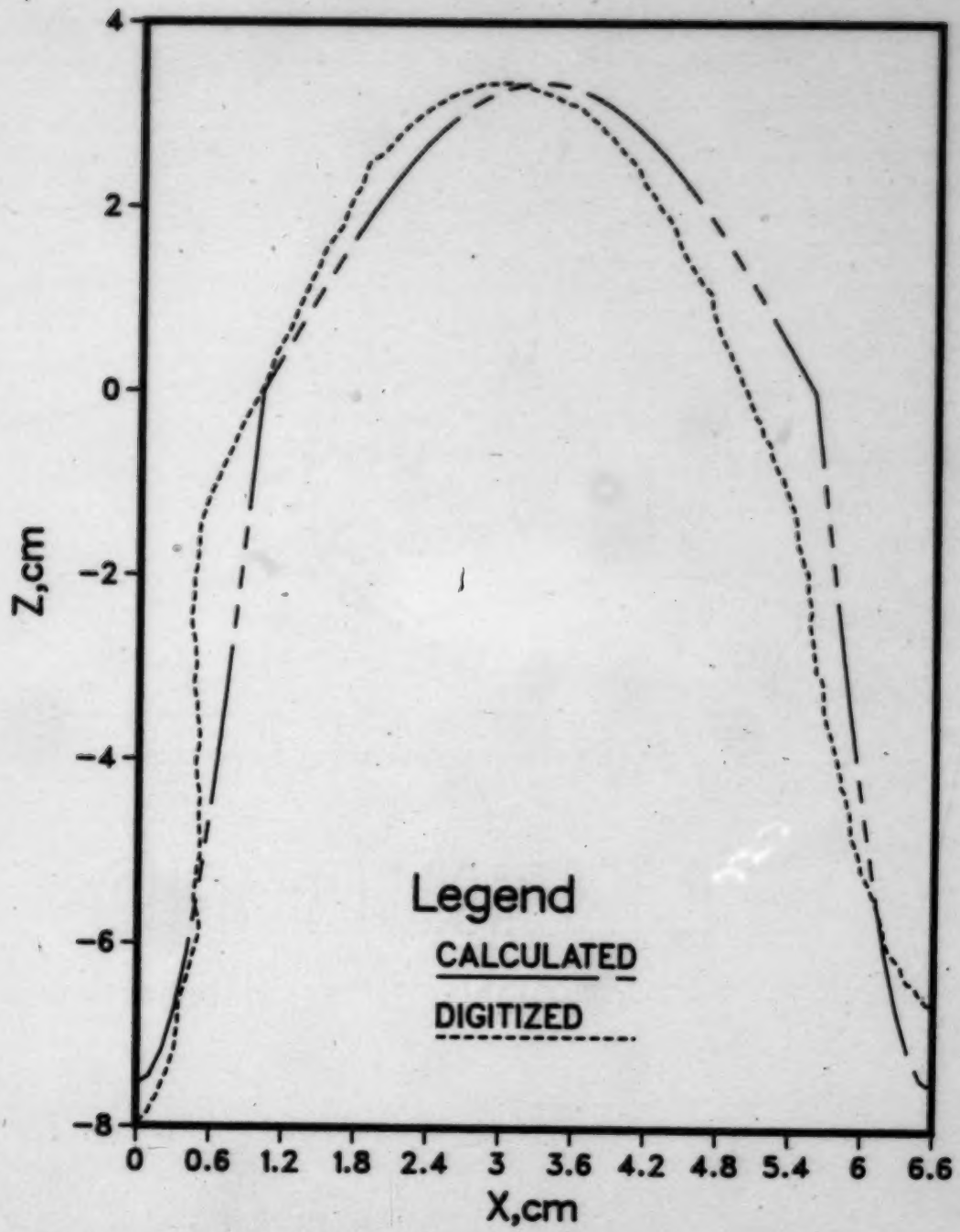

FIG.16 THE INTERFACE AT T=1132 SEC. FOR RUN 51

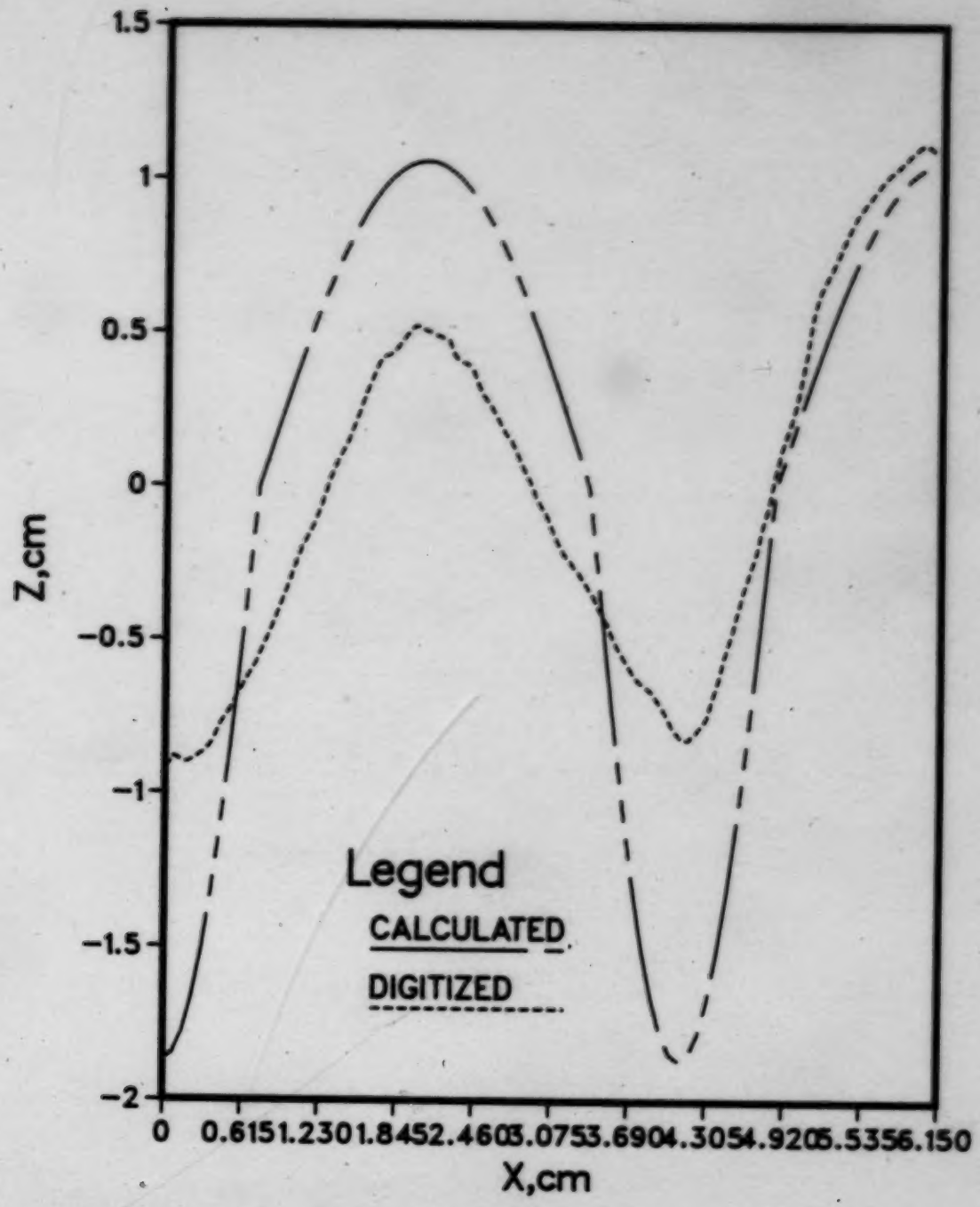

FIG.17 THE INTERFACE AT T=221 SEC. FOR RUN 13

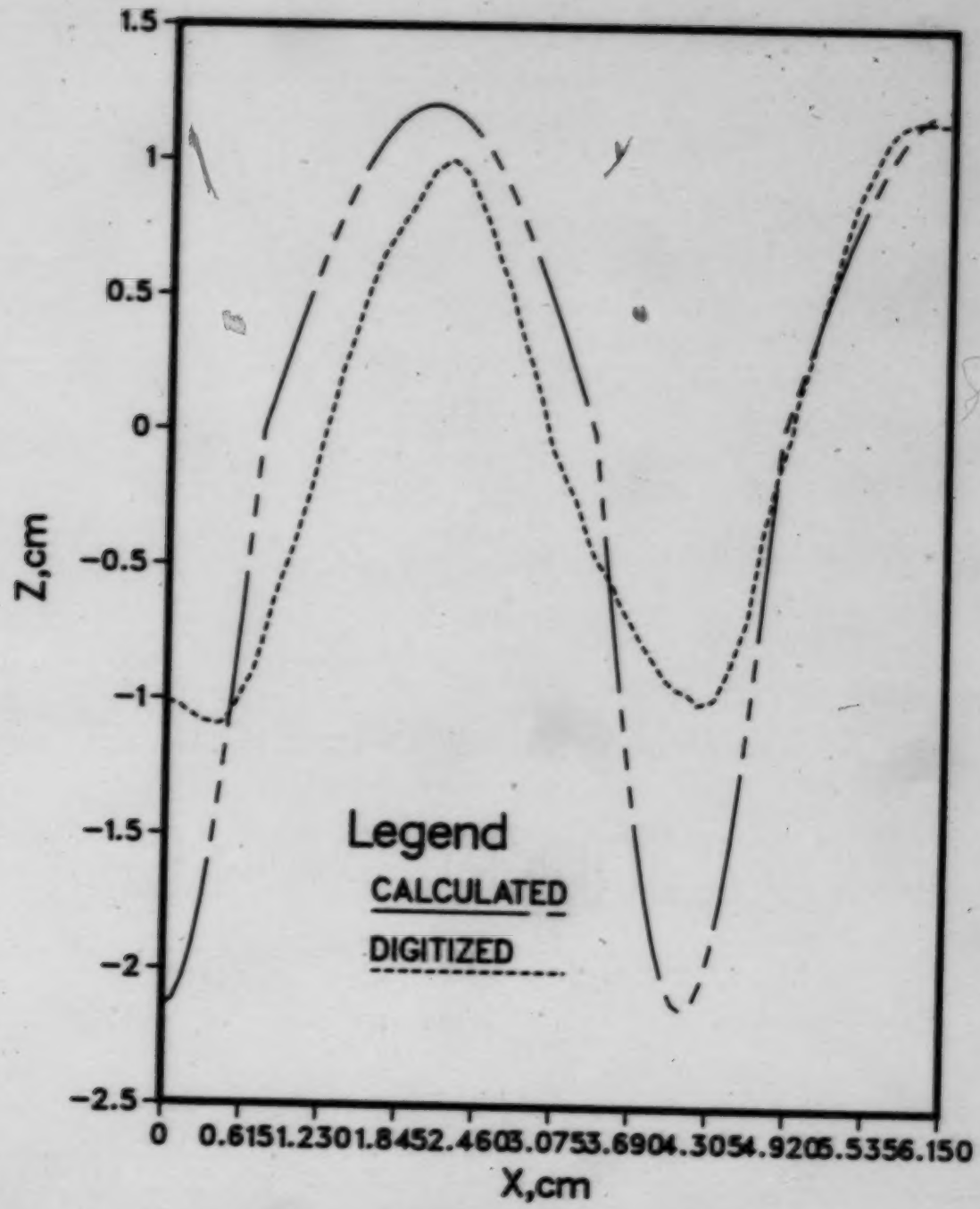

FIG.18 THE INTERFACE AT T=251 SEC. FOR RUN 13

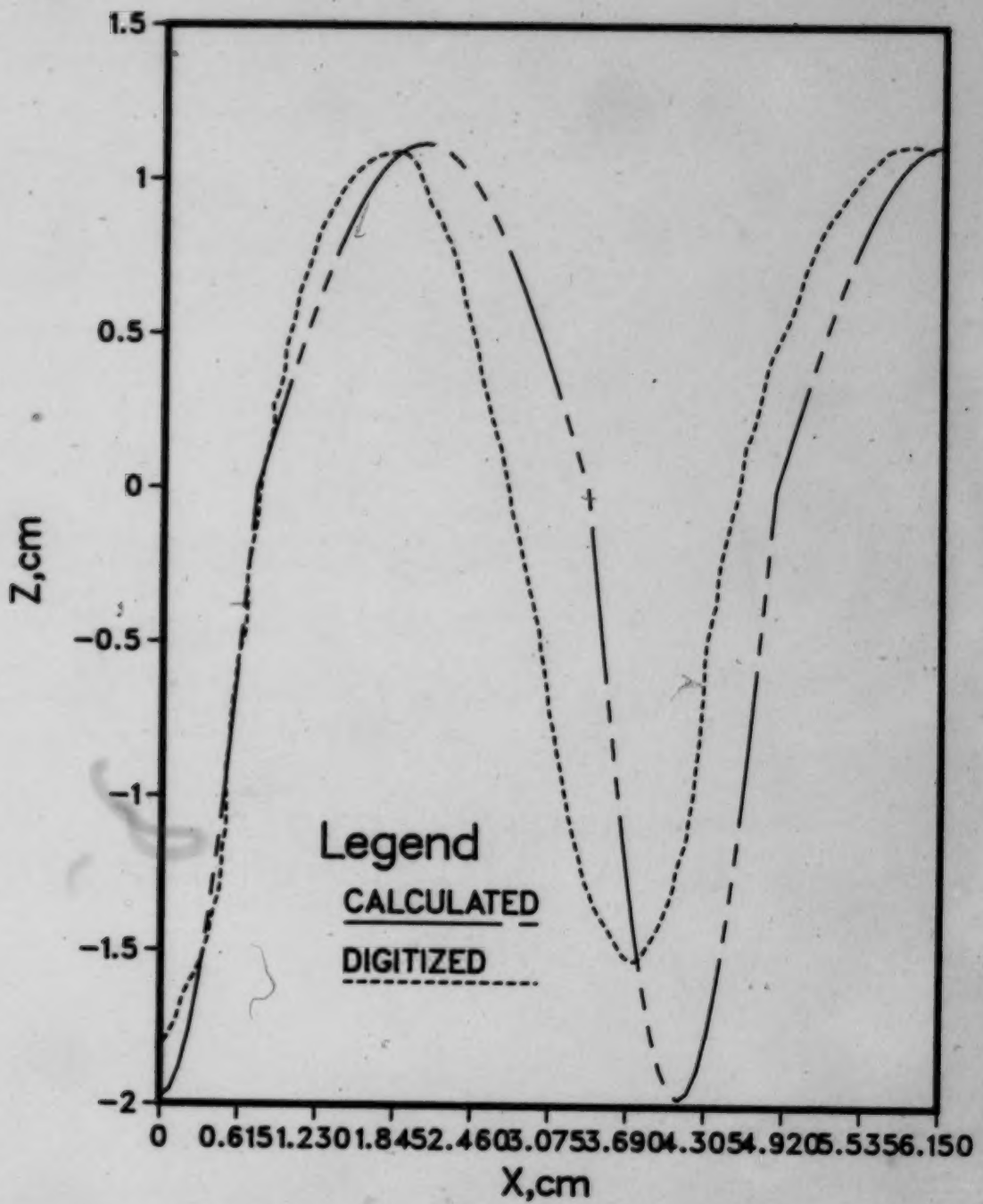

FIG.19 THE INTERFACE AT T=301 SEC. FOR RUN 13

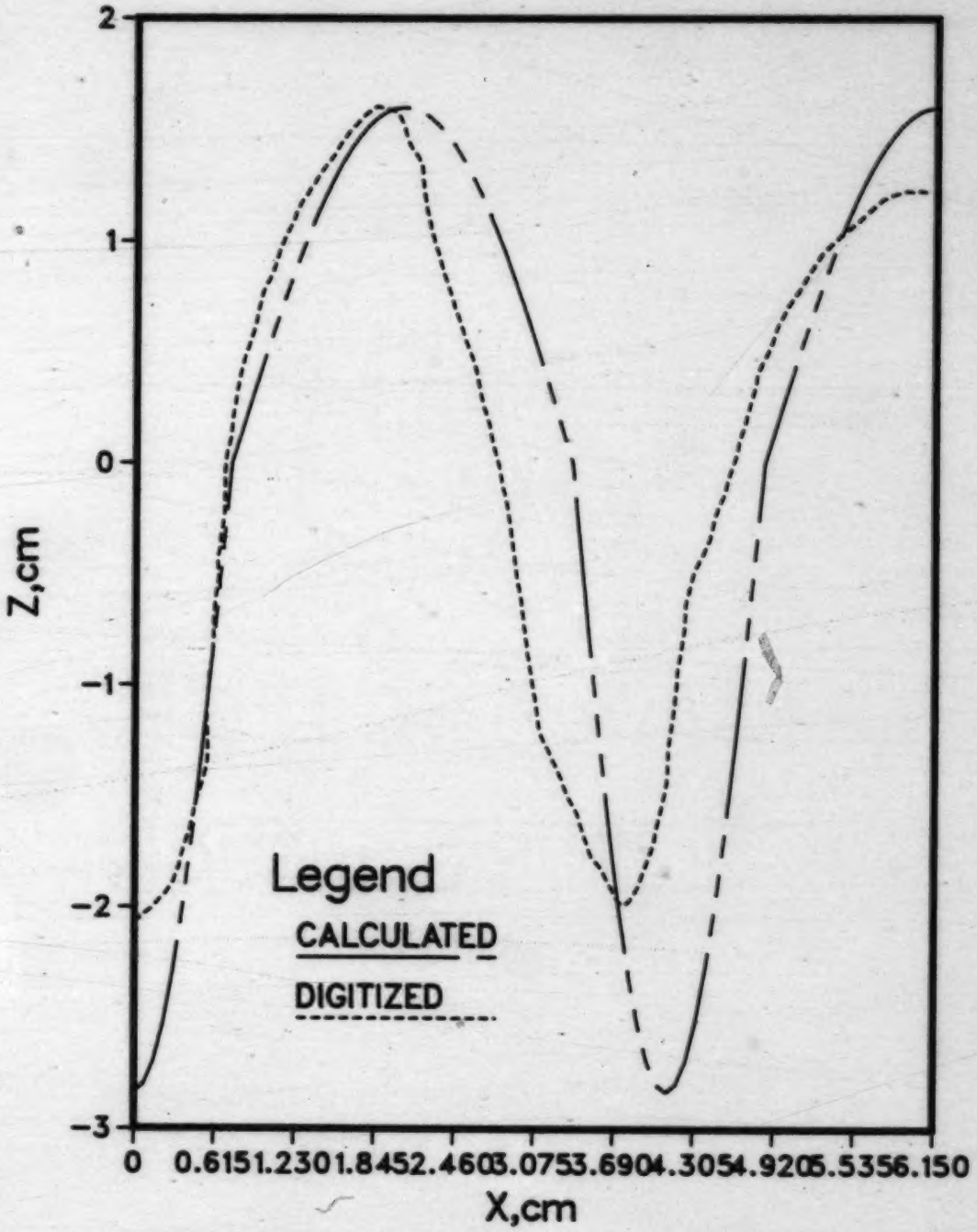

FIG.20 THE INTERFACE AT T=324 SEC. FOR RUN 13

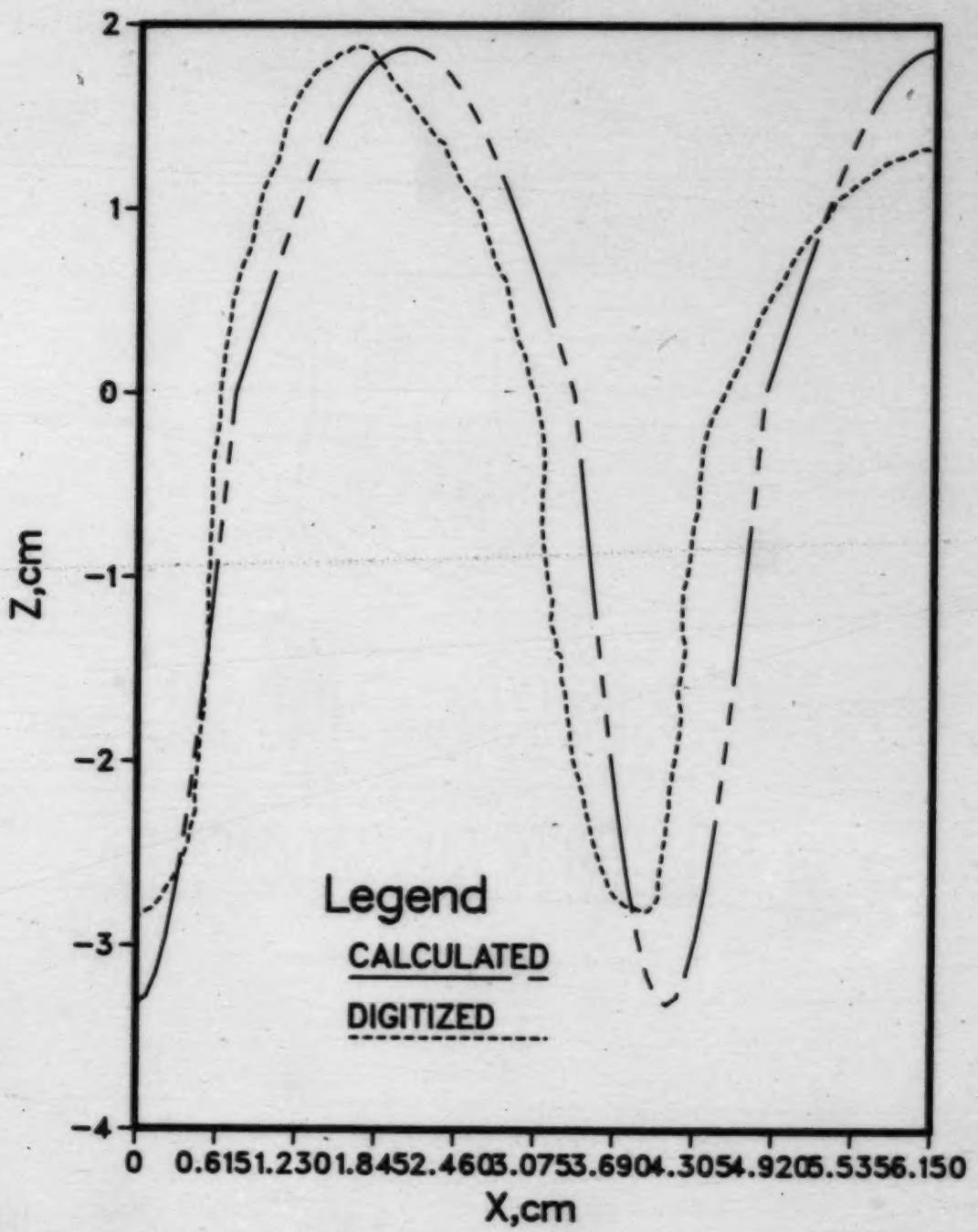

FIG.21 THE INTERFACE AT T=387 SEC. FOR RUN 13

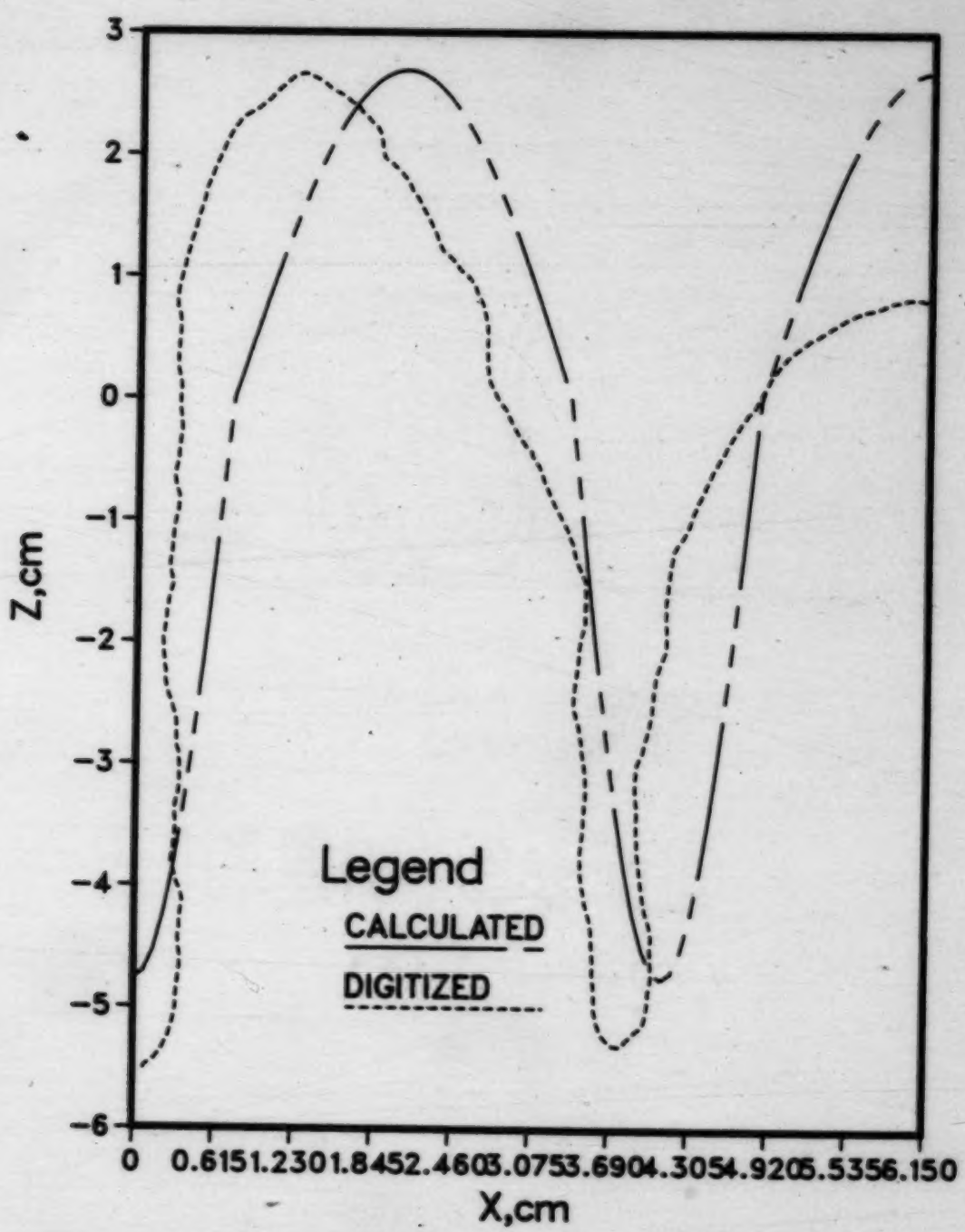

FIG.22 THE INTERFACE AT T=505 SEC. FOR RUN 13

Under these conditions the match between the experimental and theoretically predicted profiles is not good. But, once these effects diminished, the roots of the fingers stayed relatively fixed and a reasonably good match was obtained between the experimental and theoretically predicted profiles (see Figs. 11-16, 19, 20, 21, 31, 39, 40, 45-50).

When the match between the predicted and the experimental profiles is not very good, there seems to be a phase difference due to the shifting of the roots. Experiments 33 (Figs. 33-37) and 50 (Figs. 54-58) are examples of this type of match. In Experiment 33, the digitized curve leads the calculated curve by about the same amount for all but the lowest value of time. However, in Experiment 50, the shift appears to be uneven. In all the other figures, there is a small amount of lag between the calculated and the experimental curve, but there is no particular pattern for this lag. Therefore, it is likely that the lag (or lead) between the calculated and experimental curve is due to random disturbances which perturb the interface as it advances.

Under laboratory conditions, at lower modes (low Isr), the experiments generally started out at the maximum mode associated with the instability number and later one of the modes close to the maximum on the time factor versus wavelength curve distinguished itself. For instance, the maximum possible mode for Experiment 27 was mode 2 and, as can be seen from Table 2, it started at this mode. Looking

at the time constant versus wavelength curve for this experiment (see Fig.6), it is seen that for a maximum possible mode of two, the most probable mode is one. Therefore, the interface became first mode as it advanced towards the outlet end of the Hele-Shaw cell. In Fig.8, although the interface is distorted, the second mode can still be recognized; in Figs. 9 and 10 the first mode becomes more and more distinguishable, and finally in Figs. 11, 12 and 13 a good first mode is observed. Some other examples can be see in Table 2 for Experiments 7, 13, 15, 22, 30 and 32. The maximum mode, in some of the experiments, was followed by another mode which was still close to the maximum. It was found that this change, in general, was from higher modes to lower ones. If the porous medium is ideal, the most unstable mode invariably should dominate the displacement. But under laboratory conditions, there exists microscopic heterogeneities as a result of irregularities in the wettability of glass surfaces and possible dust particles on them. This causes the interface to be perturbed intermittently. Therefore, in addition to the most unstable mode, other modes which have time constants close to the most unstable one were observed in the Hele-Shaw experiments. Examples of this type of behaviour can be seen in Experiments 29, 33, 35, 49, 50 and 53 in Table 2.

At larger values of the instability number (higher modes), the experiments started out with one of the modes which had a time constant close to the maximum value rather

than the maximum possible mode that could be obtained at that velocity. Again, a change of mode towards the lower ones was observed. Experiments 38, 39, 59, 60 and 63 in Table 2 illustrate this behaviour.

As the instability number becomes further removed from the stability boundary, the ratio of viscous forces to capillary forces (capillary number) increases. Hence, the imbalance between these forces becomes larger as the mode number increases. This imbalance causes experimental profiles to be very irregular. As a consequence, it was not easy to identify the experimental mode when Isr was large. Experiments 18, 36, 46, 54, 59 and 60 are examples of such experiments in Table 2.

It was also observed that the final mode tends to be the first mode at high instability numbers (Exps. 17, 38, 59, 60 and 63) whereas at low instability numbers the final mode could be larger than mode one (Exps. 22, 33, 35 and 52). The occurrence of such a phenomenon can be attributed to two reasons: namely, the effect of competing potentials of the fluids and the effect of finite geometry of the flow system.

When a fluid/fluid interface is advancing in a porous medium, there are three potentials which determine the conditions of the flow. The first one is the viscous flow potential which arises from the difference of the mobilities of the two fluids. This potential tries to deform the interface in the form of viscous fingers. The second

potential is the gravity potential which arises because of the density difference between the displacing and the displaced fluid. It can either try to dampen the viscous fingers or enhance them, depending on the density difference, but its effect under both circumstances is constant everywhere on the interface. The third potential is the capillary potential which is a result of the curvature of the interface. It always opposes the deformation of the interface.

The incipient fingers that are formed can grow at the same rate only in the absence of any microscopic irregularities. That is, these fingers start losing symmetry when they encounter microscopic irregularities. When a given finger becomes broader, the capillary potential which tries to dampen it becomes smaller. As the viscous and gravity potentials are constant, a reduction in the capillary potential means a net overall increase in the total potential trying to drive the finger. Consequently, such a finger speeds up and dominates the displacement. The effect of this phenomenon is more pronounced at high velocities. When one finger dominates the displacement, the final configuration will be the first mode. This effect may be observed in Figures 17 to 22. Note that, on the left, as the base of the water finger (which is located at z=0) becomes broader, it speeds up (see Fig.23). Also, as can be seen from Table 2, this broadening of the finger leads to a second mode configuration. Note that, if the cell had been

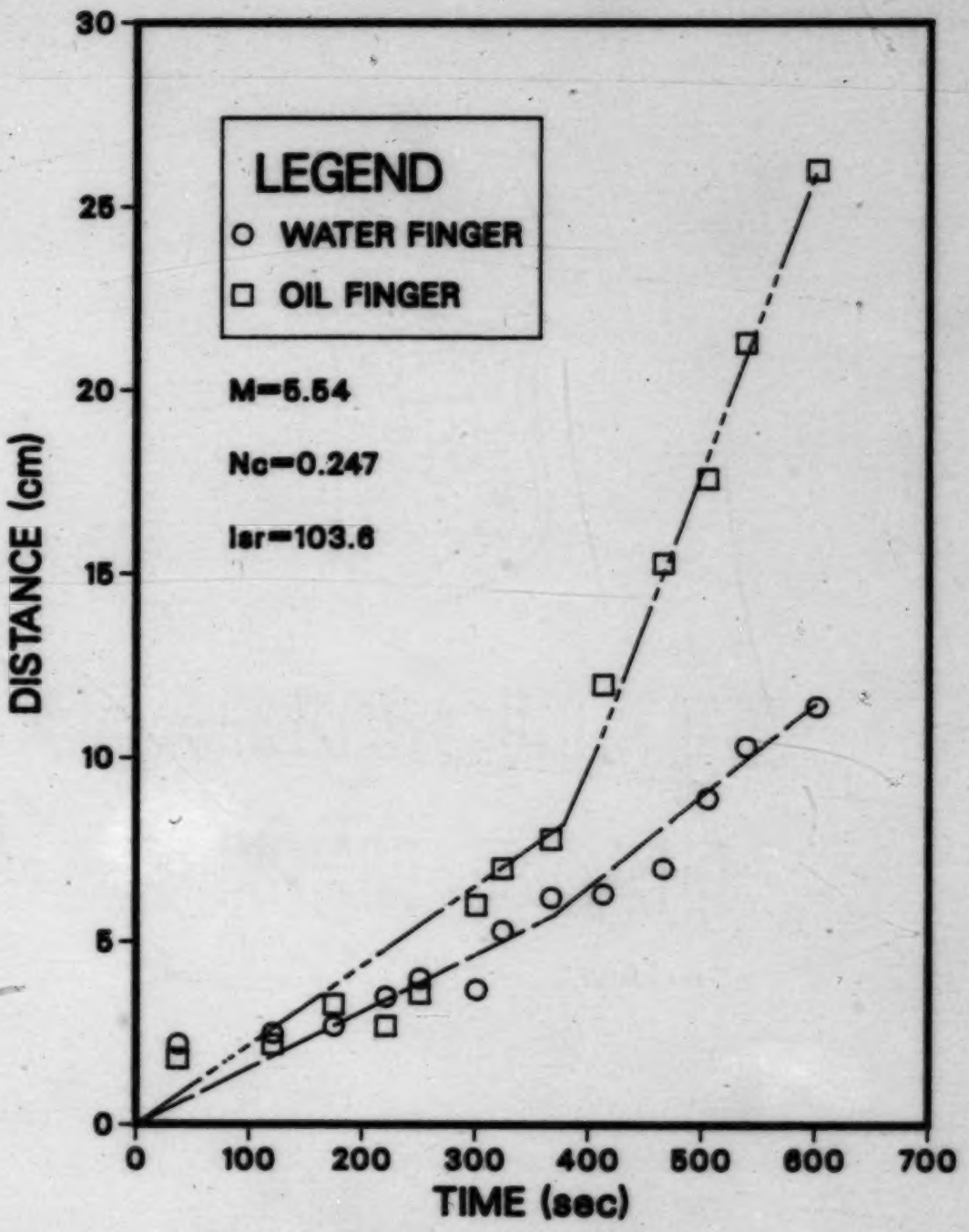

FIG.23 DISTANCE TRAVELLED BY THE TIP OF THE FINGER FOR RUN 13

longer, a first mode finger might have formed eventually.

The effect of finite geometry can be understood when such a finger which is ahead of others is considered. When a finger propagates faster than its neighbours, it bypasses more viscous fluid than the shorter fingers. The longest finger in a multifingered front is mechanistically similar to an only finger on a single finger front. Consequently, this longer finger will continue to grow faster because it has moved the region of steep pressure gradients past the viscous fluid that still lies ahead of shorter fingers. This causes the longer finger to keep moving faster, thus dampening the growth of shorter fingers. Again, this eventually results in the finger exhibiting a first mode configuration. The difference in the lengths of short and long fingers becomes more pronounced as the tip of the finger approaches the outlet. Another effect of the finite geometry could have been that the cell was not long enough for the first mode to appear in all the experiments.

In the theory developed here, a finger is modelled as a one-dimensional standing wave whose amplitude is continuously increasing with time (see Equation 18). In writing Equation 18, it was assumed that the finger roots were embedded in the initially plane interface. These roots do not change with time; i.e., they are fixed on the initially plane interface.

In the experiments, it was observed that the roots of the fingers changed as the experiments progressed. This was

not a surprise because the roots of the fingers had to be rearranged while the interface was changing modes. The intermittent perturbation of the interface, due to the effect of microscopic heterogeneities in the system, was another cause for the roots not to be fixed. For the experiments during which the roots of the fingers stayed almost fixed, the relative widths observed were in excellent agreement with the theory (e.g. Exps. 13, 31 and 51). In these experiments, the velocity of the finger increased as the interface switched to a smaller mode (see Fig.s 23, 24, 25). In Experiment 13, the interface started to change from mode 3 to mode 2 at around t=380 seconds (see Fig.23). This can also be observed in Figures 17 to 22. In Experiment 31, the interface very quickly changed from mode 4 to mode 2 after the start of the experiment and later it changed from second mode to first mode at around t=750 seconds (see Fig.24). This is also seen in Figures 29 to 34 in Appendix 5. In Experiment 51, the interface changed from mode 4 to mode 2 at around t=1200 seconds (see Fig.25). Although the data is scattered, the trend was still observed.

The reason for this increase in the velocity can be explained as follows: The energy provided to the system is constant as the injection rate is constant. This energy is stored at the interface and also is used to drive the finger. When the interface changes its mode structure to a smaller one, the total surface area is reduced, which, in turn, results in the release of some excess energy.

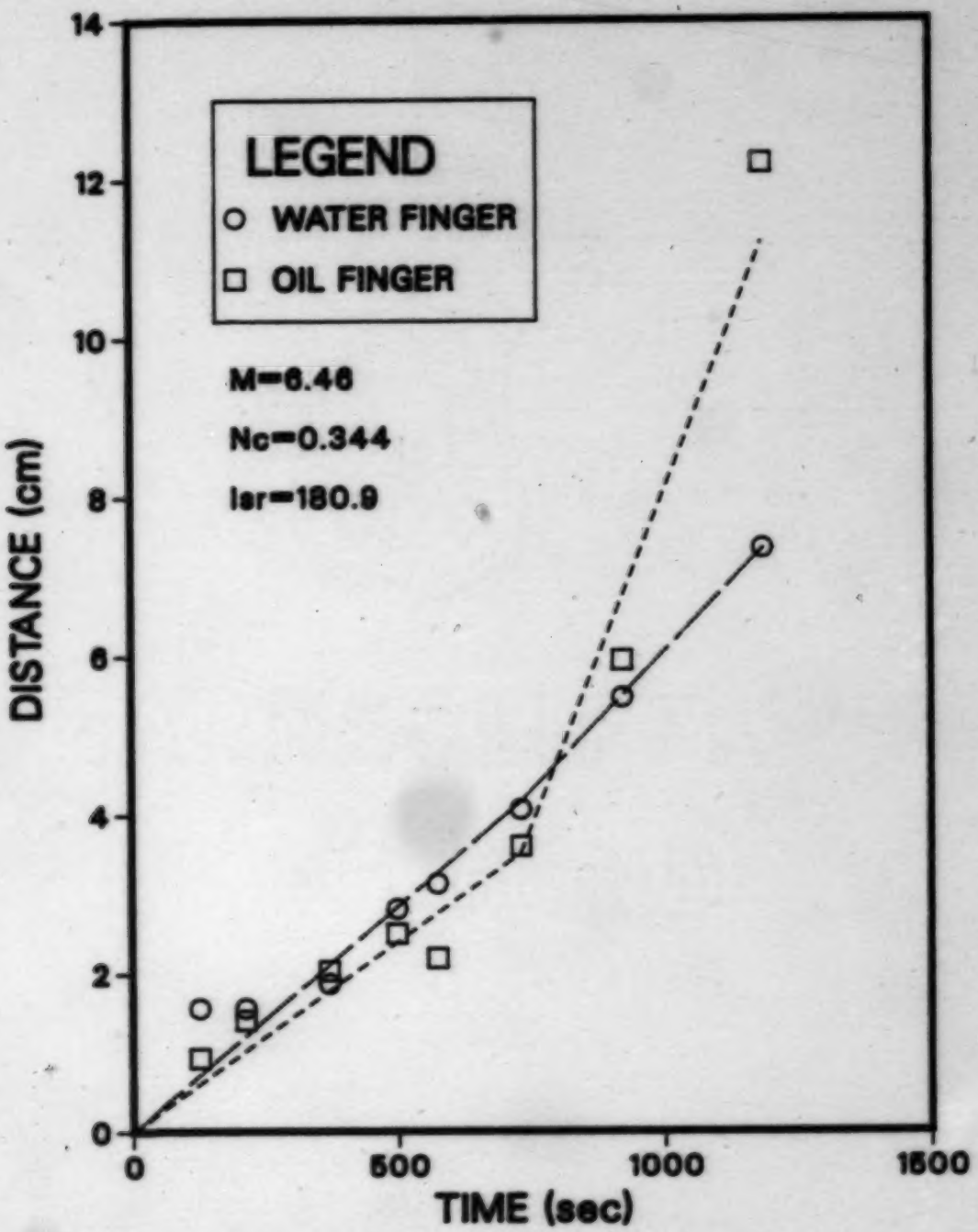

FIG.24 DISTANCE TRAVELLED BY THE TIP OF THE FINGER FOR RUN 31

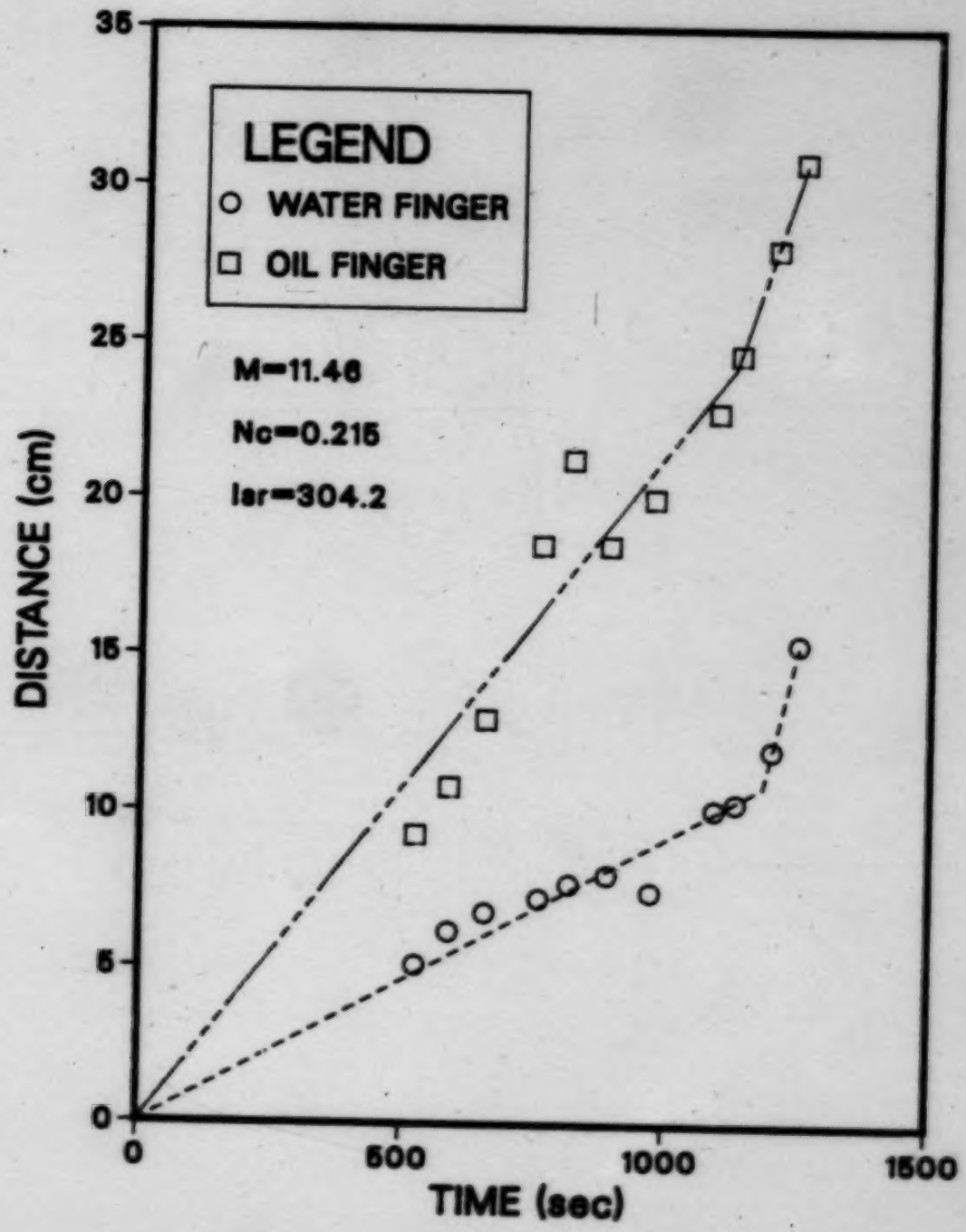

FIG.25 DISTANCE TRAVELLED BY THE TIP OF THE FINGER FOR RUN 51

This excess energy is used to drive the remaining fingers at a higher velocity. Here, the amount of energy which is converted into heat, due to the viscous friction between fluids and the Hele-Shaw cell, is assumed to be negligible.

During the experiments in which the roots of the fingers changed with time, the velocity of the water and oil finger altered depending on the direction of this change. In some experiments (e.g. Experiments 33 and 50), the root of the water finger became wider, causing the finger tip to slow down with respect to the moving boundary which is moving with the superficial velocity of the experiment. The interface is shown, for Experiment 33, in Figures 33 to 37 in Appendix 5, and for Experiment 50, in Figures 51 to 58. In both experiments, the water finger became wider, causing the oil finger to narrow as the interface advanced. As a consequence, the velocity of the water finger decreased as that of the oil finger increased. This is shown in Figures 26 and 27. Experiment 44 was an example of a different phenomenon. In this case, the interface was first mode initially and later changed to second mode (see Table 2). While this change was occurring, the water finger became wider, which caused the interface to become close to first mode again. This caused the oil finger to speed up while the velocity of the water finger remained constant (see Fig.28). In any case, the distance travelled by the tip of the water and oil fingers with respect to the moving boundary is a linear function of time.

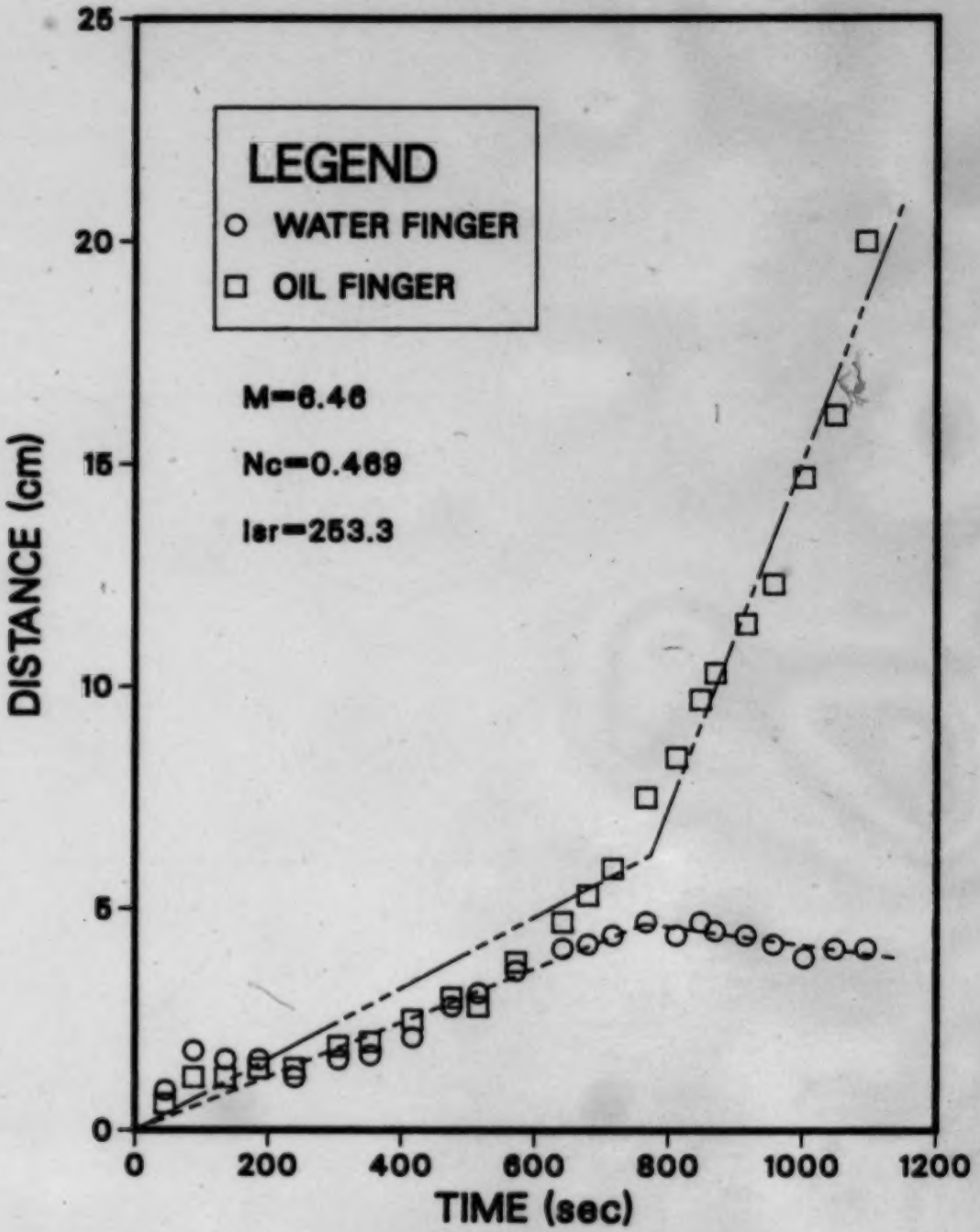

FIG.26 DISTANCE TRAVELLED BY THE TIP OF THE FINGER FOR RUN 33

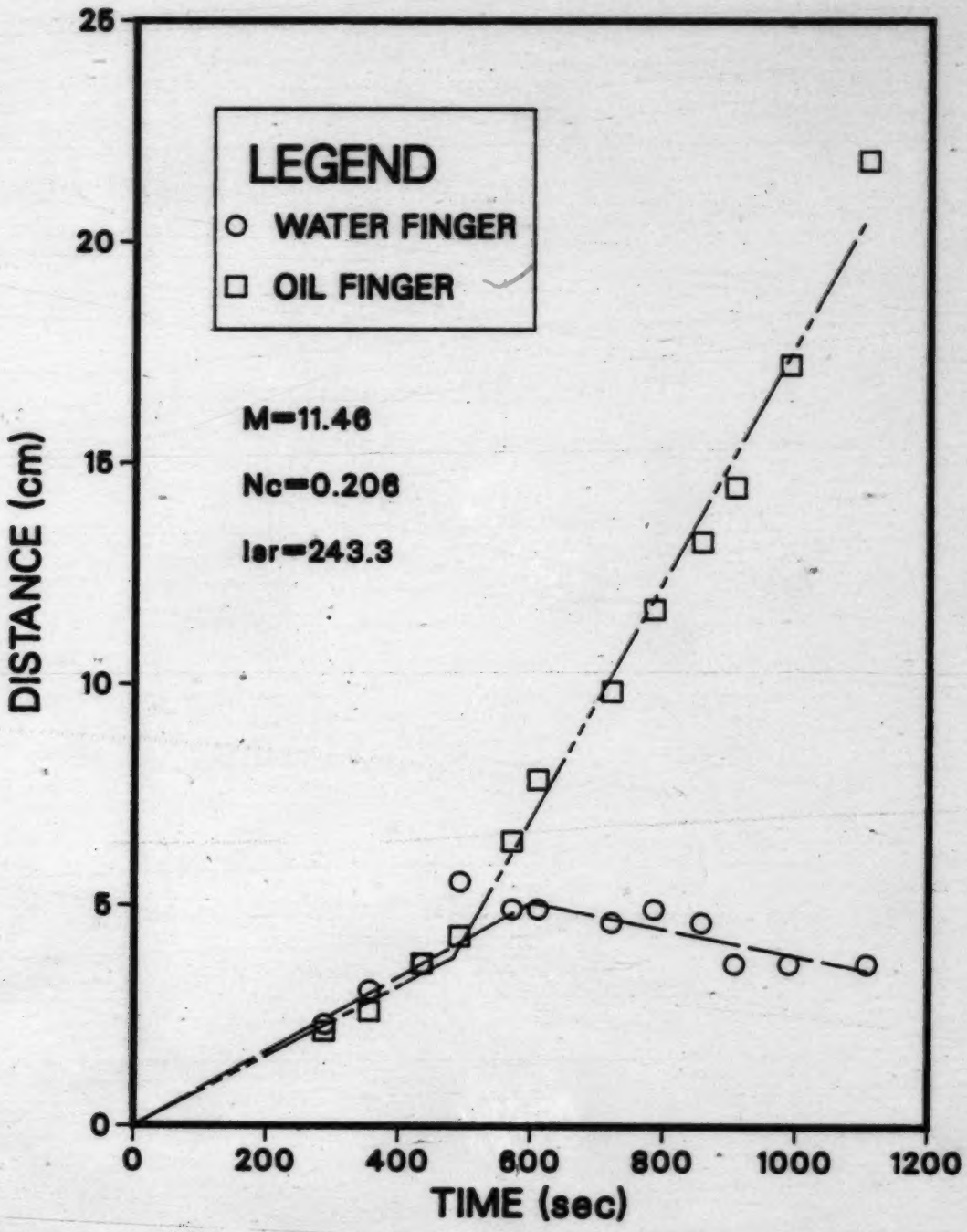

FIG.27 DISTANCE TRAVELLED BY THE TIP OF THE FINGER FOR RUN 50

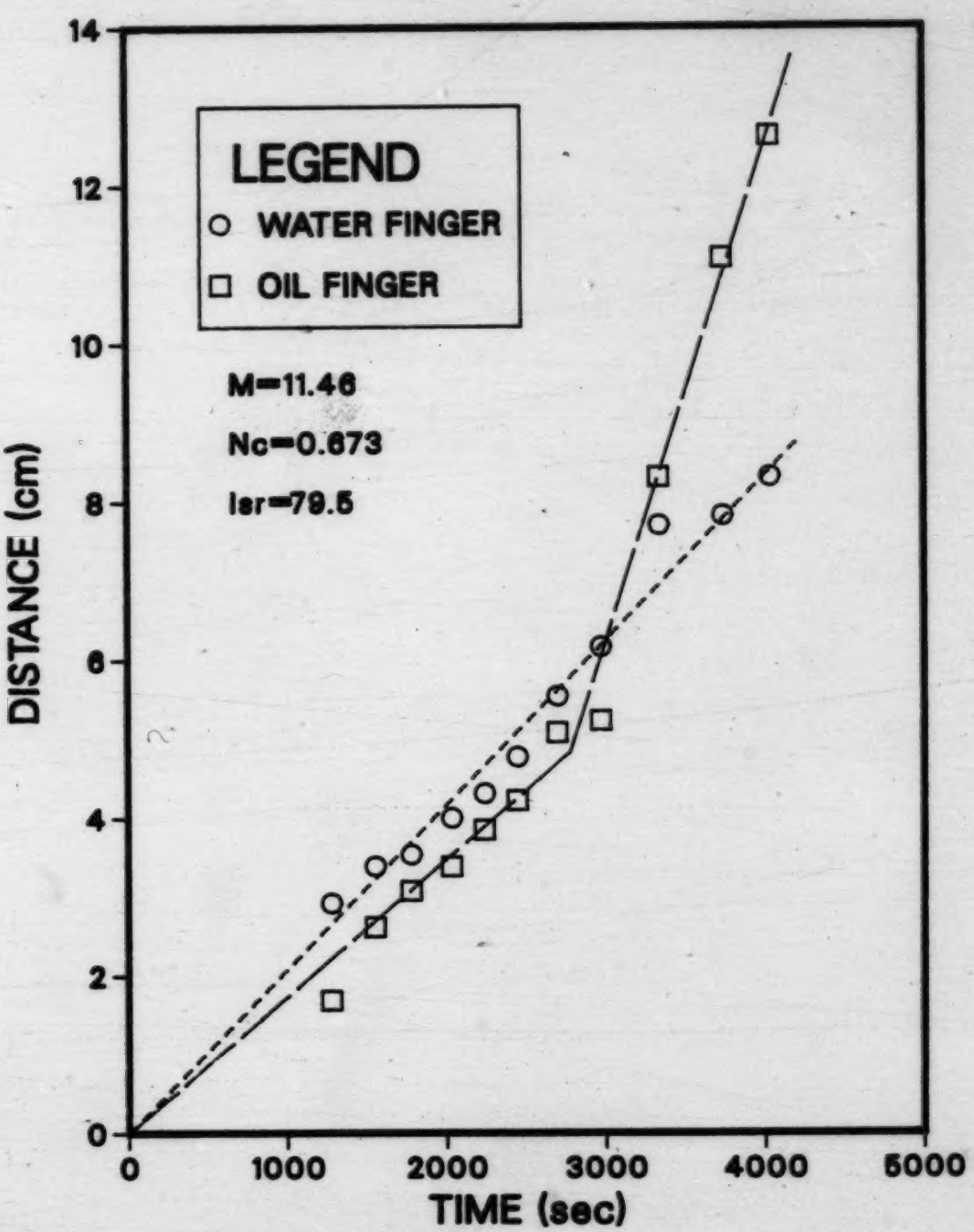

FIG.28 DISTANCE TRAVELLED BY THE TIP OF THE FINGER FOR RUN 44

Another generalization that can be made is that the water fingers in all the experiments were wider than the oil fingers. This means that Equation 41 is quantitatively correct if the roots of the fingers are fixed on the moving boundary; if the roots change rather than remaining fixed, then Equation 41 is qualitatively correct.

Some experiments were repeated to see if the reproducibility would improve by changing the wettability from water-wet to oil-wet as suggested in the literature[7]. Experiments 6,7; 12,13; 14,15,19; 17,18,20,21 and 61,62 are replicate runs for a water-wet system. A study of these runs indicates that, given the stochastic nature of the perturbations introduced by local changes in thickness and wetting, the runs were reasonably reproducible. Experiments 23,24; 27,28; 36,37,38,39,40,41; 48,49 and 51,52,53,54 are replicate runs for an oil-wet system. Again, the runs seem to be reasonably reproducible. Moreover, the oil-wet runs were about as reproducible as the water-wet runs, contrary to what has been reported in the literature.

As the theory assumes a fixed arrangement for the roots of the fingers during the life span of an experiment, the shifting, widening and narrowing of the fingers cause c_2 to change. Theoretically, c_2 is a constant. The narrowing or widening of a finger affects the distance travelled by the tip of the finger with respect to time because of material balance demands.

TABLE.3

VALUES OF c_2 AT DIFFERENT TIMES

EXPERIMENT	TIME(SEC.)	c_2
27	1424	13.8
27	1858	18.4
27	2718	29.3
27	3330	45.0
27	3685	62.2
27	3968	72.2
51	889	75.0
51	1092	89.6
51	1132	94.4
13	221	8.7
13	251	9.8
13	301	15.4
13	324	12.3
13	367	13.4
13	505	17.7
31	127	3.3
31	214	9.4
31	370	23.6
31	498	28.4

TABLE.3 (Continued)

VALUES OF c_2 AT DIFFERENT TIMES

EXPERIMENT	TIME(SEC.)	c_2
33	680	69.3
33	812	94.5
33	870	106.1
33	958	137.5
33	1003	162.5
34	308	9.7
34	413	11.2
34	493	13.2
34	525	12.9
42	5981	46.1
42	7135	49.5
42	7978	57.3
42	9976	73.1
42	12014	75.1
42	13219	76.5
42	14427	83.9
42	15092	58.9
42	16465	75.2

TABLE.3 (Continued)

VALUES OF c_2 AT DIFFERENT TIMES

EXPERIMENT	TIME(SEC.)	c_2
50	288	17.6
50	435	25.0
50	571	32.2
50	610	36.7
50	721	54.9
50	786	61.1
50	857	77.5
50	990	129.5

In particular, widening will slow down the growth and narrowing will speed up the growth in the direction of displacement. Consequently, this speeding up or slowing down of the finger, which is not accounted for in the theory, affects the value of c_2, and causes it to vary with time. This occurs because the evaluation of c_2 depends on the maximum distance travelled by the tip of the water finger at each time (see Section 6.5). The constant c_2 increased by a factor of two over the life of the finger in those experiments where the roots remained relatively fixed or

changed by small amounts. This was the case for Experiments 13, 34, 42, 51 and 27, as can be seen in Table 3. In the other experiments this increase was as much as an order of magnitude; see, for example, Experiments 31, 33 and 50 in Table 3. In addition to the narrowing and widening of the roots, another reason for c_2 to change could have been the time component of the functional form postulated for the shape of the finger. If the finger growth rate is faster than that predicted by the theory, this will result in an increase in c_2.

The fact that it is not possible to undertake a linear combination of the solutions to Equation 18 suggests that the the fluid displacement problem may be non-linear. If this is indeed true, one would expect the interface to be very sensitive to the initial and boundary conditions. Because the finger surface was very sensitive to the initial conditions and to the local heterogeneities during the experiments support the contention that the problem may be a non-linear one. Because the initial perturbation of the interface was different in each experiment, when a particular experiment started, any shape of interface could have been observed before one of the possible modes could be observed. Moreover, as the instability number increases the displacement becomes completely dominated by the heterogeneities of the system. This causes the front to be very erratic. The theory will not be able to predict the behaviour of unstable displacements at these high

instability numbers. It seems that an alternative approach must be taken to overcome the chaotic viscous fingering encountered at the high instability numbers. That is to say, it may be necessary to pass from the macroscopic scale to the "megascopic" scale, as has already been done[30,31] when passing from the microscopic scale to the macroscopic scale.

A Hele-Shaw cell was chosen for the experimental study because the assumption of a sharp interface is satisfied exactly in it, and because it enables one to focus on the force balance between the two fluids without the complications of the random geometry. Moreover, the relative permeability aspects of a real porous medium are absent in such a cell. As a result, the effects of a transition region between the two fluids are not present. One may argue that such a displacement corresponds to a real situation in which the size of the fingers is large relative to the transition region on the finger surfaces.

The viscous fingers can be created only when, in a displacement, viscous forces dominate all the other forces. Equation 55, therefore, is not explicitly dependent upon the interfacial tension. The fact that the perturbation velocity of water does not depend on the interfacial tension between the two fluids suggests that an equation similar to Equation 55 might be used to predict the perturbation velocity of solvent fingering into oil. There is some experimental evidence[29,32,33] that miscible and immiscible displacements, when dominated by viscous forces, exhibit a similar

behaviour. But there is, as yet, no theoretical basis for such a phenomenon.

SUMMARY AND CONCLUSIONS

The new approach to stability theory[21] which has recently been developed was modified for a Hele-Shaw cell. Sixty-three experiments were conducted in which the viscosity ratio, the wettability, the flow rate and the interfacial tension were changed to validate the new theory. Moreover, a method for obtaining c_2 from the experimental data was obtained. Keeping in mind the limitations of the theory, and for the experiments conducted herein, the following conclusions may be drawn.

1. Equation 60 correctly predicted the stability boundary.
2. The mode boundaries obtained through the use of Equation 63 were correct, provided the instability number was not too far removed from the stability boundary.
3. The relative widths and the shapes of the fingers were , in general, in good agreement with the theory.
4. The agreement between the experimental behaviour and the theoretically obtained time constant versus wavelength plots was good.
5. The distance travelled by the tip of the oil and water fingers with respect to the moving boundary was a linear function of time. This supports the findings of Gupta, et.al.[12,13].
6. The experiments supported the theoretical contention that the problem is non-linear. If such is the case, the individual harmonics cannot be superposed to obtain the shape of the interface.

REFERENCES

1. Taylor,G.I. "The Instability of Liquid Surfaces When Accelerated in a Direction Perpendicular to Their Planes.I", 1950, Proc. Roy. Soc. London, ser.A, vol.201, p.192
2. Lamb,H. "Hydrodynamics", Sixth ed., 1945, Dover Publications,Inc., N.Y., ch.9, p.373
3. Lewis,D.J. "The Instability of Liquid Surfaces When Accelerated in a Direction Perpendicular to Their Planes.II", 1950, Proc. Roy. Soc. London, ser.A, vol.202, p.81
4. Bellman,R. and Pennington,R.H. "Effects of Surface Tension and Viscosity on Taylor Instability", 1954, Quart. Appl. Math., vol.12, p.151
5. Saffman,P.G. and Taylor,G.I. "The Penetration of a Fluid into a Porous Medium or Hele-Shaw Cell Containing a More Viscous Fluid", 1958, Proc. Roy. Soc. London, sec.A, vol.245, p.312
6. van Meurs,P. and van der Poel,C. "A Theoretical Description of Water Drive Process Involving Viscous Fingering", 1958, Trans. AIME, vol.213, p.103
7. Chuoke,R.L.; van Meurs,P. and van der Poel,C. "The Instability of Slow, Immiscible, Viscous Liquid-Liquid Displacements in Permeable Media", 1959, Trans. AIME, vol.216, p.188 and J. Pet. Tech., July 1959, p.64

8. Outmans,H.D. "Nonlinear Theory for Frontal Stability and Viscous Fingering in Porous Media", 1962, Soc. Pet. Eng. J., June, p.165

9. Rachford,H.H. "Instability in Water Flooding Oil from Water-Wet Porous Media Containing Connate Water", 1964, Soc. Pet. Eng. J., June, p.133

10. Raghaven,R. and Marsden,S.S. "The Stability of Immiscible Liquid Layers in a Porous Medium", 1971, J. Fluid Mech., vol.48, part 1, p.143.

11. Huang,A.B.; Chikhliwala,E.D. and Yortsos,Y.C. "Linear Stability Analysis of Immiscible Displacement Including Continuously Changing Mobility and Capillary Effects: Part.II - General Basic Flow Profiles", 1984, SPE Paper No. 13163

12. Gupta,S.P.; Varnon,J.E. and Greenkorn,R.A. "Viscous Finger Wavelength Degeneration in Hele-Shaw Models", 1973, Water Resour. Res., vol.9, no.4, p.1039

13. Gupta,S.P. and Greenkorn,R.A. "An Experimental Study of Immiscible Displacement with an Unfavorable Mobility Ratio in Porous Media", 1974, Water Resour. Res., vol.10, no.2, p.371

14. Wooding,R.A. and Morel-Seytoux,H.J. "Multiphase Fluid Flow Through Porous Media", 1976, Ann. Rev. Fluid Mech., vol.8, p.233

15. White,I.; Colombera,P.M. and Philip,J.R. "Experimental Studies of Wetting Front Instability Induced by Gradual Change of Pressure Gradient and by Heterogeneous Porous Media" 1977, Soil Sci. Soc. Am. J., vol.41, p.483

16. Hagoort,J. "Displacement Stability of Water Drives in Water Wet Connate Water Bearing Reservoirs" 1974, Soc. Pet. Eng. J., Feb., p.63

17. Peters,E.J. and Flock,D.L. "The Onset of Instability During Two Phase Immiscible Displacement in Porous Media" 1981, Soc. Pet. Eng. J., April, p.249

18. Jerauld,G.R.; Davis,H.T. and Scriven,L.E. "Frontal Structure and Stability in Immiscible Displacement", 1984, SPE/DOE Paper No. 12691

19. Jerauld,G.R.; Davis,H.T. and Scriven,L.E. "Stability of Fronts of Permanent Form in Immiscible Displacement", 1984, SPE Paper No. 13164

20. Yortsos,Y.C. and Huang,A.B. "Linear Stability Analysis of Immiscible Displacement Including Continuously Changing Mobility and Capillary Effects: Part.I - Simple Basic Flow Profiles", 1984, SPE/DOE Paper No. 12692

21. Bentsen,R.G. "A New Approach to Instability Theory in Porous Media", 1985, Soc. Pet. Eng. J., October

22. Hubbert,M.K. "The Theory of Ground Water Motion and Related Papers", 1969, Hafner Publishing Co., N.Y., p.18

23. Scheidegger,A.E. "The Physics of Flow Through Porous Media", 1974, University of Toronto Press, Toronto, ch.4, p.49

24. Marle,C.M. "Multiphase Flow in Porous Media", 1981, Editions Technip, Paris, ch.7, p.219

25. Rose,W.D. "Some Problems Connected with the Use of Classical Description of Fluid/Fluid Displacement Processes", 1972, in Fundamentals of Transport Phenomena in Porous Medium, Int. Assoc. for Hydraulic Res., Elsevier Publishing Co., N.Y., p.229

26. Saffman,P.G. "Fingering in Porous Media" 1982, in Lecture Notes in Physics, vol.154: Macroscopic Properties of Disordered Media, Springer-Verlag, N.Y., p.208

27. Bear,J. "Dynamics of Fluids in Porous Media", 1972, American Elsevier Co., Inc., N.Y., ch.1, p.24

28. Bentsen,R.G. and Saeedi,J. "Liquid-Liquid Immiscible Displacement in Unconsolidated Porous Media" 1981, J. Can. Pet. Tech., Jan.-Mar., vol.20, p.93

29. Perkins,T.K. and Johnston,O.C. "A Study of Immiscible Fingering in Linear Models", 1969, Soc. Pet. Eng. J., March, p.39

30. de la Cruz,V. and Spanos,T.J.T. "Mobilization of Oil Ganglia",1983, AIChE J., vol.29, no.12, p.854

31. Whitaker,S. "Fluid Motion in Porous Media", 1969, Ind. Eng. Chem., vol.6, no.12, p.15

32. Offeringa,J. and van der Poel,C. "Displacement of Oil from Porous Media by Miscible Fluids" 1954, Trans. AIME, vol.201, p.310

33. Paterson,L. "Dispersion and Fingering in Miscible and Immiscible Fluids within a Porous Medium" 1983, Powder Tech. , vol.36, p.71

34. Hellums,J.D. and Churchill,S.W. "Dimensionless Analysis and Natural Circulation", 1961, Chem. Eng. Progr. Symp. Ser., vol.57, no.32, p.75

BIBLIOGRAPHY

Scheidegger,A.E. "Growth of Instabilities on Displacement Fronts in Porous Media" 1960, Phys. Fluids, vol.3, no.1, p.94

De Wiest,R.J.M. "Geohydrology", 1965, John Wiley & Sons Inc., N.Y.

Bear,J. "Immiscible Displacement", 1970, Adv. in Hydrosci., vol.6, p.141

Chow,C.C. and Scheidegger,A.E. "Stability Conditions for Fingering Process in Porous Media", 1972, J. Hydrology, vol.15, p.1

Prickett,T.A. "Modelling Techniques for Groundwater Evaluation", 1975, Adv. in Hydrosci., vol.10, p.1

White,I; Colombera,P.M. and Philip,J.R. "Experimental Study of Wetting Front Instability Induced by Sudden Change of Pressure", 1976, Soil Sci. Soc. Am. J., vol.40, p.824

Miller,C.A. "Stability of Interfaces", 1978, Surface and Coll. Sci., vol.10, p.227

Spanos,T.J.T. "The Surface Conditions for Viscous Displacement in a Homogeneous Porous Medium", 1979, Can. J. Phys., vol.57, p.1738

Dullien,F.A.L. "Porous Media: Fluid Transport and Pore Structure", 1979, Academic Press, N.Y.

Pitts,E. "Penetration of a Fluid into Hele-Shaw cell: The Saffman-Taylor Experiment", 1980, J. Fluid Mech., vol.97, part 1, p.53

Spanos,T.J.T. "A Stability Analysis of Immiscible Viscous Displacement in a Homogeneous Porous Medium", 1980, Can. J. Phys., vol.158, p.138

Greenkorn,R.A. "Steady Flow Through Porous Media", 1981, AIChE J., vol.27, no.4, p.529

McLean,J.W. and Saffman,P.G. "The Effect of Surface Tension on the Shape of Fingers in a Hele-Shaw Cell", 1981, J. Fluid Mech., vol.102, p.455

Greenkorn,R.A. "Flow Phenomena in Porous Media", 1983, Marcell Dekker Inc., N.Y.

Paterson,L.; Hornof,V. and Neale,G. "Visualization of a Surfactant Flood of an Oil Saturated Porous Medium", 1984, Soc. Pet. Eng. J., June, p.325

Park,C.W.; Gorell,S. and Homsy,G.H. "Two Phase Displacement in Hele-Shaw Cells: Experiments on Viscously Driven Instabilities", 1984, J. Fluid Mech., vol.141, p.257

APPENDIX 1

SOLUTION OF ONE DIMENSIONAL WAVE EQUATION BY SEPARATION OF VARIABLES

The equation to be solved is Equation 18 which is given by,

$$-\frac{1}{a^2 f(t)}\frac{\partial^2 \eta}{\partial t^2} = \frac{\partial^2 \eta}{\partial x^2} \tag{18}$$

Assume a solution of the form

$$\eta(x,t) = F(x) \cdot T(t) \tag{1.1}$$

The boundary conditions are :

$$0 \leq x \leq L_x$$

$$0 \leq t \leq \infty \tag{1.2}$$

In order that the root of the finger be embedded in the linear interface which initially separates the two fluids,

it is necessary that

$$F(L_x) = 0 \tag{1.3}$$

Furthermore, as the normal perturbation velocity vanishes at the wall of the Hele-Shaw cell

$$F'(0) = 0 \tag{1.4}$$

Differentiate Equation 1.1 with respect to time and distance

$$\frac{\partial^2 \eta}{\partial t^2} = FT'' \tag{1.5}$$

$$\frac{\partial^2 \eta}{\partial x^2} = TF'' \tag{1.6}$$

substitute into Equation 18 and divide by FT to obtain

$$\frac{F''}{F} = -\frac{1}{a^2 f(t)}\frac{T''}{T} = k \qquad (1.7)$$

where k is a constant which means that two ordinary differential equations are obtained from Equation 1.7, i.e.

$$F'' - Fk = 0 \qquad (1.8)$$

$$T'' + a^2 f(t) Tk = 0 \qquad (1.9)$$

First, try k=0 ; the general solution of Equation 1.8 is

$$F = ax + b \qquad (1.10)$$

where a and b are arbitrary constants. Application of the boundary conditions leads to a=b=0 ; therefore k=0 is of no interest. Second, try $k=\mu^2$, where μ is a constant . The general solution in this case is

$$F(x) = c_1 \mathrm{Sinh}\mu x + c_2 \mathrm{Cosh}\mu x \qquad (1.11)$$

where c_1 and c_2 are arbitrary constants and the application of the boundary conditions leads to $c_1=c_2=0$; therefore this case is of no interest either. Finally, let us try

$$k=-\alpha^2 \qquad (1.12)$$

which is obviously the solution. The general solution is given by

$$F(x) = A\mathrm{Cos}\alpha x + B\mathrm{Sin}\alpha x \qquad (1.13)$$

where A and B are arbitrary constants, and application of the boundary conditions yields the present solution

$$F(x) = A\cos\alpha x \tag{1.14}$$

where

$$\alpha = \frac{(2m-1)\pi}{2L_x} \quad ; m=1,2,3... \tag{20}$$

The solution of Equation 18 now becomes

$$n(x,t) = \cos\alpha \times T(t) \tag{19}$$

where A was arbitrarily set to one.

Now from Equation 1.9 and 1.12 we obtain

$$T'' - a^2 f(t) \alpha^2 T = 0 \tag{1.15}$$

Assume a functional form for T(t)

$$T(t) = \frac{A}{\alpha} \ln\cosh\alpha at \tag{31}$$

Substitute Equation 31 in Equation 1.15 and solve for f(t)

$$f(t) = \frac{\mathrm{Sech}^2 \alpha at}{\ln\cosh\alpha at} \tag{32}$$

Therefore the final solution of the one dimensional wave equation is :

$$\eta(x,t) = \frac{A}{\alpha} \cos\alpha x \times \ln\cosh\alpha at \tag{33}$$

APPENDIX 2

CAPILLARY PRESSURE EQUATIONS FOR THE HELE-SHAW CELL

In porous medium capillary pressure can be written in the following general form'

$$P_c = \sigma_e (C_1 + C_2) + P_c(t) \qquad (2.1)$$

where σ_e is the effective interfacial tension and is equal to σ_{ow} for a Hele-Shaw cell. While $P_c(t)$ is independent of the macroscopic interface, it may be a function of time. It accounts for the capillary pressure drop across the microscopic interface. As there is no microscopic interface in a Hele-Shaw cell, $P_c(t)=0$; therefore we finally have

$$P_c = \sigma_{ow} (C_1 + C_2) \qquad (2.2)$$

where C_1 and C_2 are principal curvatures of the interface.

According to Saffman and Taylor[1], the pressure drop across the interface in a Hele-Shaw cell can be written as

$$P_c = P_w - P_o = \sigma_{ow} \left(\frac{2}{h} + \frac{1}{R}\right) \qquad (2.3)$$

where the term 2/h accounts for the constant transverse (y-z plane) curvature of the interface and 1/R accounts for the curvature in the plane of flow (x-z plane). The curvature in the plane of flow can be approximated by

$$\frac{1}{R} = -\frac{\partial^2 \eta}{\partial x^2} \qquad (2.4)$$

and from the solution by separation of variables

$$\frac{\partial^2 \eta}{\partial x^2} = -\alpha^2 \eta \qquad (2.5)$$

Finally Equation 21 is obtained by substituting this equation in Equation 2.3 ,

$$P_c = \sigma_{ow} \left(\frac{2}{h} + \alpha^2 \eta\right) \tag{2.4}$$

from Equation 3, therefore,

$$P_c = \sigma_{ow} \left(\frac{2}{h} + \frac{\partial^2 \eta}{\partial x^2}\right) \tag{21}$$

APPENDIX 3

THE DERIVATION OF THE CAPILLARY NUMBER FOR A HELE-SHAW CELL

In this section, the method of Hellums and Churchill[3] will be utilized to derive the capillary number for a Hele-Shaw cell.

(a) Express the problem in terms of differential and algebraic equations, boundary and initial conditions:

$$q_w = - \frac{h^2 A}{12\mu_w} \left(\frac{\partial P_w}{\partial x} + g\rho_w \mathrm{Cos}\theta \right) \tag{3.1}$$

$$q_o = - \frac{h^2 A}{12\mu_o} \left(\frac{\partial P_o}{\partial x} + g\rho_o \mathrm{Cos}\theta \right) \tag{3.2}$$

$$\frac{\partial q_w}{\partial x} = \frac{\partial q_o}{\partial x} = 0 \tag{3.3}$$

$$P_c = P_o - P_w \tag{3.4}$$

(b) Substitute for each variable in the problem a dimensionless variable by dividing the original variable by an arbitrary reference quantity having the same dimensions:

$$\zeta = \frac{x}{L} \tag{3.5}$$

$$f_w = \frac{q_w}{q_T} \tag{3.6}$$

$$f_o = \frac{q_o}{q_T} \tag{3.7}$$

$$\pi_c = \frac{P_c}{\sigma_{ow}(2/h)} \tag{3.8}$$

(c) From the definitions in part b, express the dimensional variable in terms of the reference quantities and dimensionless variables and insert these in the equations of part a:

$$f_w q_T = - \frac{h^2 A}{12\mu_w} \left(\frac{1}{L} \frac{\partial P_w}{\partial \xi} + g\rho_w \cos\theta\right) \tag{3.9}$$

$$(1-f_w) q_t = - \frac{h^2 A}{12\mu_o} \left(\frac{1}{L} \frac{\partial P_o}{\partial \xi} + g\rho_o \cos\theta\right) \tag{3.10}$$

$$\frac{\partial f_w}{\partial \xi} = 0 \tag{3.11}$$

$$\frac{\partial \pi_c}{\partial \xi} = \frac{h}{2\sigma_{ow}} \left(\frac{\partial P_o}{\partial \xi} - \frac{\partial P_w}{\partial \xi}\right) \tag{3.12}$$

Combine Equations 3.10 and 3.9 with 3.12

$$\frac{\partial \pi_c}{\partial \xi} = \frac{6\mu_w q_T L}{\sigma_{ow} hA}\left[f_w + (1-f_w)\frac{\mu_o}{\mu_w} + \frac{h^2 g(\rho_o-\rho_w)\cos\theta}{12V\mu_w}\right] \qquad (3.13)$$

Therefore ;

$$N_c = \frac{6\mu_w VL}{\sigma_{ow} h} \qquad (3.14)$$

$$N_g = \frac{h^2 g(\rho_o-\rho_w)\cos\theta}{12\mu_w V} \qquad (26)$$

$$M = \frac{\mu_o}{\mu_w} \qquad (27)$$

APPENDIX 4

CALCULATION OF THE TOTAL BASE AREA OF THE FINGERS

In general, for any mode m, the total base area of the water fingers is given by

$$A_{bw} = mL_{xw}h \tag{4.1}$$

It can be shown, on the initially straight interface, that (see Equation 58)

$$\frac{L_{xw}}{L_x} = \frac{1}{m}\left(\frac{\alpha_o}{\alpha_o+\alpha_w}\right) \tag{4.2}$$

Upon introducing Equation 40 into Equation 58, the following equation is obtained

$$L_{xw} = \frac{L_x}{m}\frac{M^{1/3}}{1+M^{1/3}} \tag{4.3}$$

Introduction of Equation 4.3 in Equation 4.1 leads to

$$A_{bw} = L_x h \frac{M^{1/3}}{1+M^{1/3}} \tag{4.4}$$

It is seen, from Equation 4.4, that the total base area of the water fingers will be constant for a particular cell and fluid pair, regardless of the number of fingers present, as Equation 4.4 is not a function of m. If the total base area of water fingers is independent of the number of fingers present, the total base area of oil fingers must also be independent of number of fingers because of material balance demands.

APPENDIX 5

ADDITIONAL PLOTS OF INTERFACE AT DIFFERENT TIMES FOR RUNS 31, 33, 34, 42 AND 50

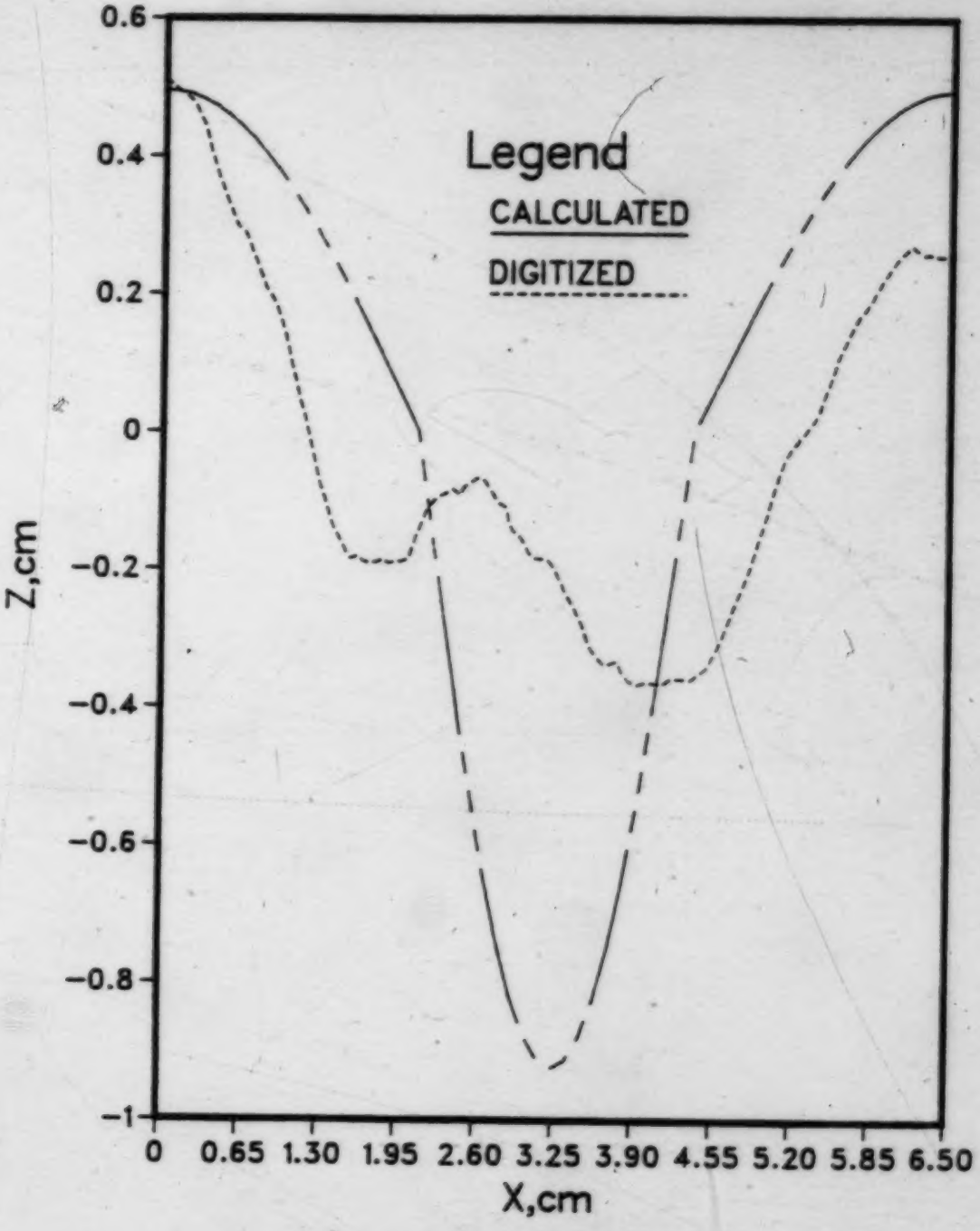

FIG.29 THE INTERFACE AT T=127 SEC. FOR RUN 31

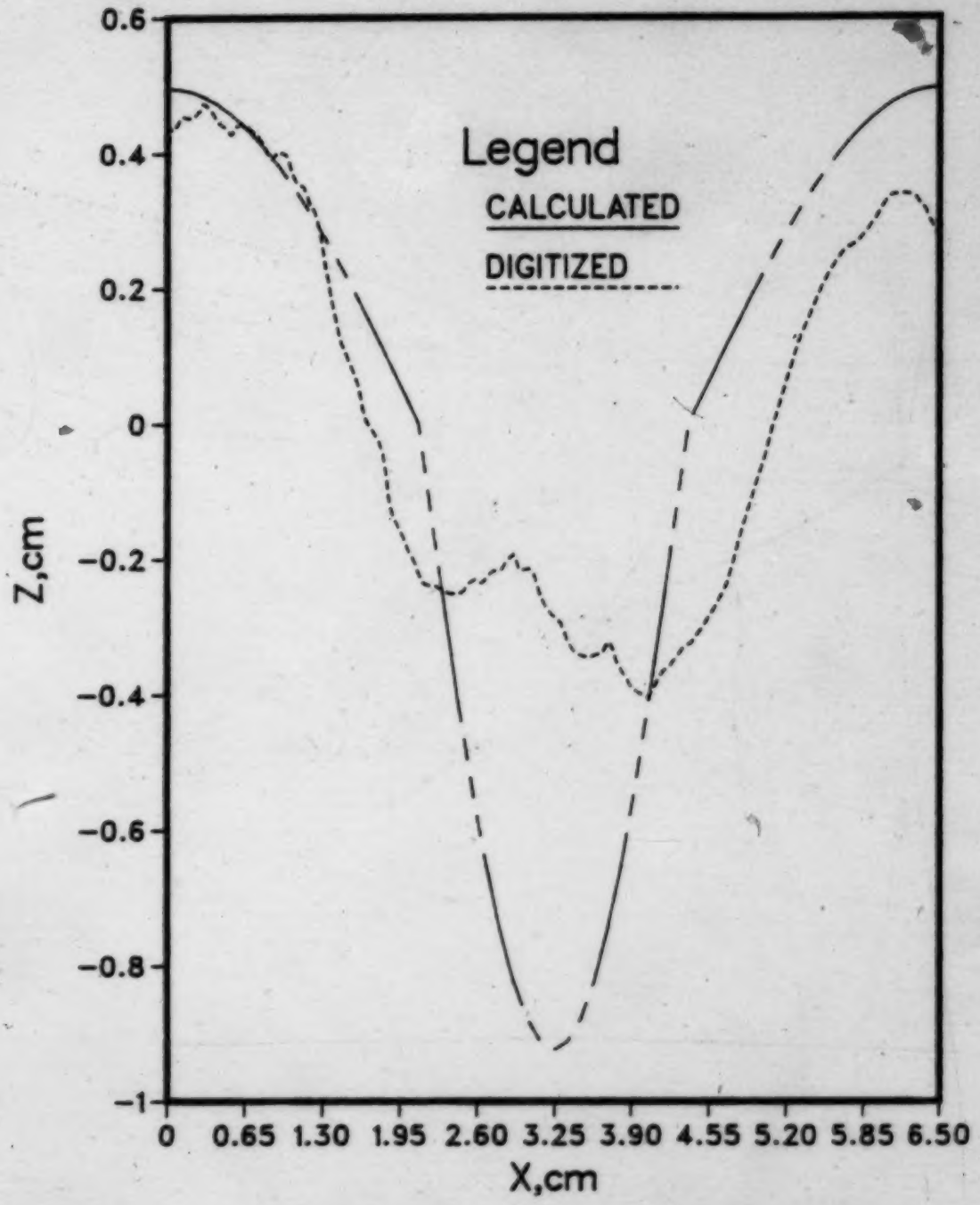

FIG.30 THE INTERFACE AT T=214 SEC. FOR RUN 31

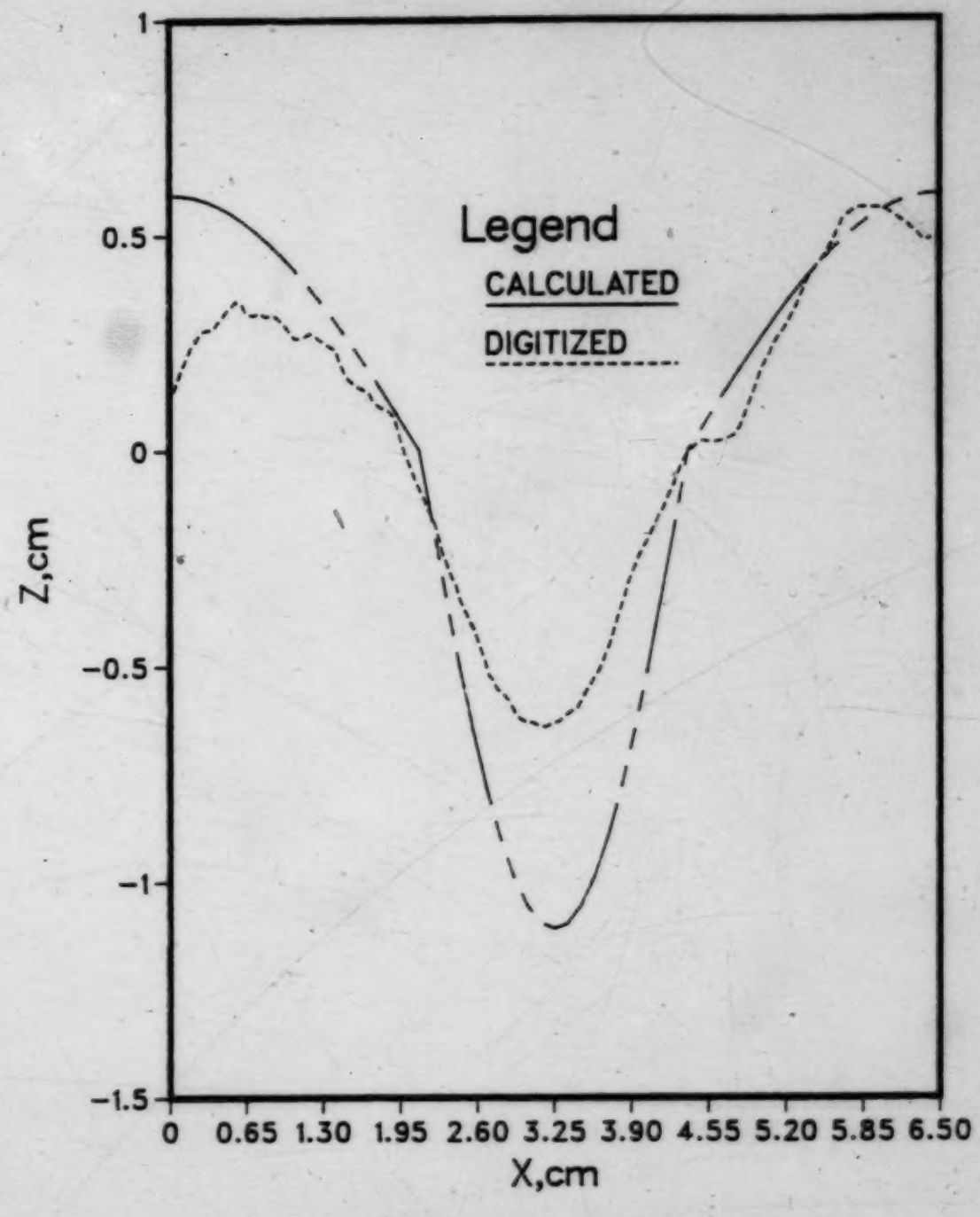

FIG.31 THE INTERFACE AT T=370 SEC. FOR RUN 31

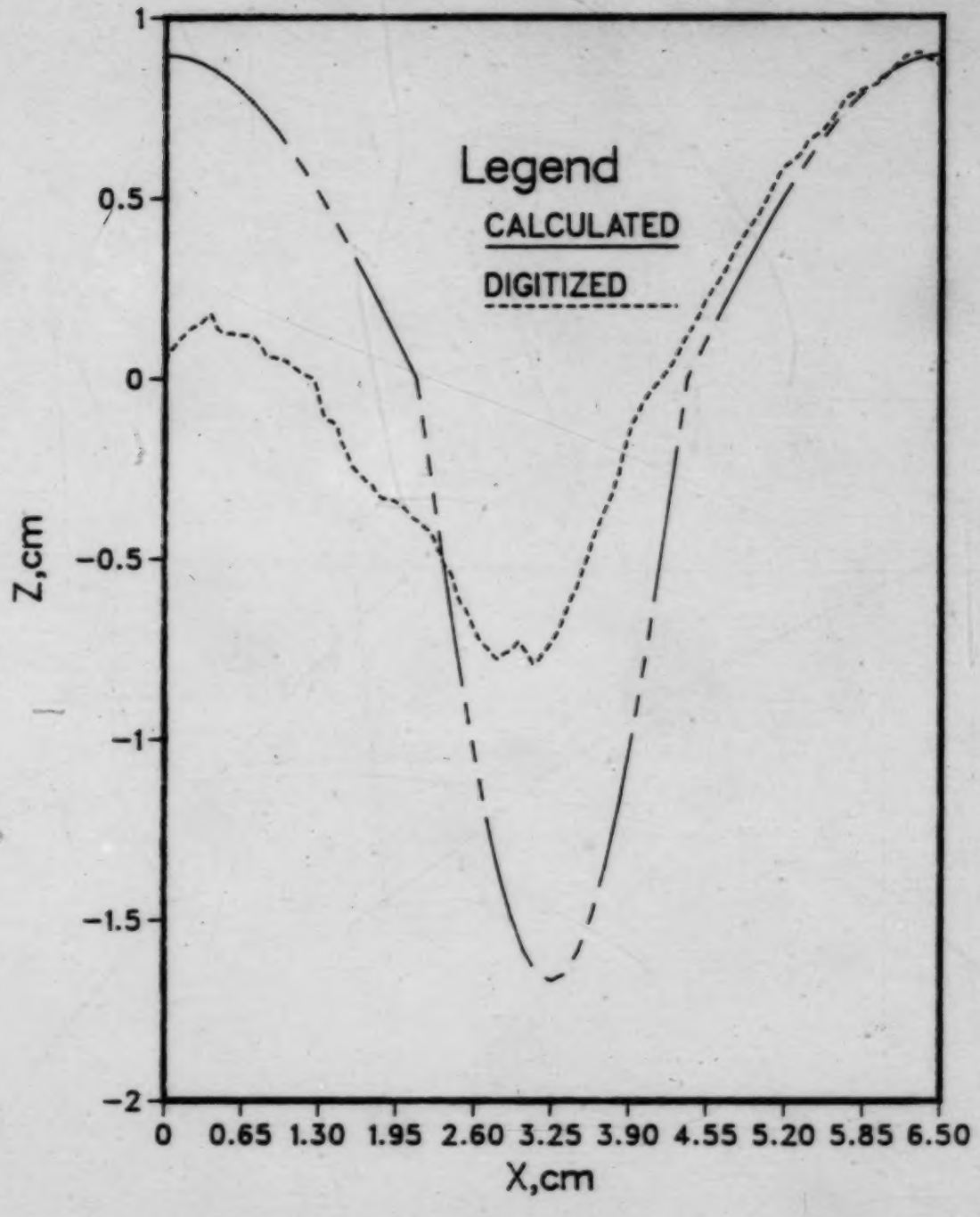

FIG.32 THE INTERFACE AT T=498 SEC. FOR RUN 31

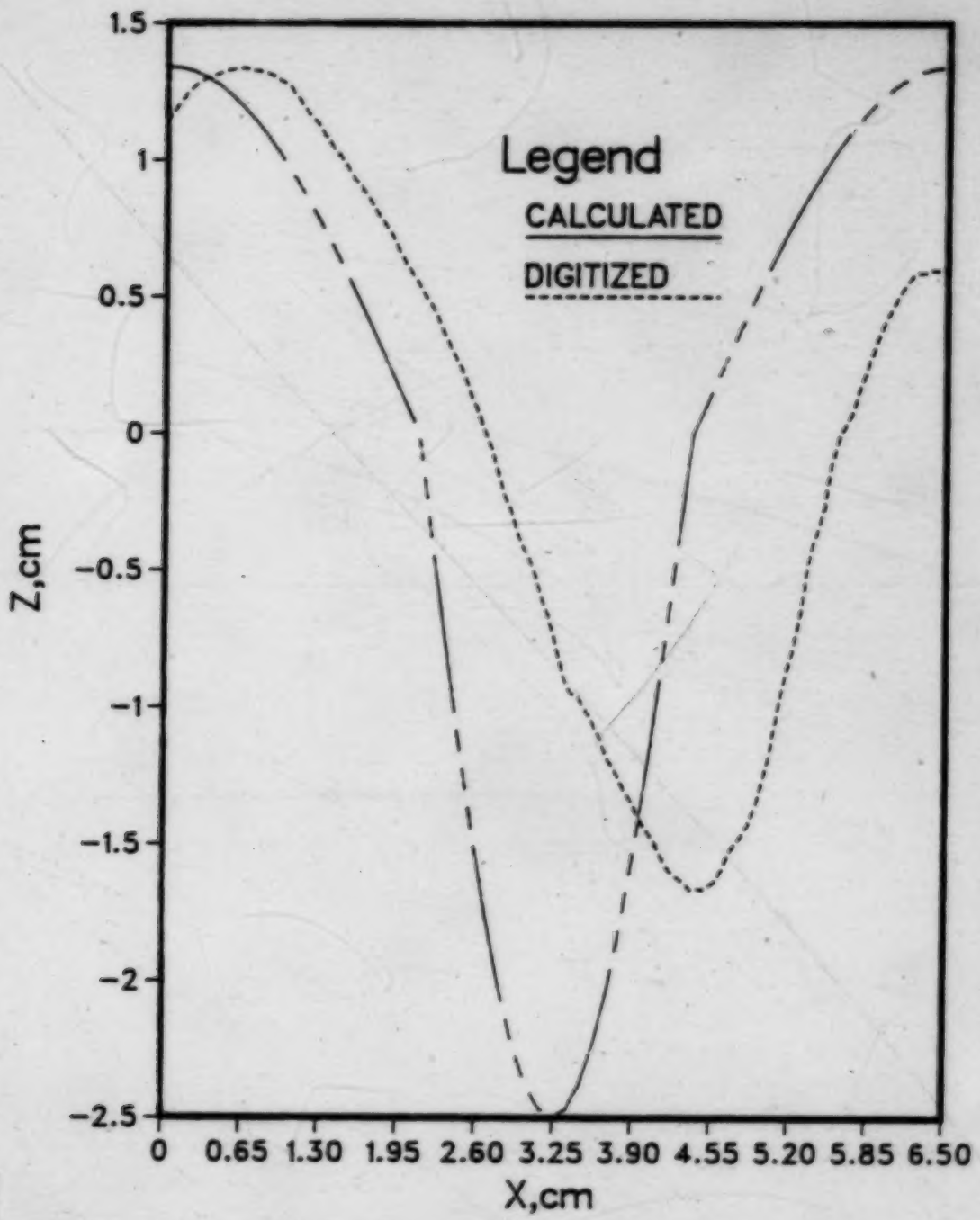

FIG.33 THE INTERFACE AT T=680 SEC. FOR RUN 33

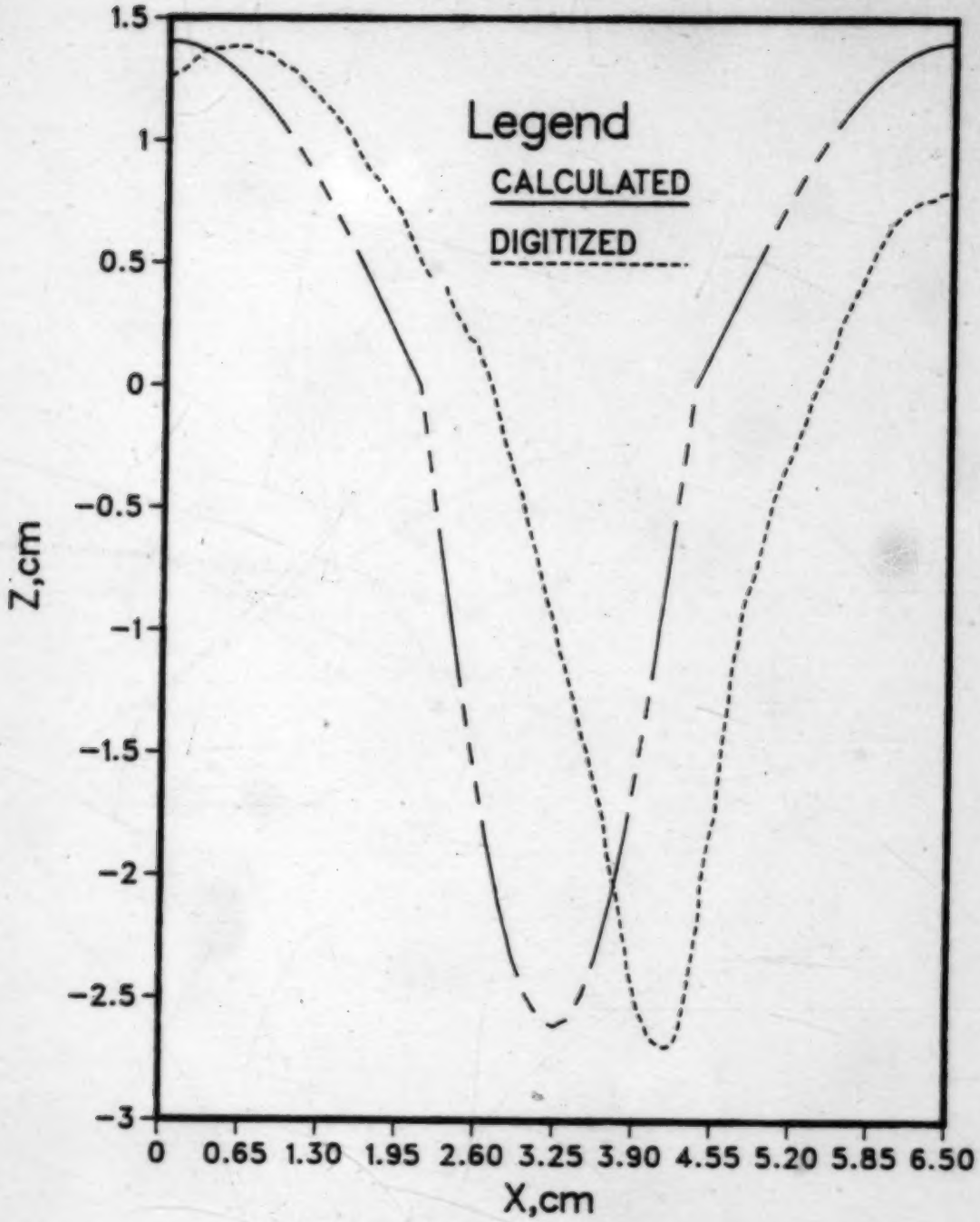

FIG.34 THE INTERFACE AT T=812 SEC. FOR RUN 33

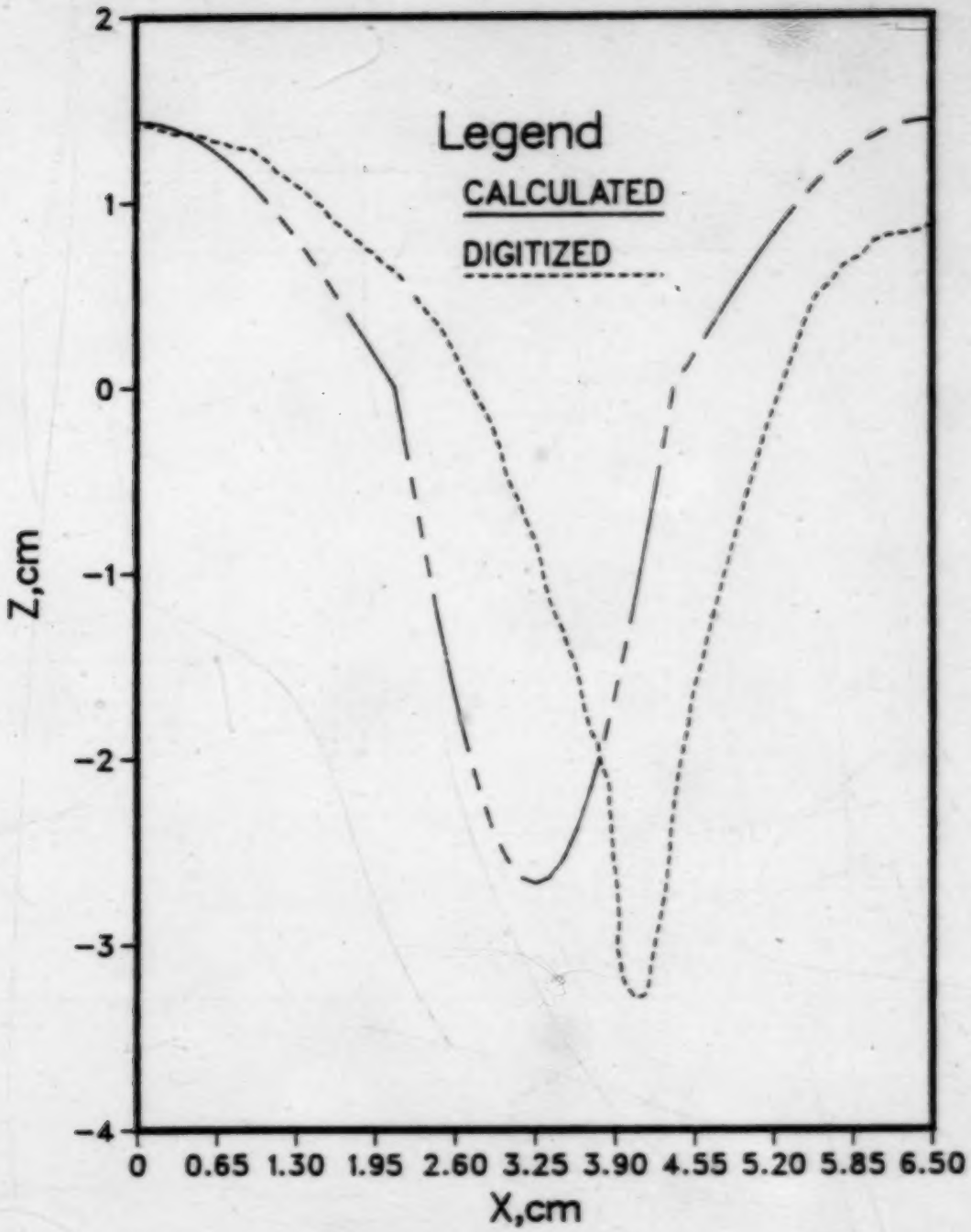

FIG.35 THE INTERFACE AT T=870 SEC. FOR RUN 33

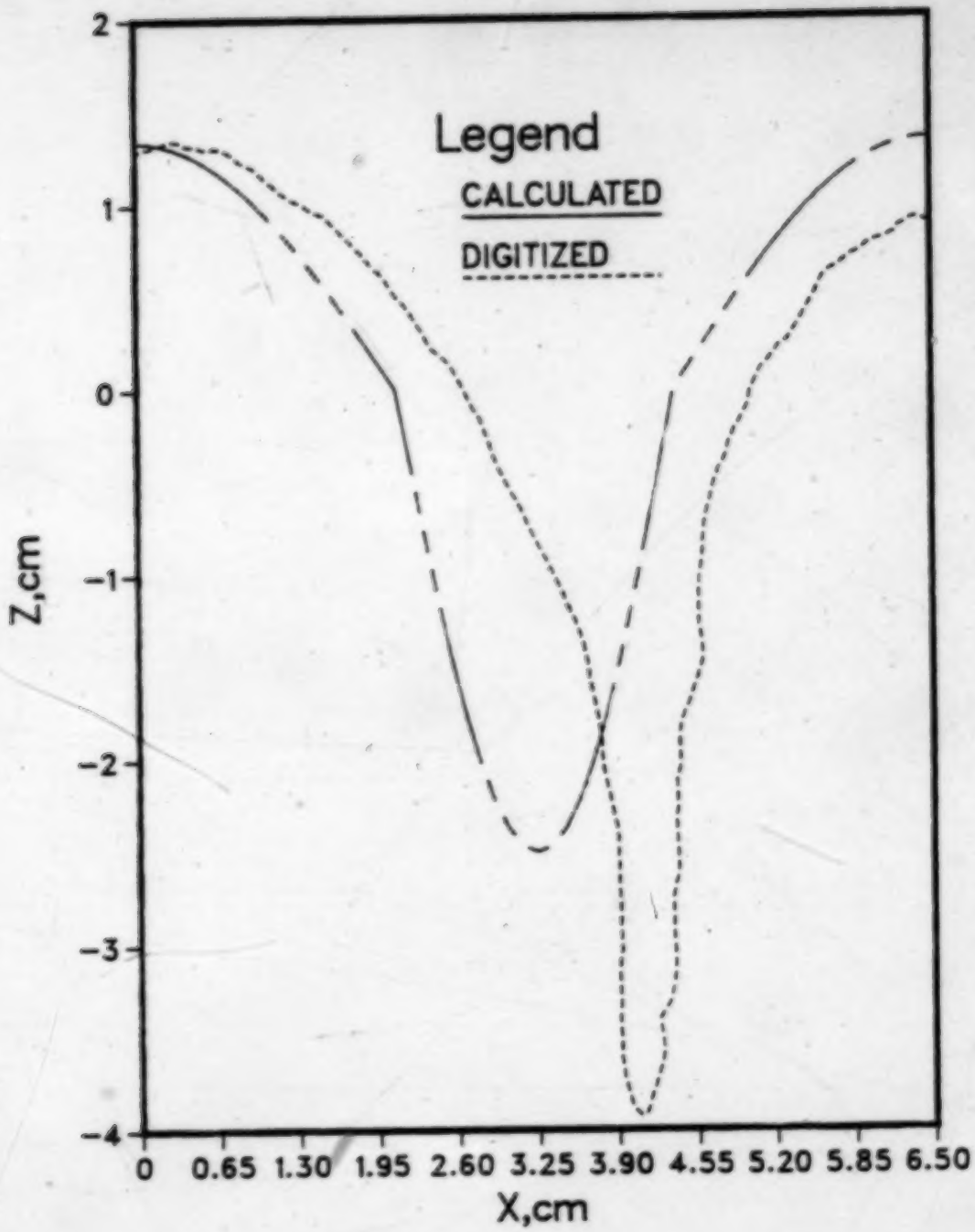

FIG.36 THE INTERFACE AT T=968 SEC. FOR RUN 33

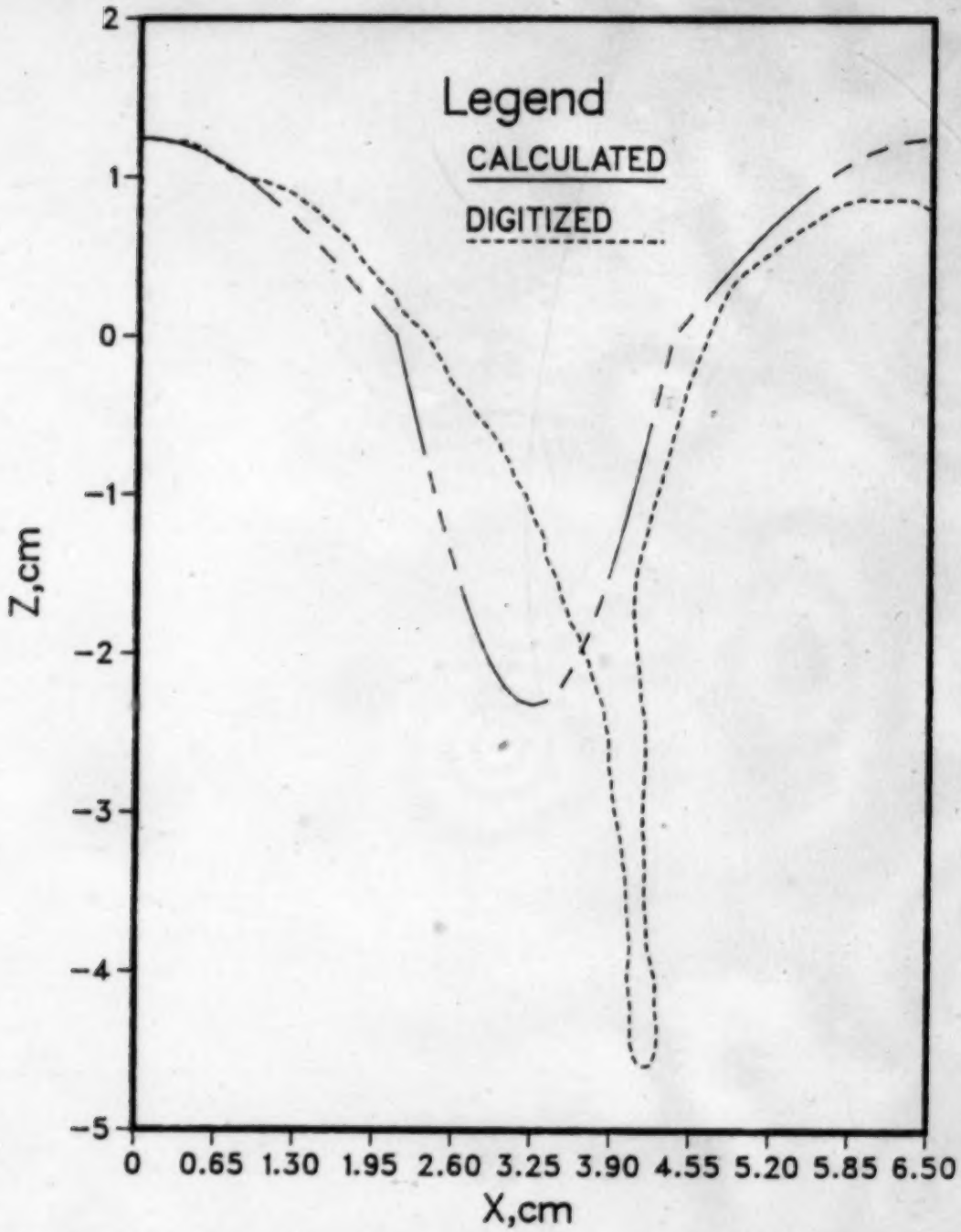

FIG.37 THE INTERFACE AT T=1008 SEC. FOR RUN 33

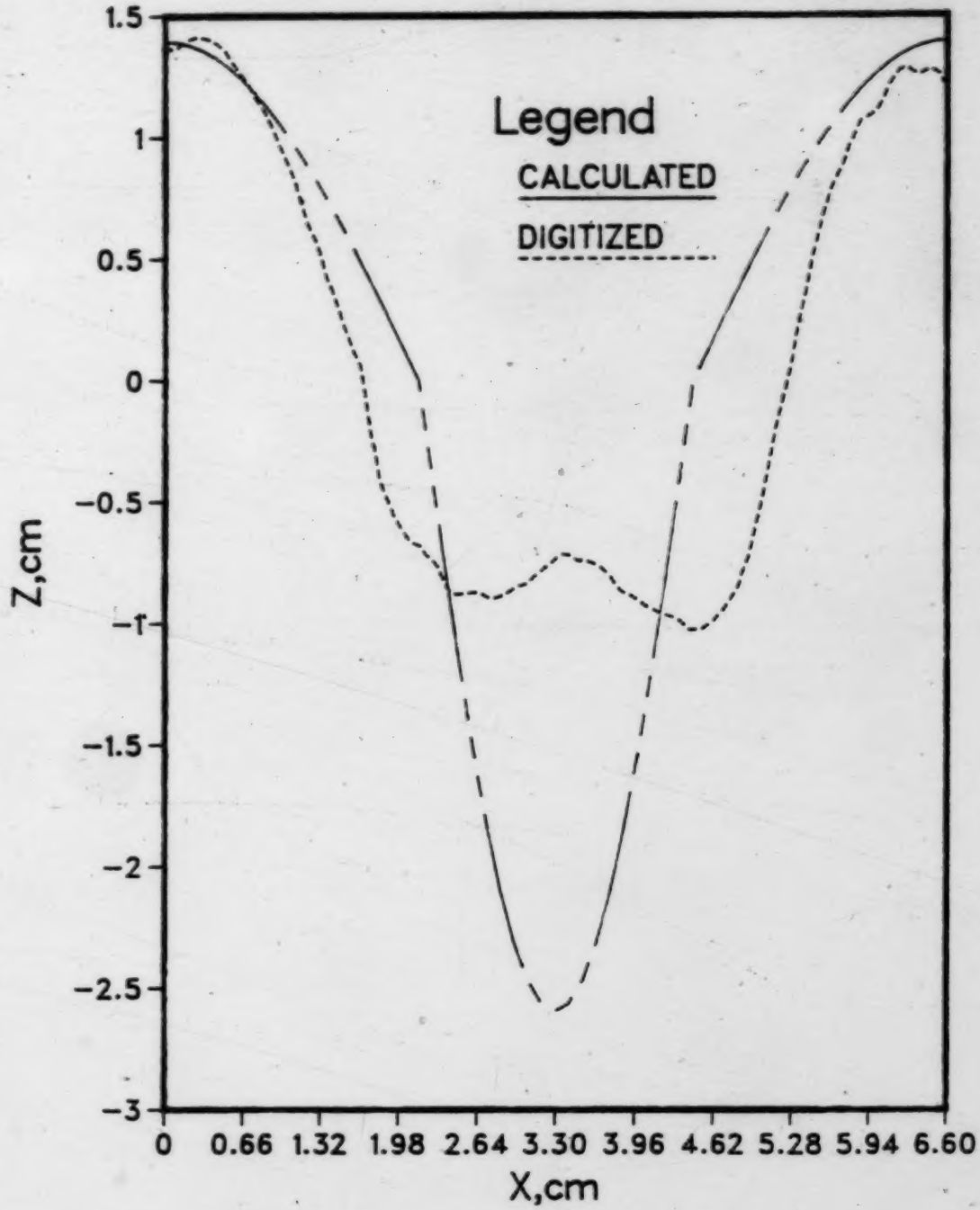

FIG.38 THE INTERFACE AT T=308 SEC. FOR RUN 34

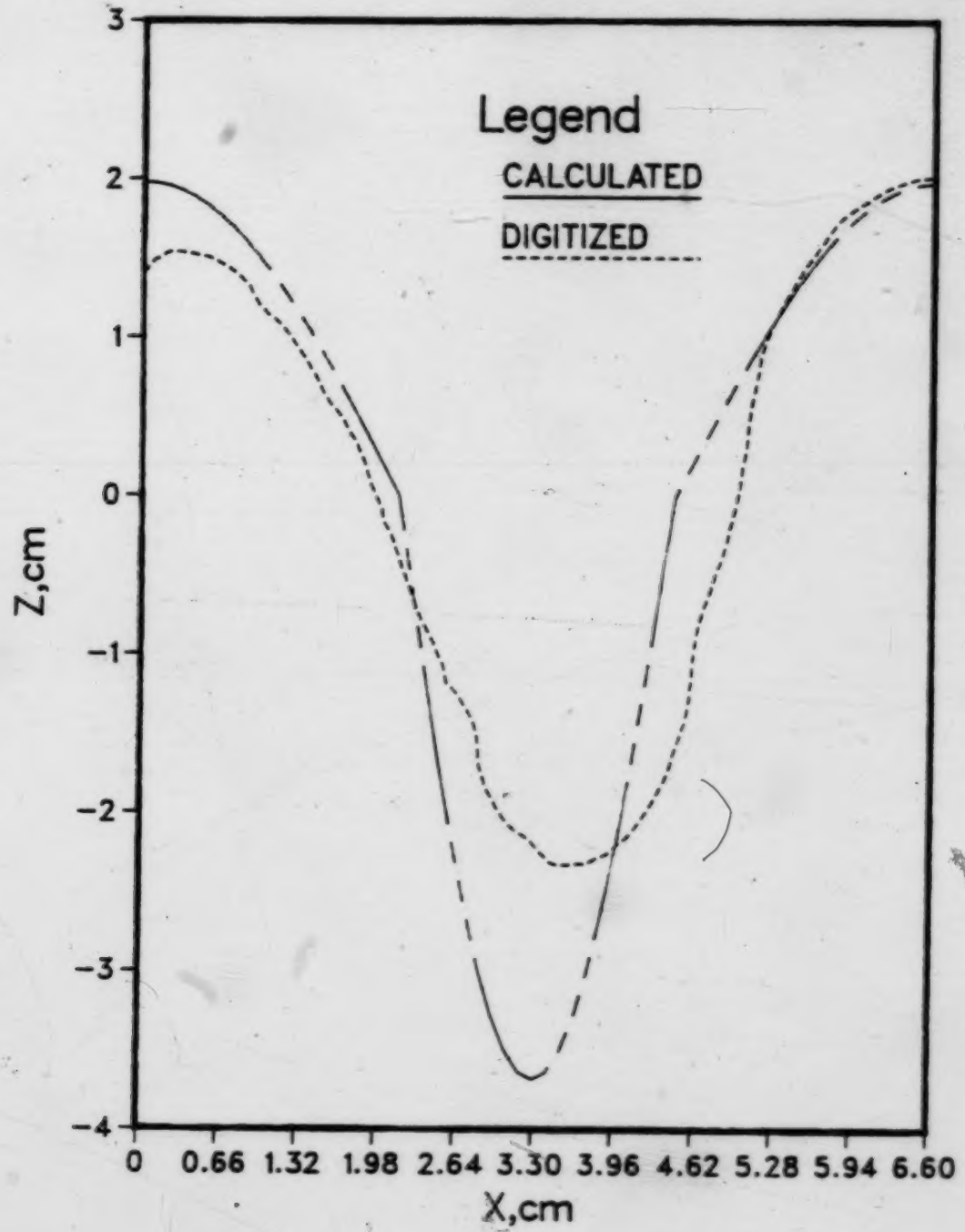

FIG.39 THE INTERFACE AT T=413 SEC.
FOR RUN 34

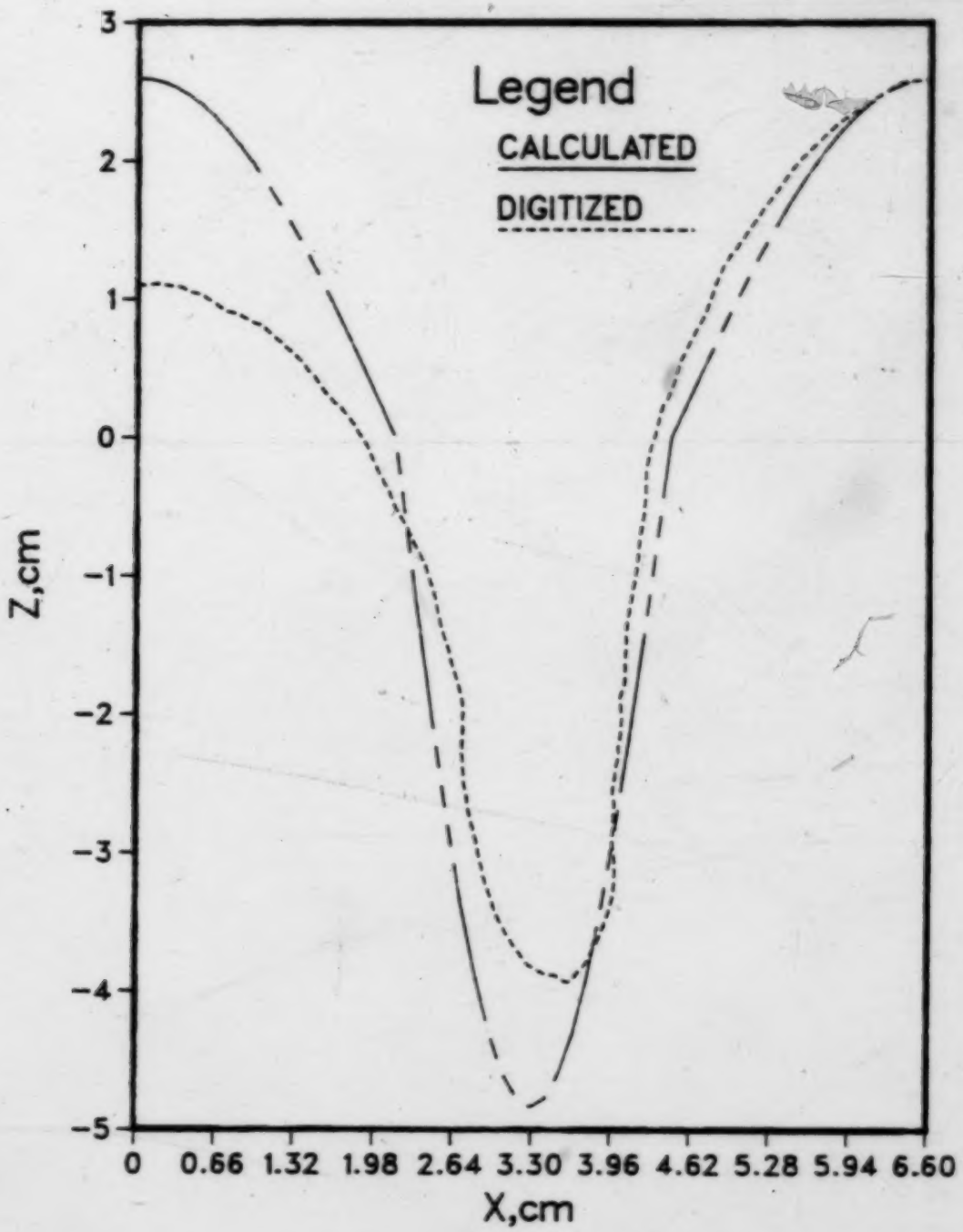

FIG.40 THE INTERFACE AT T=493 SEC. FOR RUN 34

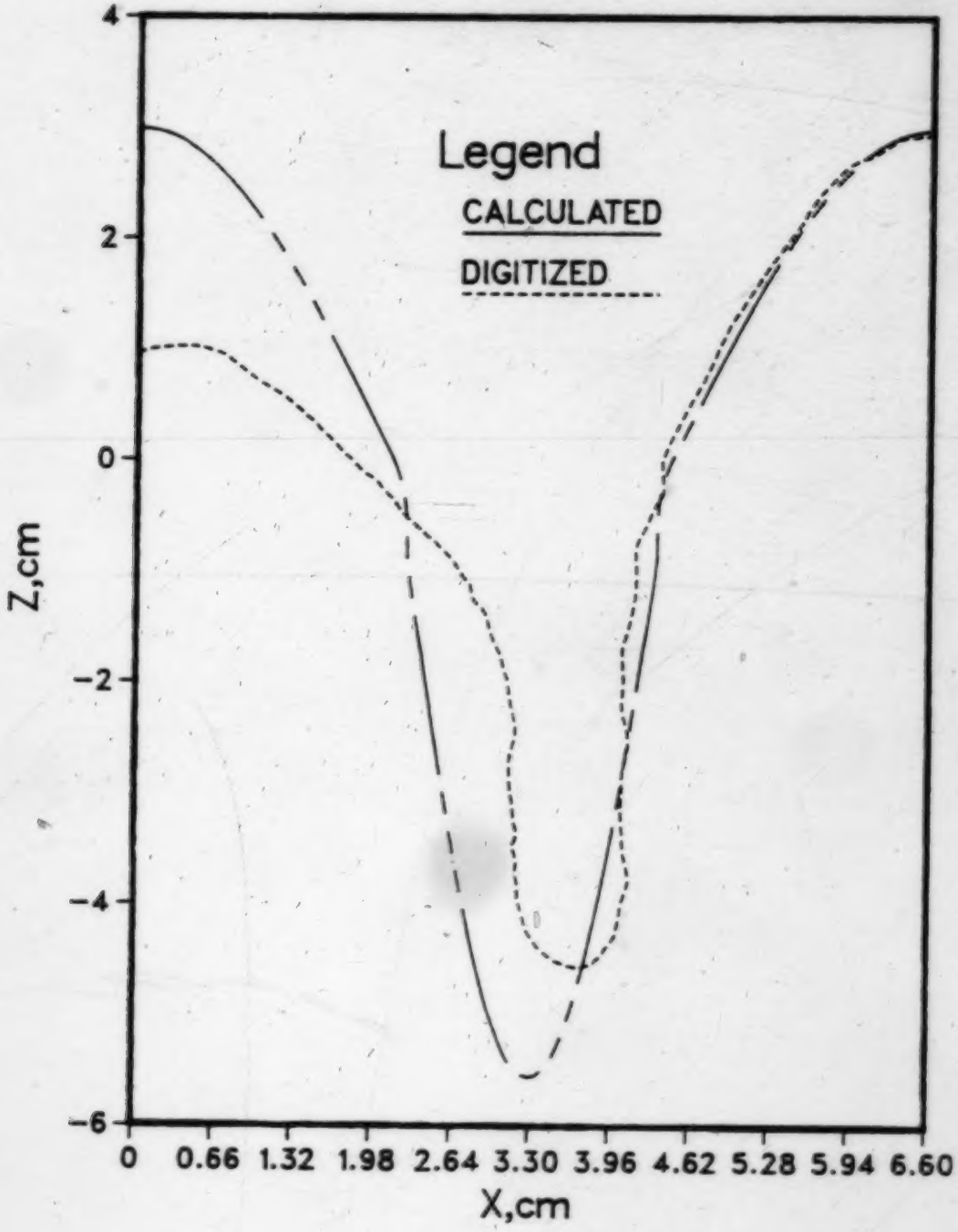

FIG.41 THE INTERFACE AT T=525 SEC. FOR RUN 34

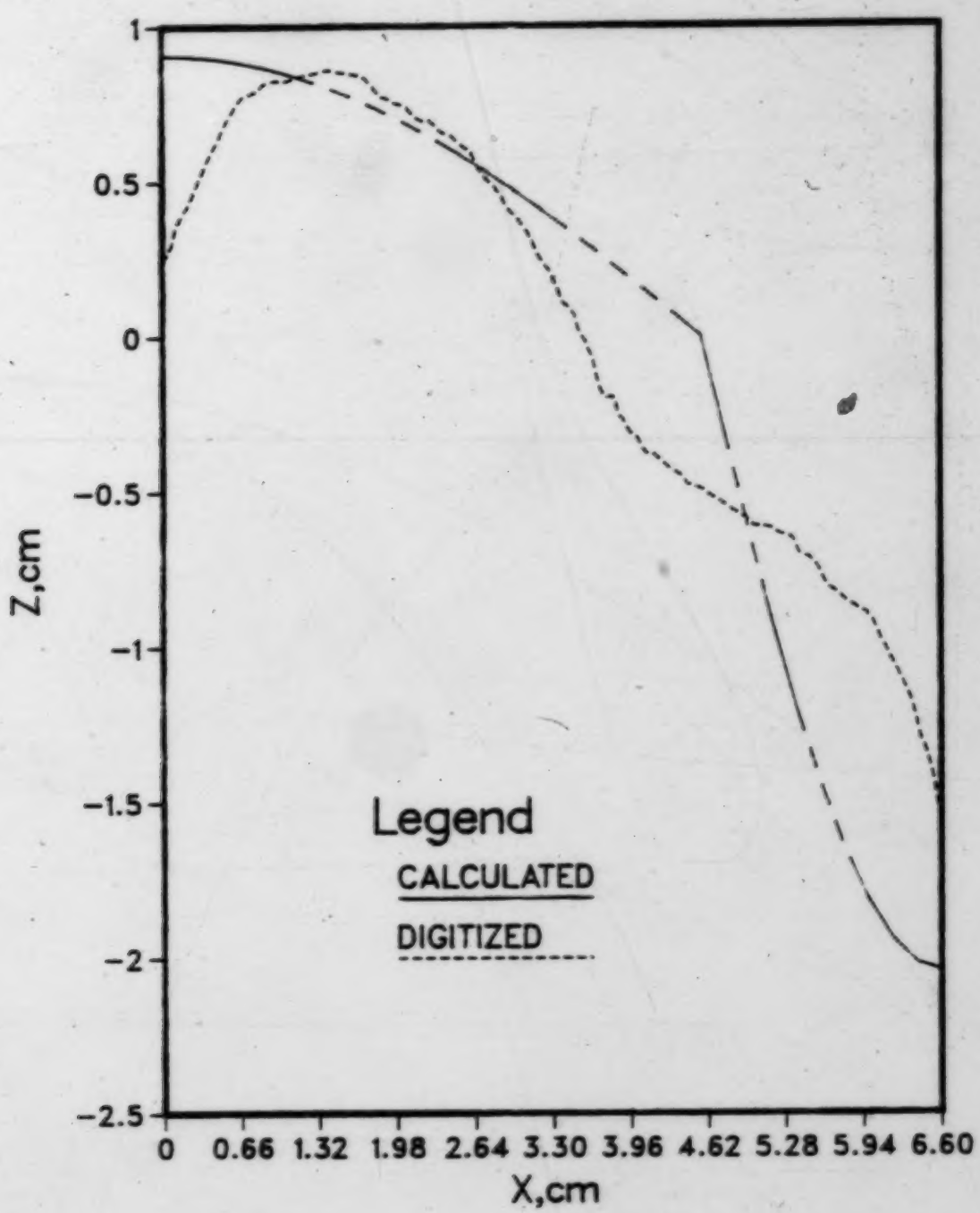

FIG.42 THE INTERFACE AT T=5981 SEC. FOR RUN 42

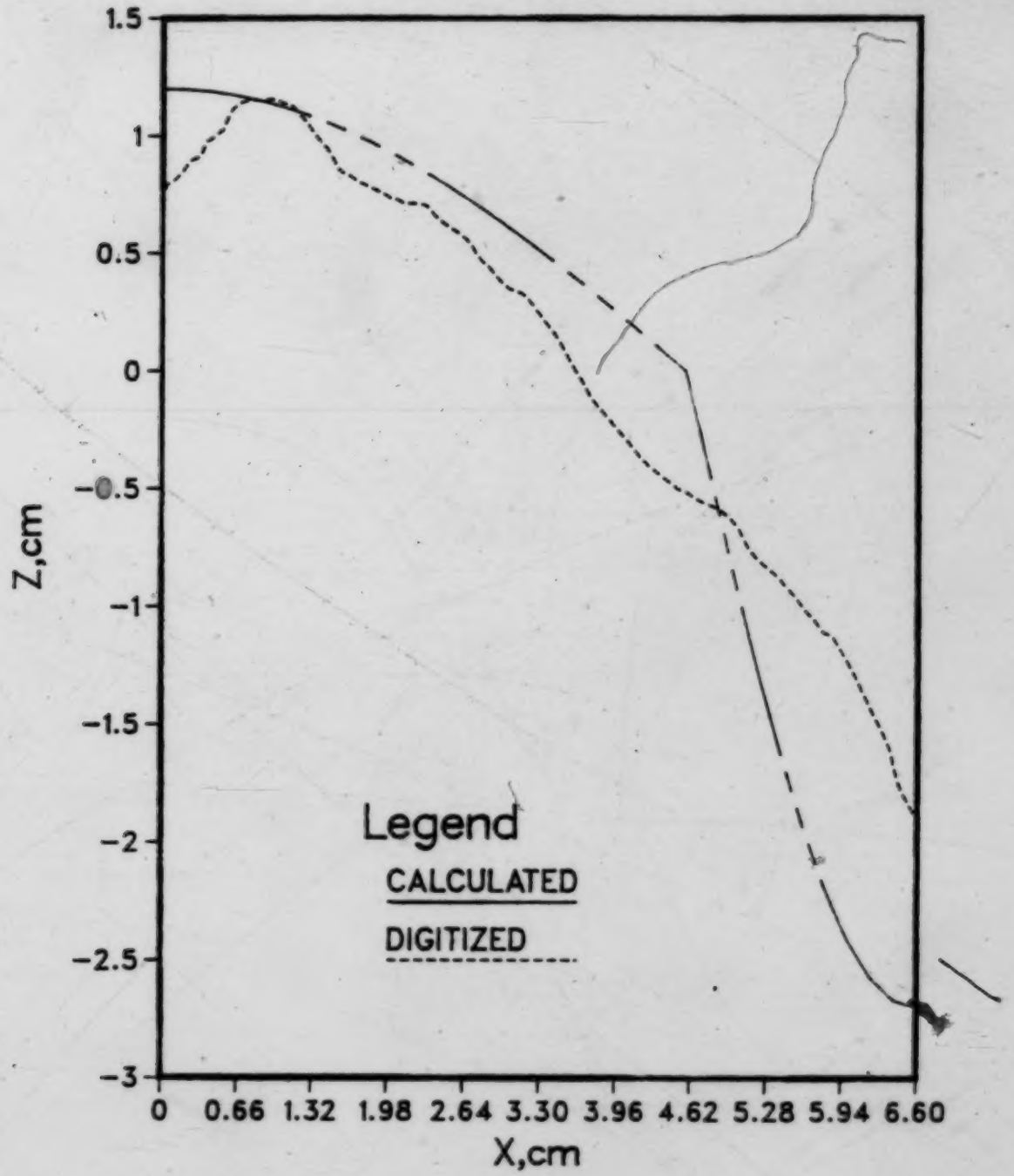

FIG.43 THE INTERFACE AT T=7135 SEC. FOR RUN 42

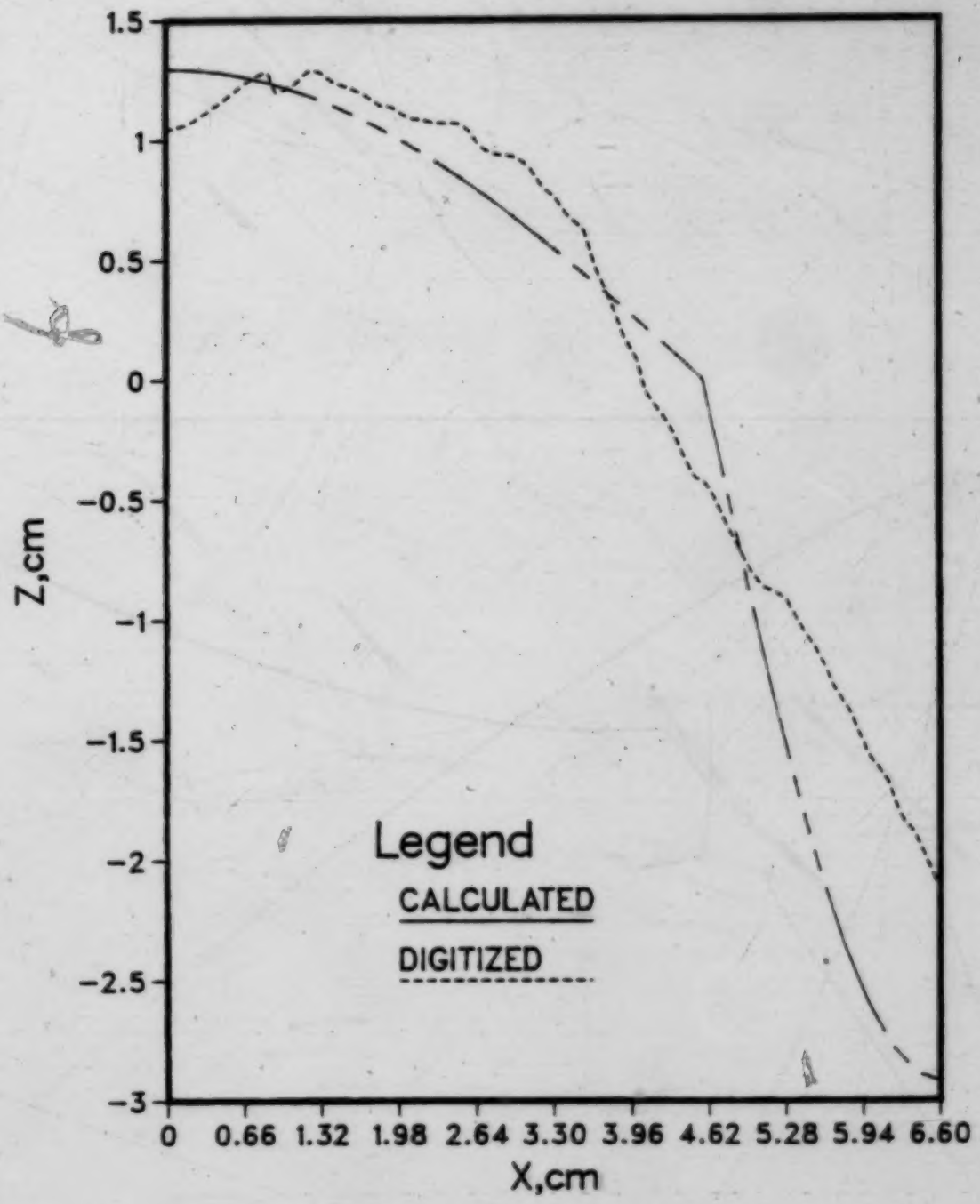

FIG.44 THE INTERFACE AT T=7878 SEC. FOR RUN 42

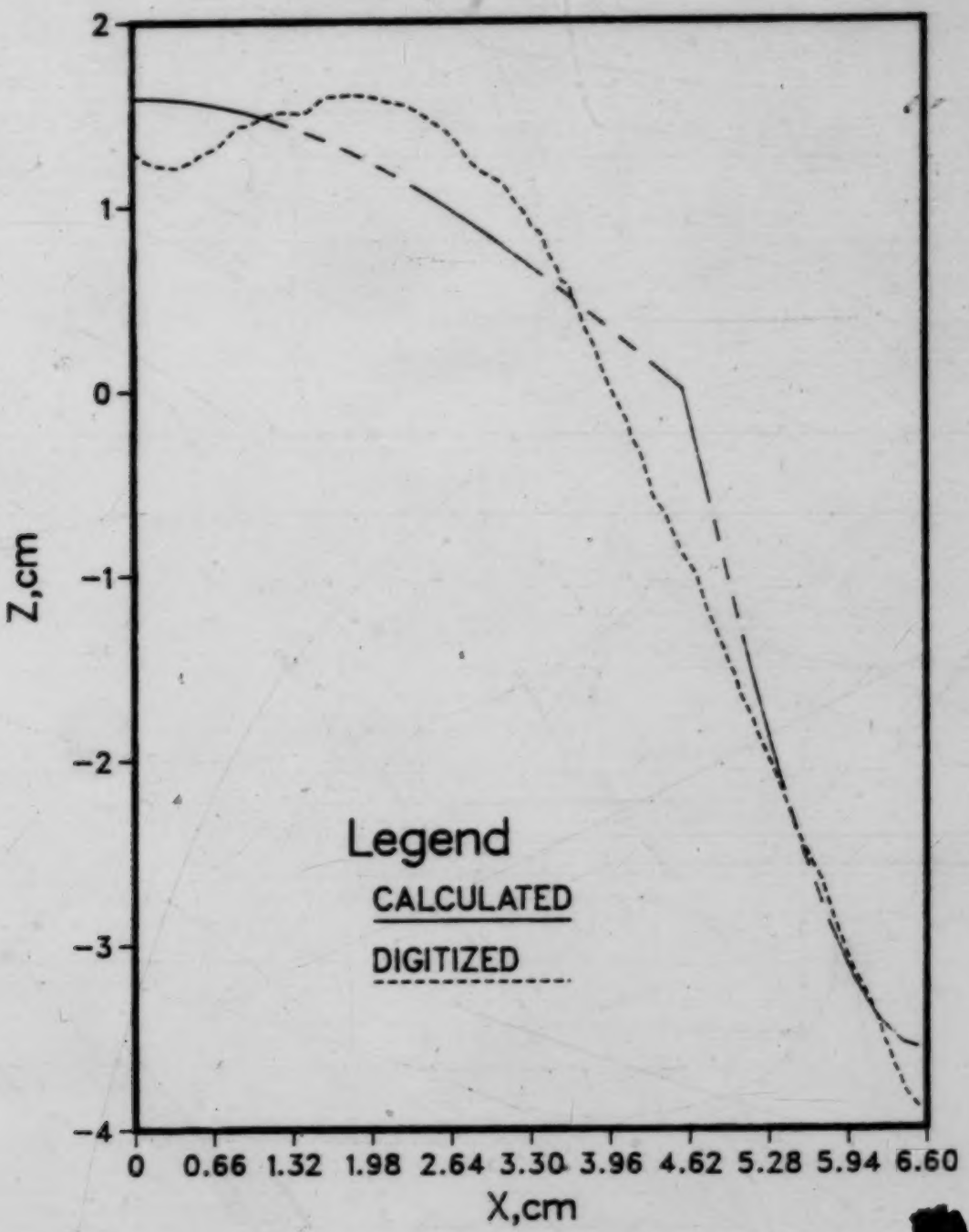

FIG.45 THE INTERFACE AT T=9976 SEC.
FOR RUN 42

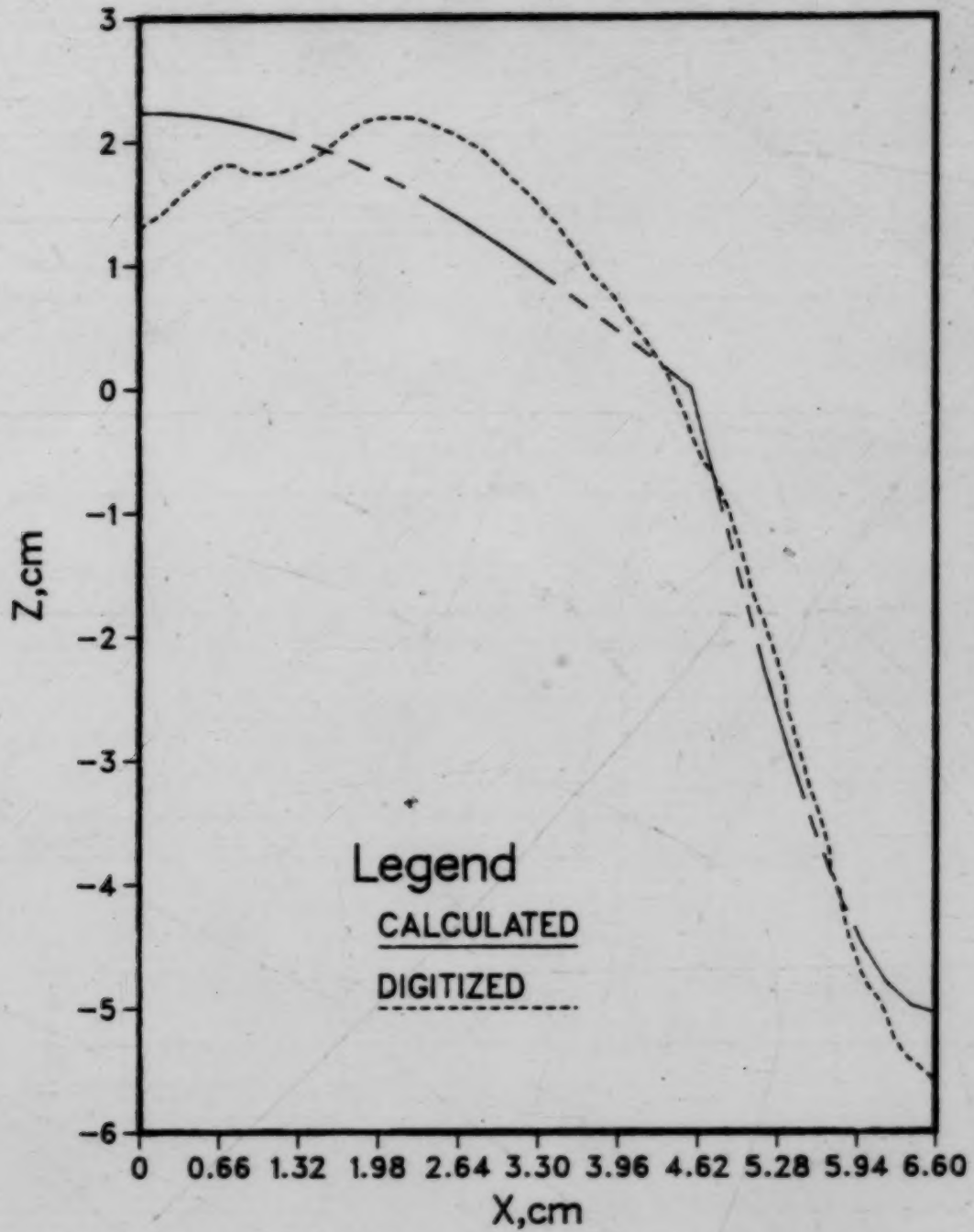

FIG.46 THE INTERFACE AT T=12014 SEC. FOR RUN 42

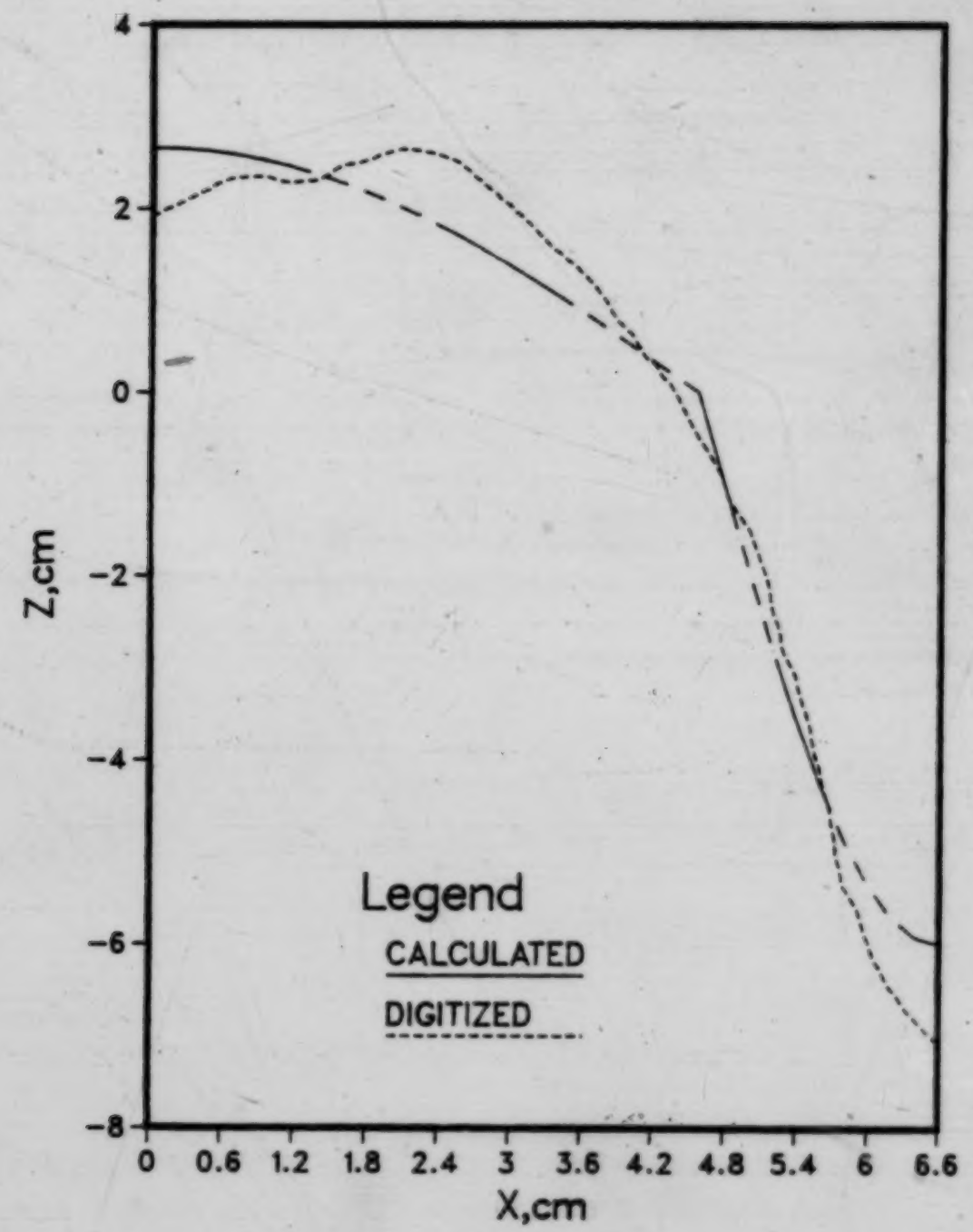

FIG.47 THE INTERFACE AT T=13219 SEC. FOR RUN 42

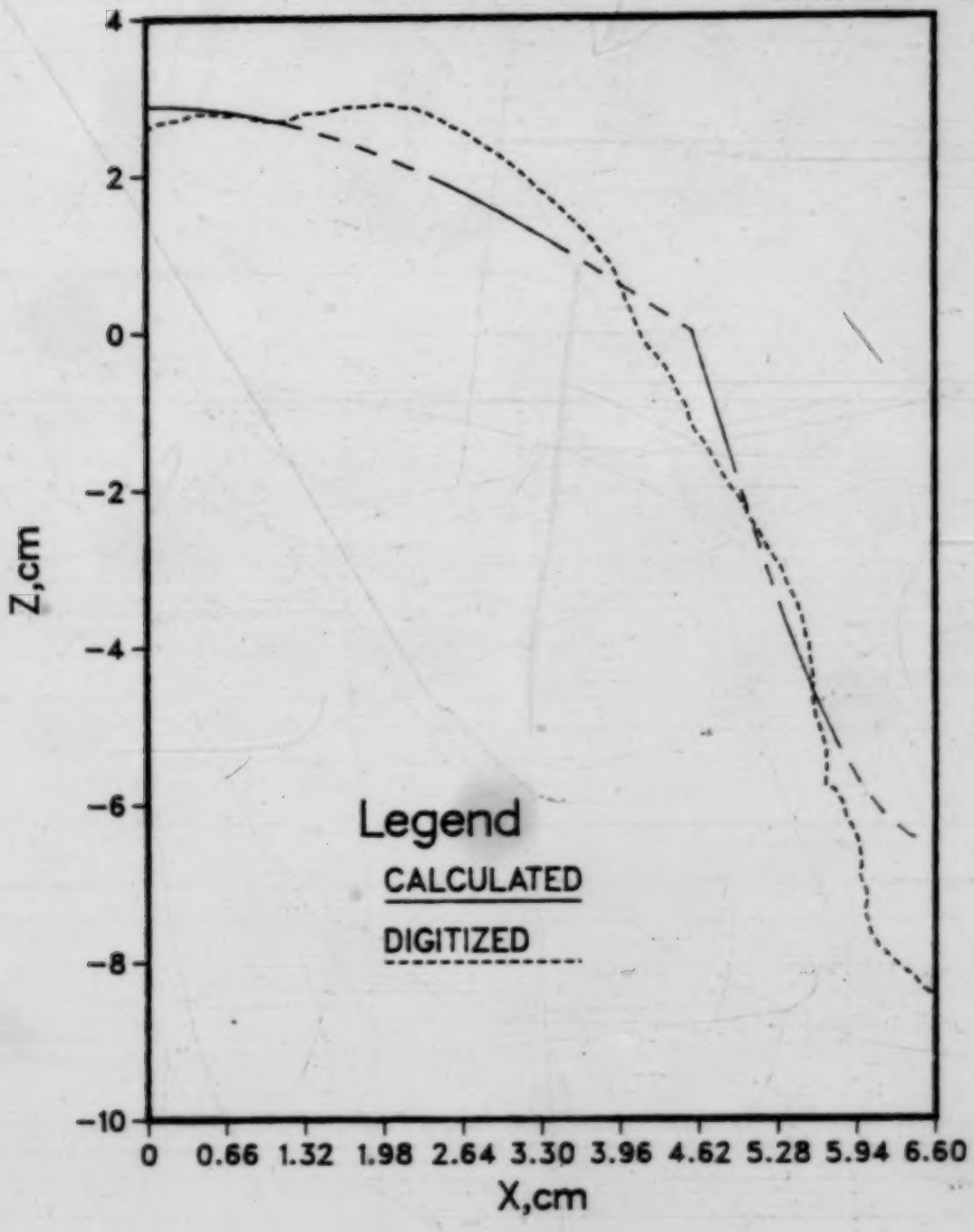

FIG.48 THE INTERFACE AT T=14427 SEC. FOR RUN 42

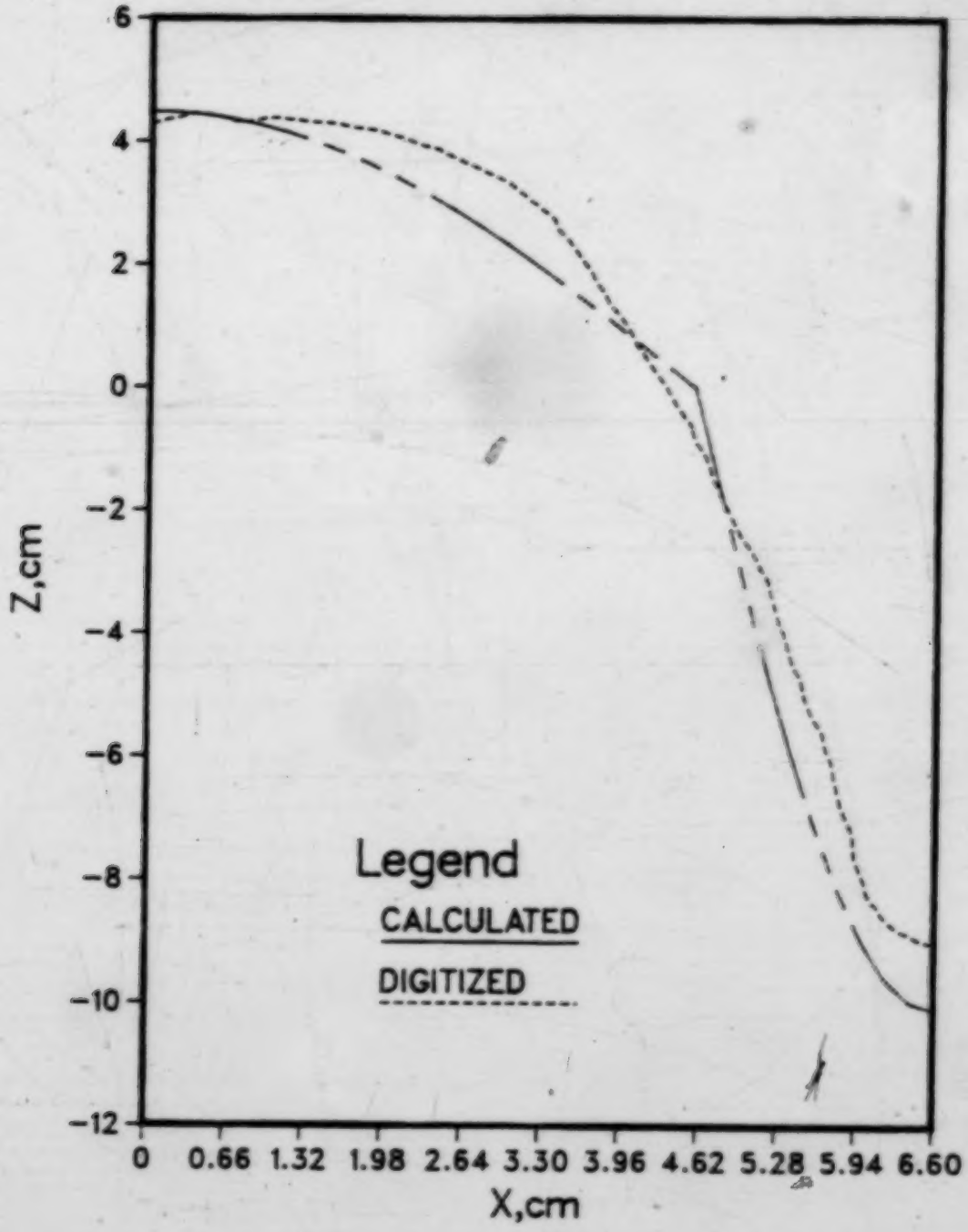

FIG.49 THE INTERFACE AT T=15092 SEC. FOR RUN 42

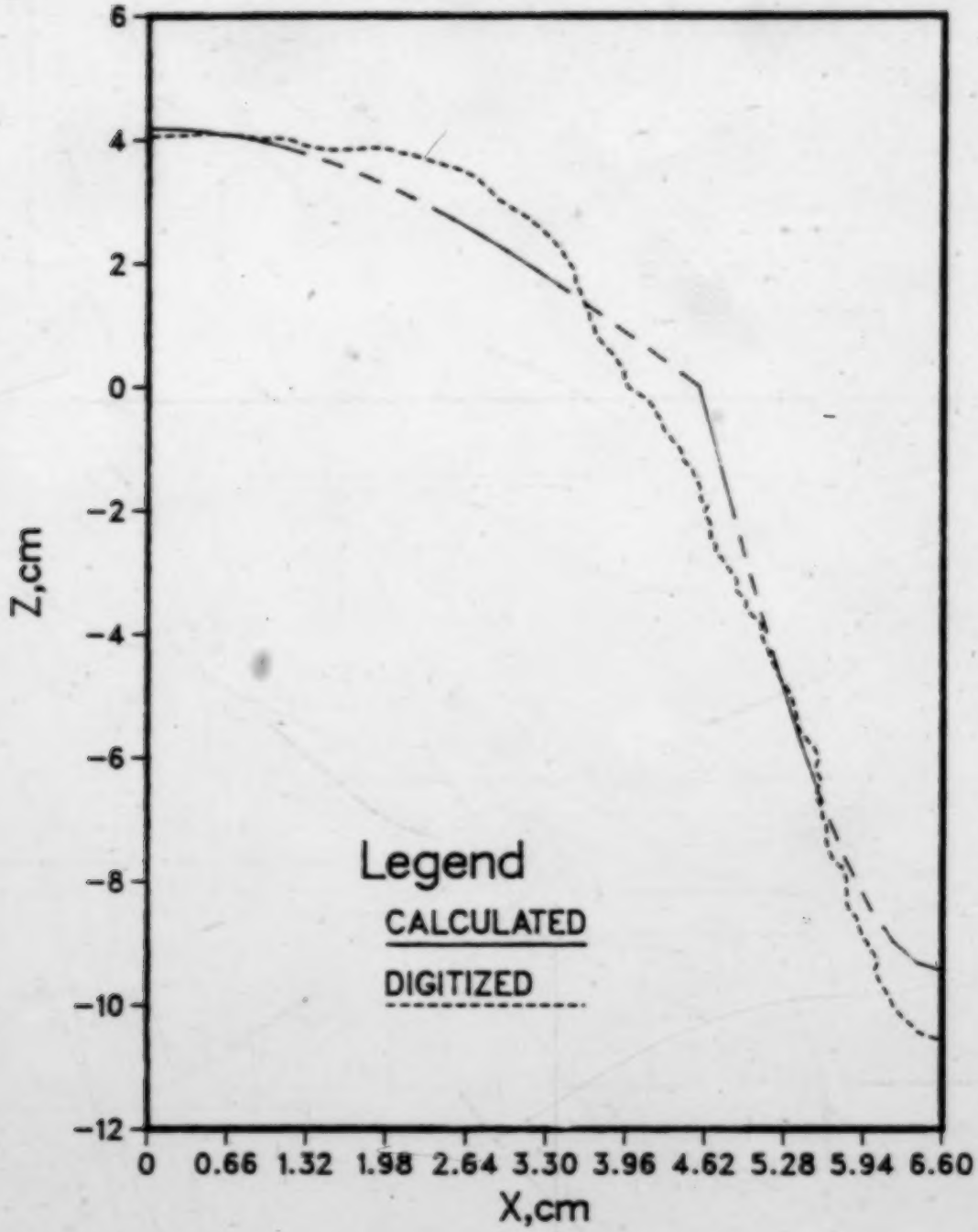

FIG.60 THE INTERFACE AT T=16466 SEC.
FOR RUN 42

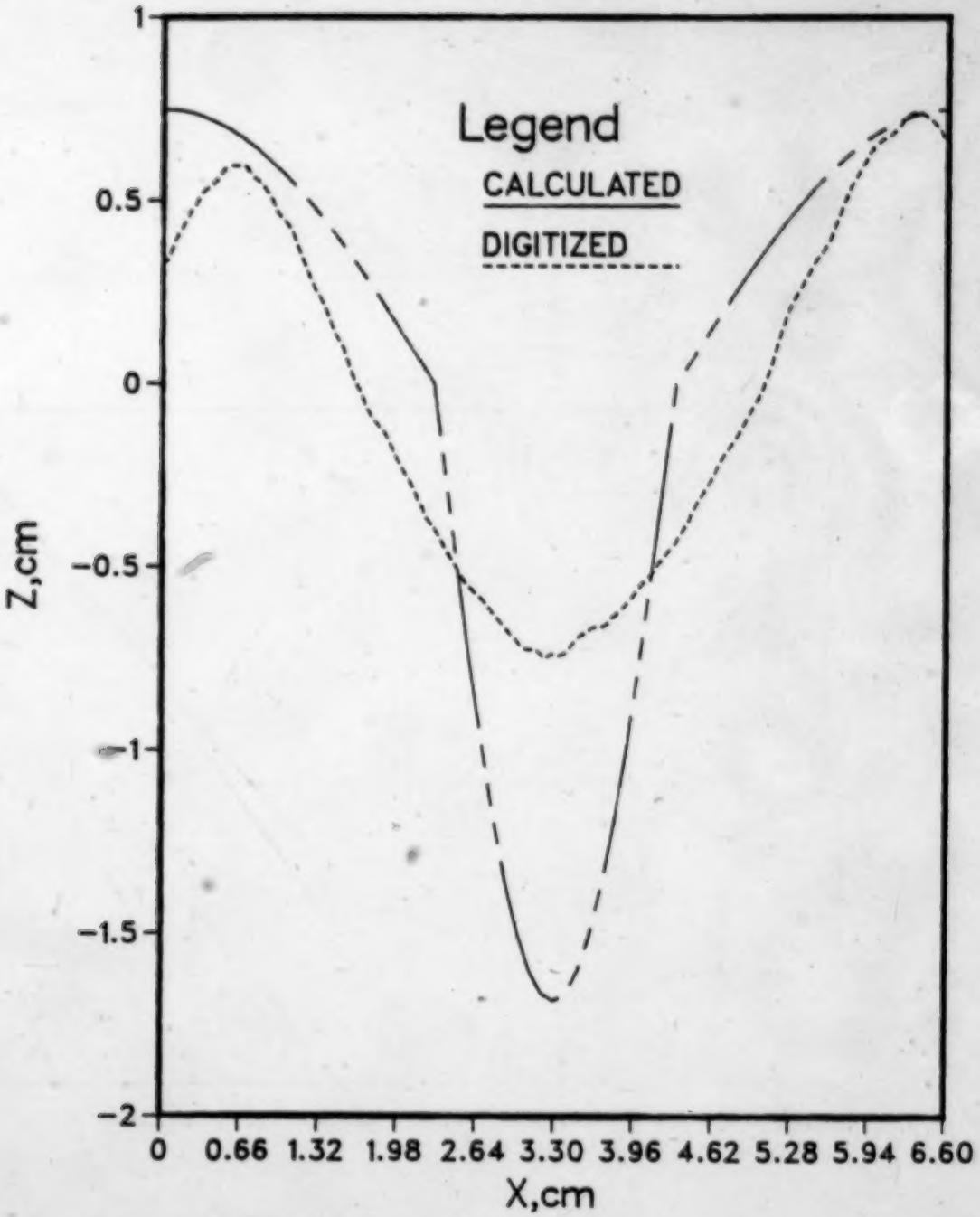

FIG.51 THE INTERFACE AT T=288 SEC. FOR RUN 50

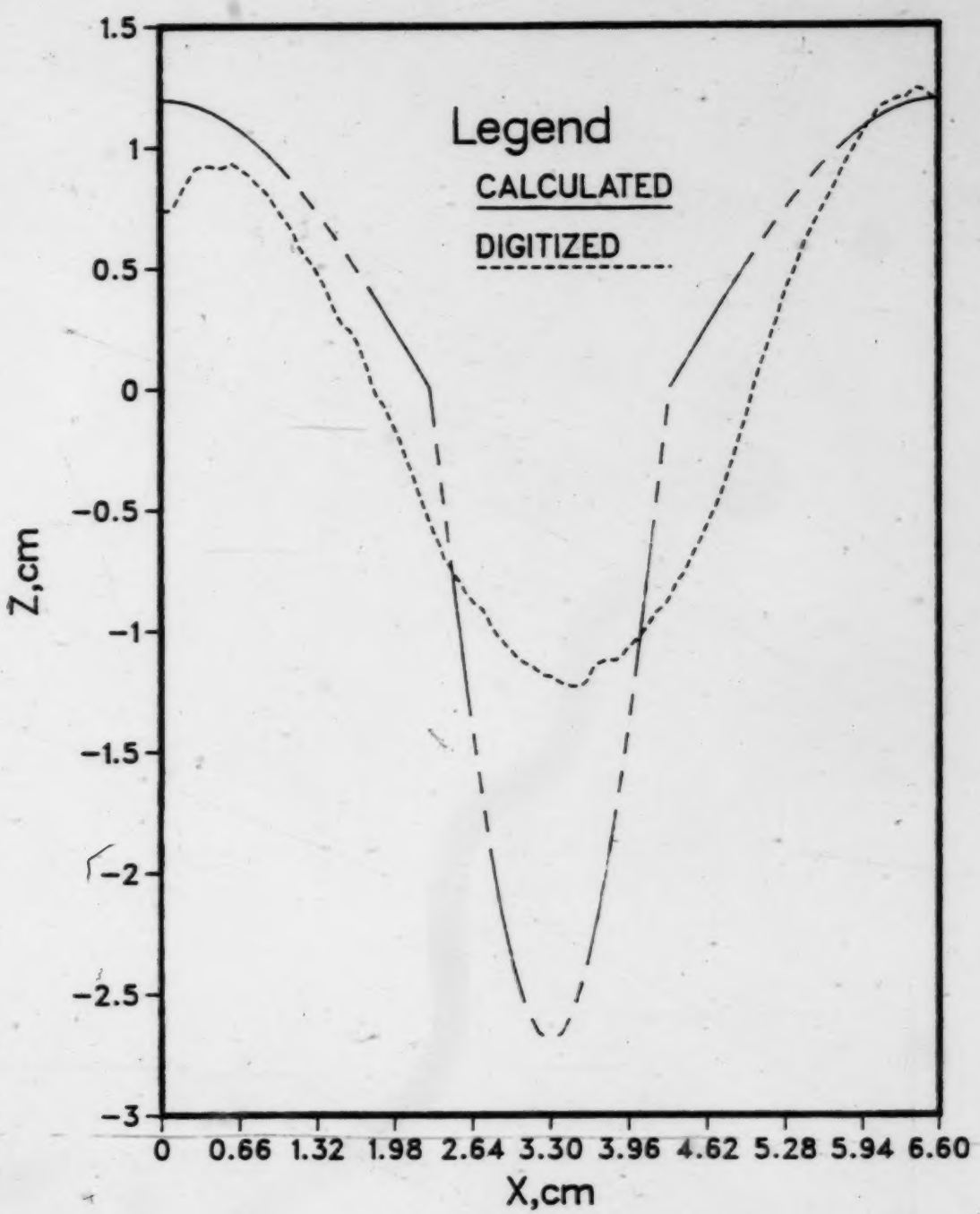

FIG.52 THE INTERFACE AT T=435 SEC. FOR RUN 50

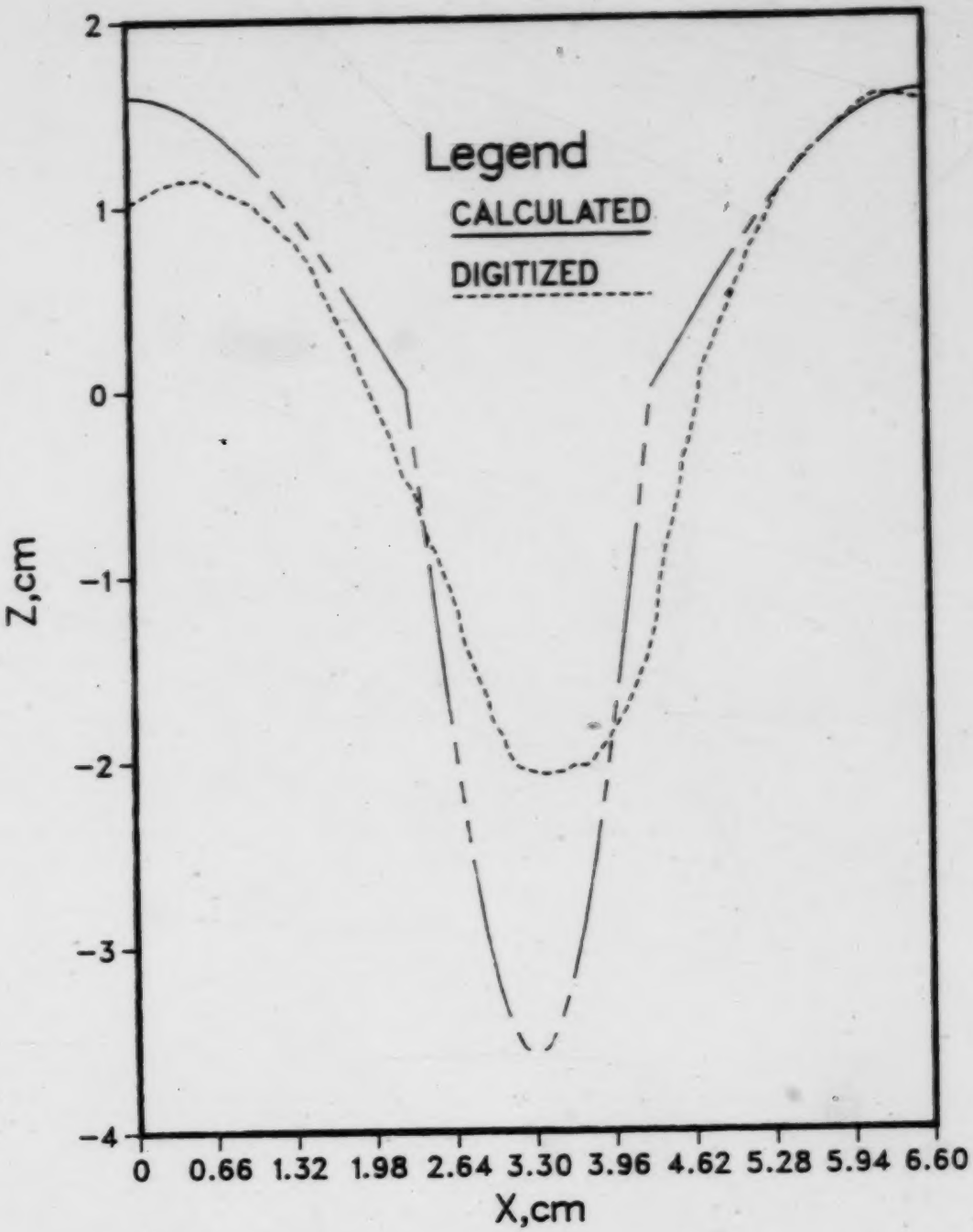

FIG.53 THE INTERFACE AT T=671 SEC.
FOR RUN 50

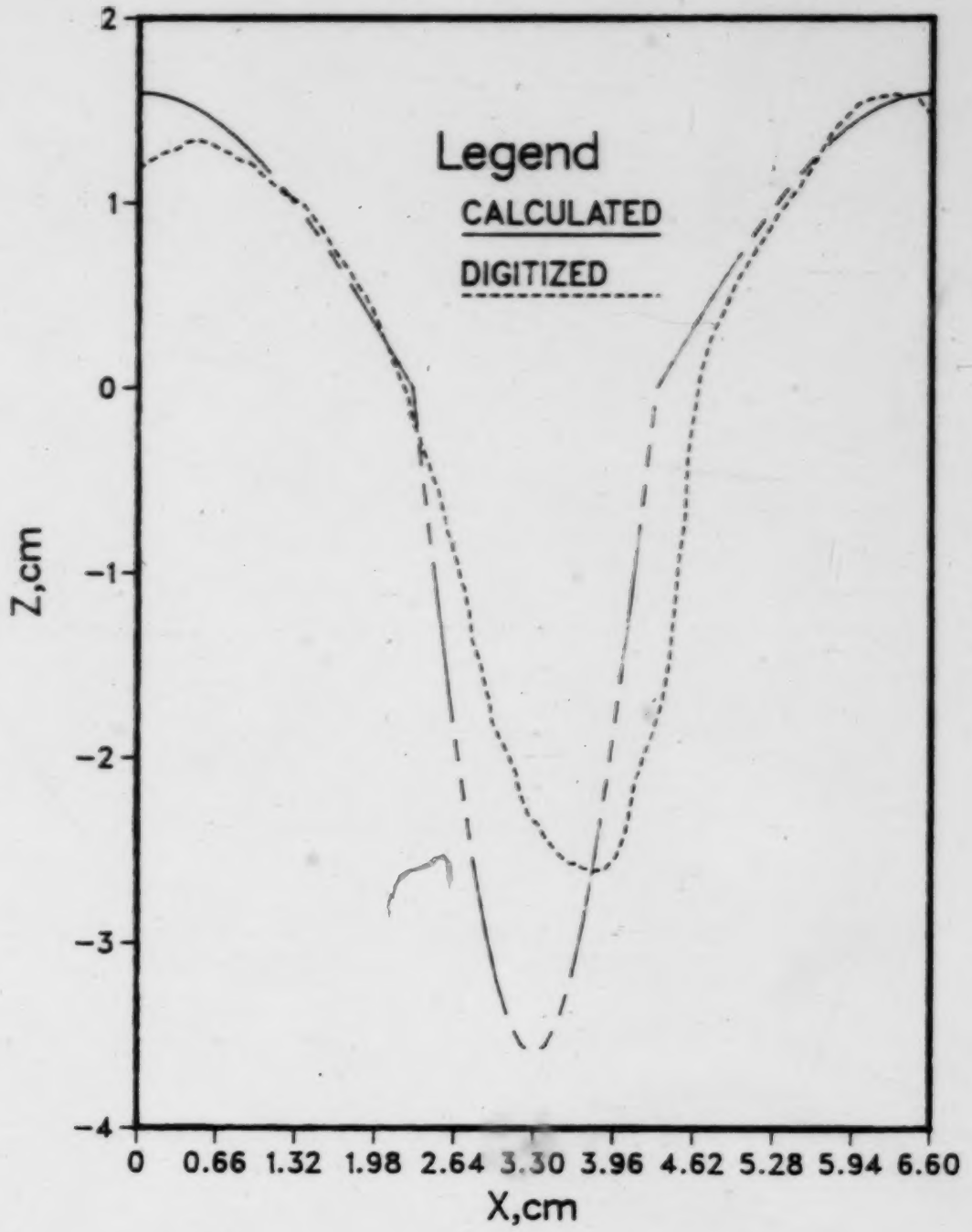

FIG.54 THE INTERFACE AT T=610 SEC.
FOR RUN 50

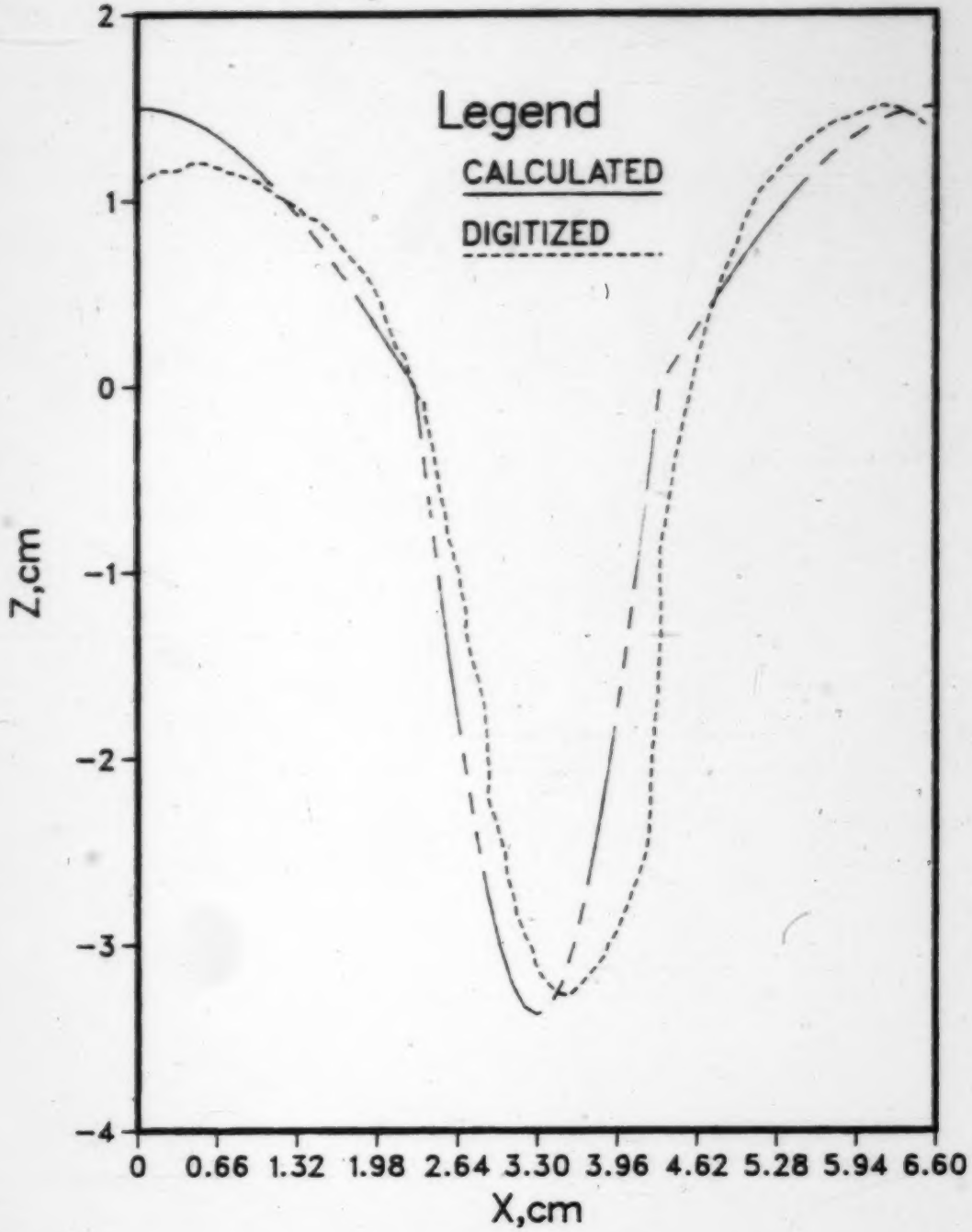

FIG.55 THE INTERFACE AT T=721 SEC. FOR RUN 60

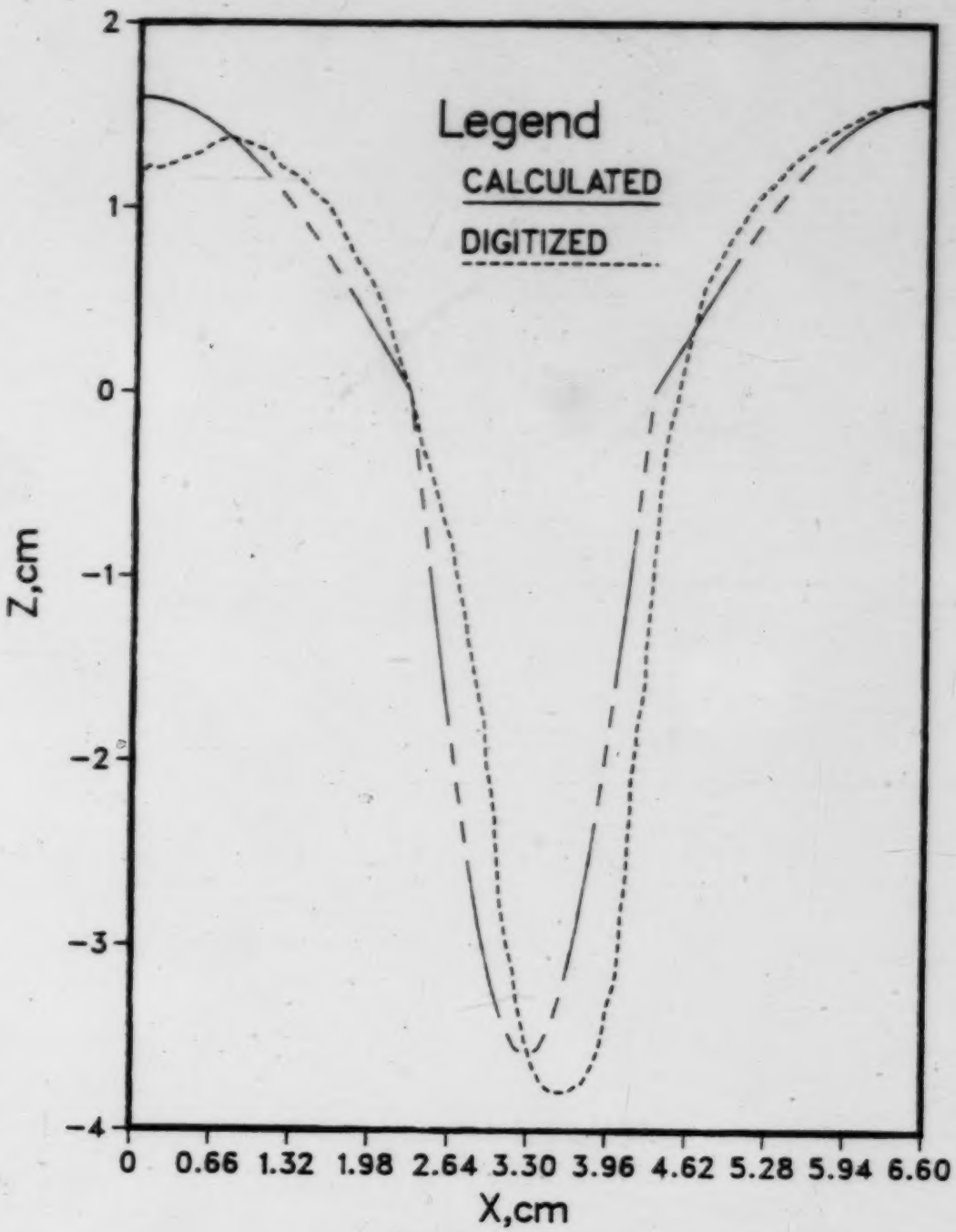

FIG.56 THE INTERFACE AT T=786 SEC. FOR RUN 50

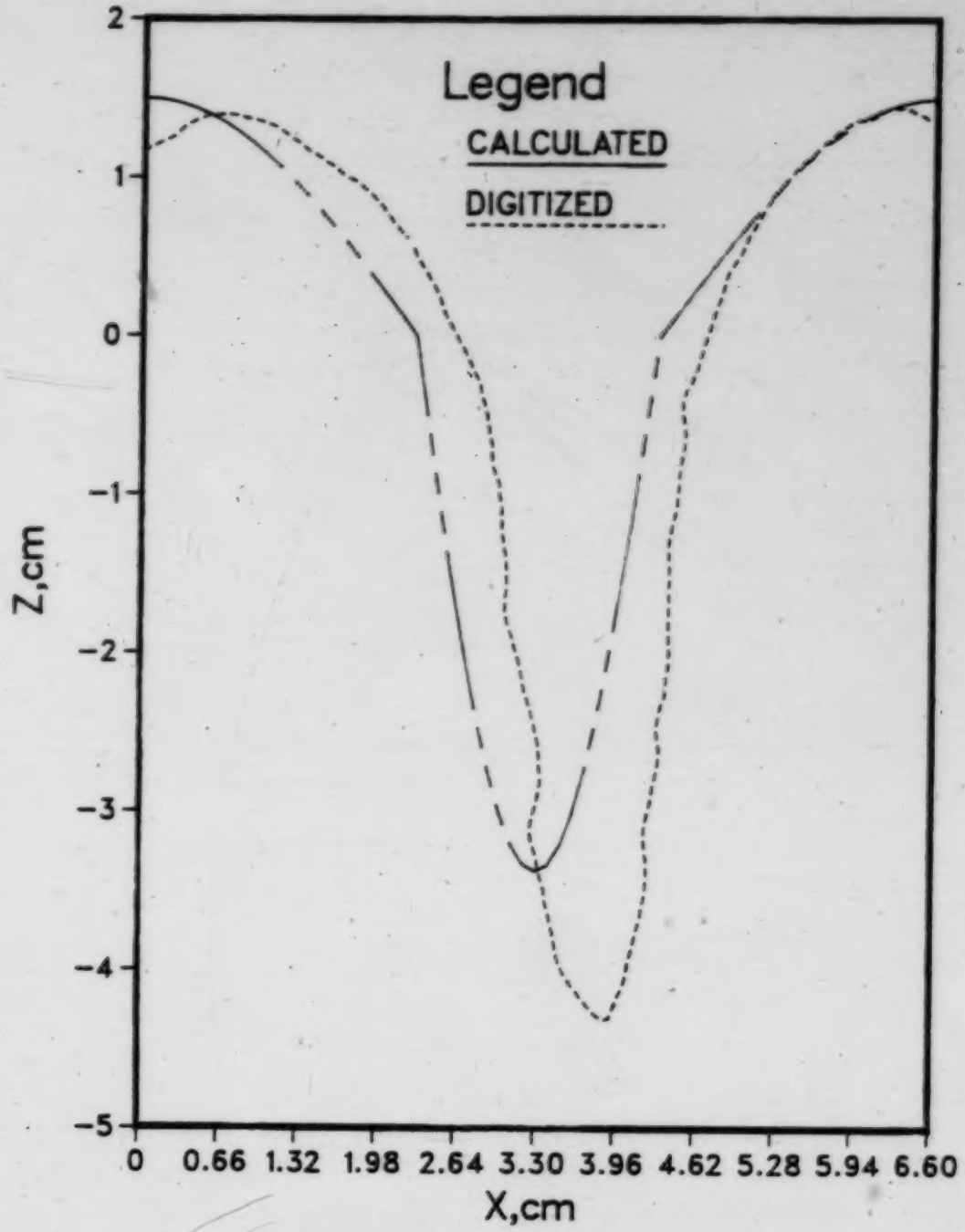

FIG.57 THE INTERFACE AT T=857 SEC.
FOR RUN 60

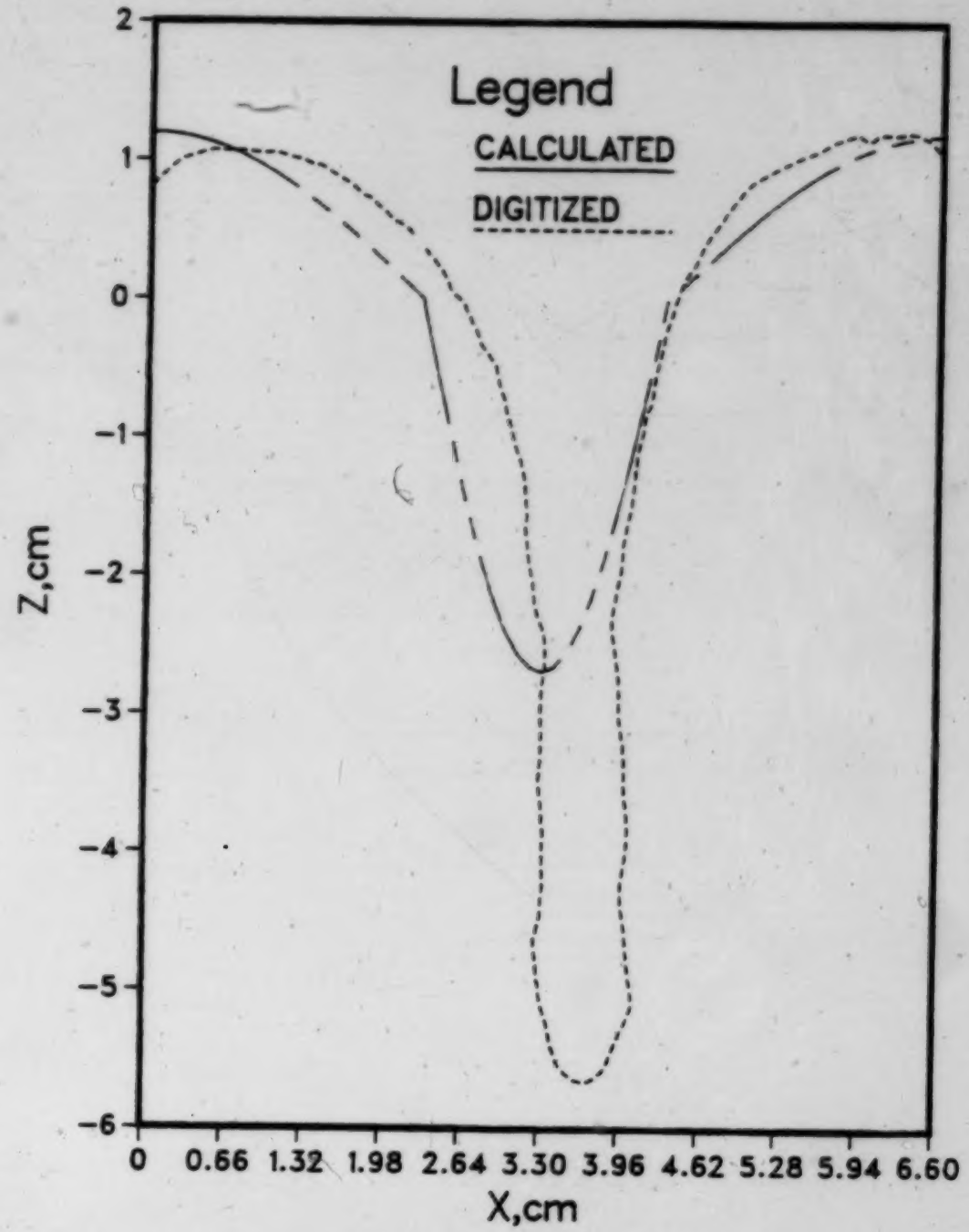

FIG.58 THE INTERFACE AT T=990 SEC.
FOR RUN 60